Dissertation submitted to the
Combined Faculties for the Natural Sciences and for Mathematics
of the Ruperto-Carola University of Heidelberg, Germany
for the degree of
Doctor of Natural Sciences

Presented by:

Dipl.-Ing. (FH) Jasmin Fabian, MSc of Biotechnology
born in: Schwetzingen, 26.08.1982
Oral-examination:

Impact of HBV and HCV infection on TGF-β signaling

Referees:

Prof. Dr. S. Wölfl, University of Heidelberg, Germany

Prof. Dr. S. Dooley, University of Heidelberg, Germany

Für meinen Papa

Harald Fabian

TABLE OF CONTENTS

LIST OF ABBREVITIONS

α-SMA	Alpha smooth muscle actin
APS	Ammonium persulfate
BSA	Bovine serum albumin
CDKIs	Cyclin dependent kinase inhibitors
CTGF	Connective tissue growth factor
DAPK	Death-associated protein kinase
DDB2	DNA damage-binding protein 2
DMEM	Dulbecco's Modified Eagle's Medium
DMSO	Dimethyl sulfoxide
DN	Dysplastic nodules
DNA	Deoxyribonucleic acid
EDTA	Ethylene diamine tetraacetate
EMT	Epithelial-mesenchymal transition
ER	Endoplasmatic reticulum
Erk	Extracellular signal-regulated kinase
FCS	Fetal Calf Serum
FMDV	Foot-and-mouth disease virus
GADD45β	Growth arrest and DNA-damage-inducible, 45 beta
Grb2	Growth factor receptor binding protein 2
HBeAg	Hepatitis B virus e antigen
HBsAg	Hepatitis B virus s antigen
HBSS	Hank's Buffered Salt Solution
HBV	Hepatitis B virus
HBx	Hepatitis B virus x protein
HCC	Hepatocellular carcinoma
HCV	Hepatitis C virus
HIF	Hypoxia inducible factor
HIPK2	Homeodomain-interacting protein kinase 2
HSCs	Hepatic stellate cells
IFN-α	Interferon, alpha
INHBE	Inhibin, beta
IRES	Internal ribosomal entry site

JAK	Janus kinase
JNK	c-Jun N-terminal kinase
kb	kilo base
LDH	Lactate dehydrogenase
MAPK	Mitogen-activated protein (MAP) kinases
MPA	Mycophenolic acid
mRNA	messenger RNA
miRNA	micro RNA
mTOR	Mammalian target of rapamycin
MTT	3-[4,5-dimethylthiazol-2-yl]-2,5-diphenyltetrazolium bromide
NASH	nonalcoholic steatohepatitis
NP-40	Nonidet™ P40 substitute
ORF	Open reading frame
PAI-I	Plasminogen activator inhibitor-1
PCR	Polymerase chain reaction
PFA	Paraformaldehyde
PGA	Pepsinogen
PHHs	Primary human hepatocytes
pre-miR	Primary miRNA
pri-miR	Precursor miRNA
RNA	Ribonucleic acid
ROS	Reactive oxygen species
SBE	Smad binding element
SDS	Sodium dodecyl sulfate
Shc	Src homology domain 2-containing protein
SPATA	spermatogenesis-associated gene
TEMED	N,N,N',N'-tetramethylethylenediamine
TIEGI	TGF-β-inducible early response gene I
TβRI	TGF-β receptor type I
TβRII	TGF-β receptor type II
TGF-β	Transforming growth factor, beta
TNF-α	Tumor necrosis factor, alpha
TP	Terminal protein
TSP-I	Thrombospondin-I

TYMS	Thymidylate synthase
UTR	Untranslated region

1 SUMMARY

HCC is the most common type of cancer, often induced by viral infection with hepatitis B virus (HBV) or hepatitis C virus (HCV). Transforming growth factor-β (TGF-β) is an important cytokine upon liver damage as in wound healing and liver fibrosis due to its proapoptotic, antiproliferative and immunosuppressive functions on the epithelium. This work investigated the impact of HBV and HCV infection on TGF-β dependent signaling, its outcome and on the progression of chronic liver disease to HCC.

cDNA microarrays were generated of primary human hepatocytes (PHHs) infected with HBV and treated with TGF-β for 1 and 24hrs, respectively. Gene expression analysis revealed that HBV regulated p53 and mTOR signaling pathway, the latter one known as being downstream of the Akt survival signaling pathway. Upon TGF-β treatment, HBV infection abrogated TGF-β signaling in PHHs and reduced the number of TGF-β regulated target genes. HepG2.2.15 cells, which replicate HBV, show decreased Smad3 phosphorylation and transcriptional activity, and impaired TGF-β induced apoptosis. HBV replication increased Akt phosphorylation, but deactivation of Akt by its specific inhibitor LY294002 sensitized HepG2.2.15 cells for TGF-β induced apoptosis. This effect was Smad3 independent. TGF-β induced apoptosis upon Akt deactivation could be reduced by p38 MAPK inhibitor SB203580.

To investigate the impact of HCV on TGF-β signaling, Huh7 cells were stably transfected with HCV core protein (Huh7-HCV core cells). In these cells, TGF-β dependent Smad3 phosphorylation and transcriptional activity were reduced, TGF-β induced apoptosis was abolished, and TGF-β target genes involved in cell cycle arrest, like GADD45β, p15, and p21 were downregulated. HCV core protein further induced expression of the pro-fibrotic cytokine connective tissue growth factor (CTGF), which was however TGF-β independent.

In summary, the data of this thesis suggest, that HBV infection and HCV core protein interfere with canonical TGF-β signaling. Upon HBV infection, survival signaling pathways are induced, which counteract TGF-β signaling. Replication of HBV and overexpression of HCV core protein blunted Smad3 signaling and TGF-β induced apoptosis was abrogated. These results indicate that viral infection facilitates the escape of hepatocytes from the TGF-β induced apoptosis to assure viral survival in the hepatocytes.

1 ZUSAMMENFASSUNG

HCC ist eine der häufigsten Krebsarten, meist ausgelöst durch eine Infektion mit dem Hepatitis B Virus (HBV) oder Hepatitis C Virus (HCV). Aufgrund der proapoptotischen, antiproliferativen und immunsuppressiven Funktionen auf das Epithelium, ist Transforming Growth Factor-β (TGF-β) ein wichtiges Zytokin bei Leberschäden wie Wundheilung und Leberfibrose. Diese Arbeit untersuchte den Einfluß einer HBV und HCV Infektion auf TGF-β abhängige Signalwege, deren zelluläre Effekte und Entwicklung von chronischer Lebererkrankung zum HCC.

HBV infizierte primäre humane Hepatozyten (PHHs) wurden für eine, beziehungsweise 24h, mit TGF-β behandelt und anschließend cDNA Mikroarrays generiert. Die Genexpressionsanalyse zeigte, dass HBV den p53 und mTOR Signalweg reguliert, letzterer wird über den Akt Survival Signalweg moduliert. Die Behandlung der HBV infizierten PHHs mit TGF-β zeigte, dass HBV die TGF-β Signalwirkung aufhob und die Anzahl der TGF-β regulierten Zielgene reduzierte. Die HBV replizierenden HepG2.2.15 Zellen zeigten eine reduzierte Smad3 Phosphorylierung und transkriptionale Aktivität, sowie eine geminderte TGF-β induzierte Apoptose. Des Weiteren erhöhte die HBV Replikation die Akt Phosphorylierung. Durch Deaktivierung von Akt, mit dem Akt spezifischen Inhibitor LY294002, konnten HepG2.2.15 Zellen für TGF-β induzierte Apoptose sensibilisiert werden. Dieser Effekt war Smad3 unabhängig. Die TGF-β induzierte Apoptose aufgrund der Deaktivierung von Akt konnte wiederum durch den p38 MAPK Inhibitor SB203580 reduziert werden.

Um den Einfluß von HCV auf TGF-β abhängige Signalwege zu untersuchen, wurden Huh7 Zellen mit dem HCV core Protein stabil transfiziert (Huh7-HCV core cells). Diese Zellen zeigten eine reduzierte TGF-β abhängige Smad3 Phosphorylierung und transkriptionale Aktivität. Des Weiteren war die TGF-β induzierte Apoptose aufgehoben, und TGF-β Zielgene, die im Zellzyklusarrest involviert sind, wie GADD45β, p15 und p21, waren herunterreguliert. Unabhängig von TGF-β induzierte das HCV core Protein die Expression des profibrotischen Zytokins Connective Tissue Growth Factor (CTGF). Zusammenfassend kann gesagt werden, dass die Ergebnisse dieser Arbeit darauf hindeuten, dass eine HBV Infektion und das HCV core Protein den kanonischen TGF-β Signalweg beeinträchtigen. Durch die HBV Infektion werden Überlebenssignalwege induziert, die dem TGF-β Signalweg entgegenwirken. Replikation von HBV und Überexpression des HCV core Proteins verminderten die Smad3 Signalleitung, sowie

die TGF-β induzierte Apoptose. Diese Ergebnisse weisen darauf hin, dass die virale Infektion Hepatozyten vor TGF-β induzierter Apoptose schützt, um das virale Überleben im Hepatozyten sicherzustellen.

2 INTRODUCTION

2.1 HCC

Hepatocellular carcinoma (HCC) belongs to the most frequent malignant tumors worldwide accounting for about 6% of all human cancers, with 564,000 new cases each year. Of liver cancers, HCC is the most common form, with a high mortality rate [1]. Etiologic factors associated with HCC are alcoholism, nonalcoholic steatohepatitis (NASH), aflatoxin B1 exposure and infection with Hepatitis B and C viruses (HBV/HCV), the latter two being responsible for 80% of HCCs [2]. However, HCC rate is much higher in low income countries, which is due to the higher incidence of HBV and HCV (Figure 1). The development of HBV vaccination has highly reduced the rate of HBV-induced HCC. Further, improvements in early detection of HCC, like regular ultrasound examination and α-fetoprotein testing, have limited the impact of HCC [3]. The primary curative treatment is surgical resection; however, it is restricted to small tumors. Patients with large tumors (greater than Ø10cm) can only be treated with molecular targeted therapies [4]. Due to the different etiologic factors HCC is very heterogenic, making the development of a curative treatment difficult. Sorafenib is a multikinase inhibitor, inhibiting several tyrosine protein kinases (VEGFR and PDGFR) and RAF/MEK/ERK cascade inhibitor. It induces apoptosis in neoplastic liver cells and attracted attention in treatment of HCC as it improved overall survival [5]. Interestingly, Ras/MAP kinase signaling was found to increase TGF-β expression and thus may be one explanation for the increased expression of TGF-β in HCC cells [6]. This was already investigated in 1991 by Ito et al. who found elevated TGF-β expression in HCC tissue [7]. Under healthy conditions, TGF-β signaling functions as a tumor-suppressor that cancer cells have to bypass in order to proliferate. However, in malignant cells TGF-β signaling is also known to function as a tumor promoter, inducing migration/ invasion upon epithelial-mesenchymal transition (EMT). The ability to switch TGF-β signaling from tumor-suppressive to tumor-promotive, may account as survival and proliferation advantage for the tumor cells. Mechanisms explaining this often-observed phenomenon will be described in more detail below.

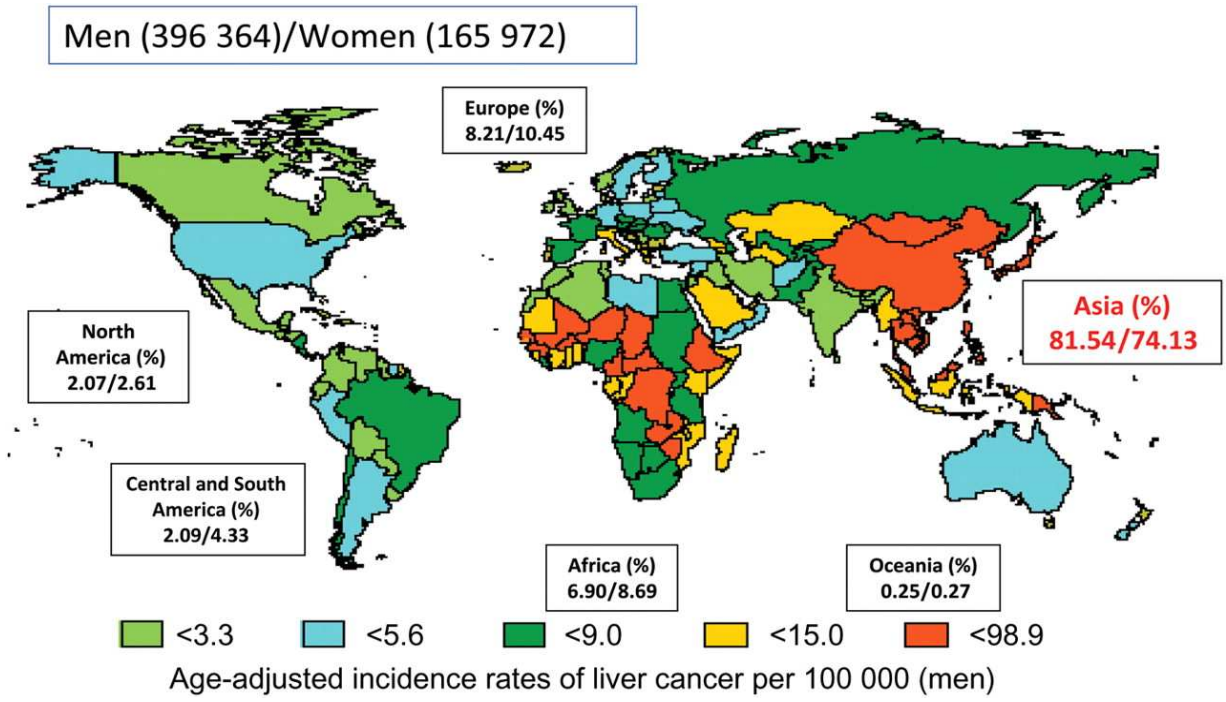

Figure 1: Liver cancer in the world (taken from [8]).

2.2 TGF-β

TGF-β is a multifunctional profibrotic cytokine, which exists in 3 isoforms. Isoform 1 has been described to be involved in pathogenesis of liver inflammation, fibrosis, cirrhosis, and HCC upon misregulation of its signaling pathway [9] [10]. As TGF-β1 has been found to be upregulated in many liver tumors [9] [11], it is thought to play a major role in at least a subset of cases displaying HBV- and HCV-induced carcinogenesis. Specifically, TGF-β controls cell proliferation, differentiation, apoptosis, migration, extracellular matrix remodeling, immune functions, and tumor invasion and metastasis [10]. Under healthy conditions, TGF-β1 secretion is restricted to Kupffer cells and is involved in liver homeostasis [12]. It is known as a growth factor for mesenchymal cells or as an inhibitor of proliferation of epithelial cells [13] [14]; for example, in fibrosis progression, TGF-β1 induces activation and proliferation of hepatic stellate cells (HSCs), whereas in "normal" hepatocytes, its outcome is cytostatic with provision of proliferation arrest and apoptosis [15]. TGF-β-induced growth inhibition and apoptosis is associated with its function as a tumor-suppressor. Interestingly, during the course of liver disease, hepatocytes become a major source of TGF-β with an autocrine effect. TGF-β1 signaling may switch from being tumor-suppressive to tumor-promoting [16], triggering

proliferation, motility, invasion and metastasis (Figure 2). Thus, TGF-β signaling is also implicated in the process of epithelial mesenchymal transition (EMT), a significant feature of tumor progression [17], which was recently also discussed to be involved in earlier stages of CLD [18]. EMT is actually found during embryogenesis and wound healing responses in adults. However, EMT has been linked to cancer, as it allows epithelial cells to migrate and to invade surrounding tissue [19]. *In vivo* and *in vitro* studies have shown that TGF-β is involved in EMT [20] as it downregulates expression of epithelial markers like E-Cadherin, and ZO-1, and it upregulates mesenchymal markers like, vimentin, fibronectin, α-smooth muscle actin (α-SMA), or N-Cadherin [21]. Hence, TGF-β expression and its signaling pathway are thought to provide several advantages for tumor cells during cancer progression under certain circumstances [22]. Nevertheless, the specific conditions that induce the switch from cytostatic to tumorigenic for TGF-β have not been elucidated thoroughly yet.

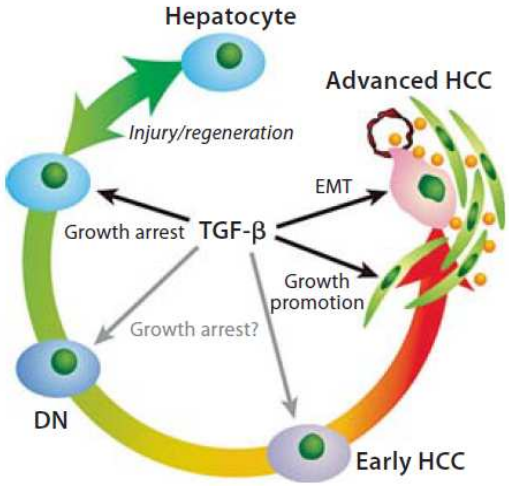

Figure 2: The role of TGF-β during the course of liver injury and regeneration towards hepatocarcinogenesis. TGF-β inhibits the proliferation during liver injury and regeneration. The switch of tumor-suppressive to tumor-promoting of TGF-β occurs during dysplastic nodules (DN) and early HCC. In advanced HCC cells TGF-β induces growth inhibition and EMT and contributes to tumor invasion through tumor-stromal interaction (taken from [23]).

2.2.1 Canonical Smad-mediated TGF-β signal transduction

The canonical TGF-β pathway is activated due to binding of bioactive TGF-β to its receptor type II (TβRII) (ALK5). This complex further interacts and activates TGF-β type

I receptor, forming a heterotetrameric complex. The receptor proteins Smad2 and 3 become phosphorylated upon recruitment and interaction with TGF-β receptor type I (TβRI) serine and threonine residues. The activated Receptor (R)-Smad2 and 3 release from the receptor upon formation of a trimeric complex with the Common mediator (Co)-Smad4, which is then able to translocate to the nucleus (Figure 3). By binding to promoters containing the minimal smad binding element (SBE) 5'-CAGAC-3', the complex is able to activate or inhibit the expression of TGF-β target genes, like the upregulation of Plasminogen activator inhibitor-1 (PAI-I), procollagen I and III, CTGF, p15, p21, GADD45β or the repression of c-myc, Bcl-xL, HGF, and Id-1 [24] [25]. Although Smad2 and Smad3 are highly homologous, it has been shown, that there are functional differences between these two proteins. Yanagisawa et al. 1998 showed that overexpression of Smad3 in lung epithelial cells resulted in apoptosis upon TGF-β treatment, whereas Smad2 had not such a great impact [26]. Further, overexpression of dominant negative Smad3 in Hep3B cells inhibits TGF-β-induced apoptosis [27]. Recruitment of several different transcription factors, corepressors and coactivators further defines the signature of transcribed genes which is highly dependent on cell type and physiological context [28]. The expression of a specific set of transcription factors, corepressors and coactivators, might be one explanation how tumor cells can switch off the cytostatic, but not the tumor-promoting branch of TGF-β signaling. Furthermore, the different transcription factor complexes themselves are highly regulated by other signaling pathways, leading to crosstalk between TGF-β and other signaling pathways. Among the transcribed genes is the Inhibitory (I)-Smad Smad7, a negative feedback inhibitor of TGF-β signaling. One of its mechanisms to inhibit TGF-β signaling is by hindering Smad binding to the receptor and thereby their phosphorylation and activation. Further, Smad7 interferes with Smad-DNA complex formation in the nucleus [29].

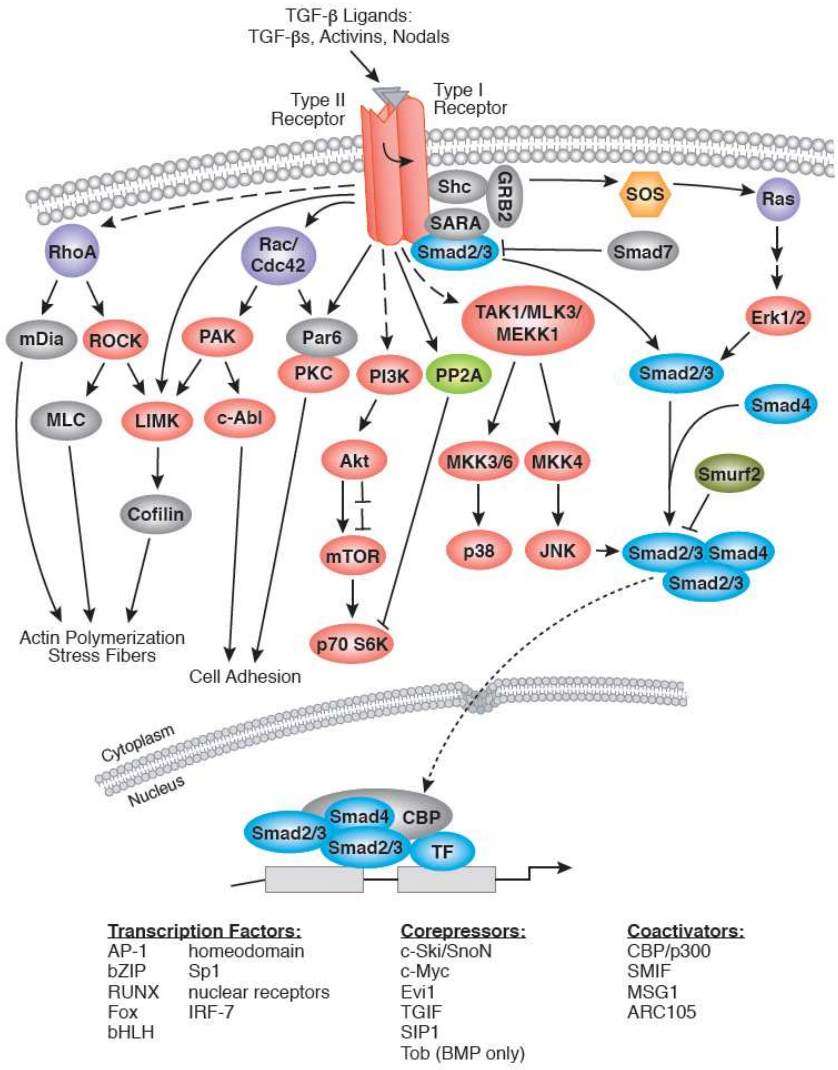

Figure 3: TGF-β signaling pathways. TGF-β signals through Smad and non-Smad pathways to regulate transcription of its target genes. TGF-β binds to TβRII to form an activated complex with TβRI, which is in turn able to c-terminally phosphorylate and activate Smad2 and 3. Both Smads form a trimeric complex with Smad4 and accumulate in the nucleus. Expression and repression of TGF-β target genes is performed in cooperation with transcription factors, corepressors and coactivators to regulate target gene expression. JNK and MAPK also phosphorylate Smads to influence their activation. Interaction of activated TβR complex with non-Smad signaling pathways including PI3K, Akt, p38, JNK, RhoA, and Erk can further influence gene transcription and cell fate. For detailed information see text (adapted from www.cellsignal.com; October 2012).

2.2.2 Non-canonical TGF-β signaling and crosstalk

Three different mechanisms have been defined leading to non-canonical TGF-β signaling. First, binding of TGF-β to the receptor complex results in the activation of

proteins from other signaling pathways, including GTPases Rac1, Cdc42, RhoA and Ras, the MAP kinases c-Jun N-terminal kinase (JNK), extracellular signal-regulated kinase (ERK), p38 MAP kinase, growth and survival promoting PI3K/AKT/TOR pathway, and tyrosine kinases FAK, Src and Abl [30] [31] (Figure 3). The phosphorylation of different proteins is mainly achieved by the dual specificity of the receptors acting as tyrosine and serine/threonine kinase which results in the recruitment of several adaptor proteins [32]. For example, p38 MAPK activation can be mediated via Src in breast cancer cells. Src phosphorylates TβRII, thereby recruiting growth factor receptor binding protein 2 (Grb2) and Src homology domain 2-containing protein (Shc) which are associated with adapter proteins responsible for p38 MAPK activation promoting oncogenic signaling by TGF-β [33]. Bhowmick et al. 2001 reported that in NMuMG cells activation of RhoA-dependent signaling by TGF-β induces stress fiber formation and mesenchymal-/ EMT-like characteristics [34]. Second, non-Smad signaling pathways can lead to phosphorylation and activation of Smad proteins. For example, in epithelial R-1B/L17 cells it was found, that ERK pathway can trigger direct phosphorylation of R-Smads in their linker region, which impairs their nuclear translocation [35]. JNK phosphorylates Jun in COS-7, HepG2, and Mv1Lu cells, resulting in a complex formation of Smad2 and its corepressor protein TGIF leading to inhibition of Smad2-dependent transcription [36]. Third, activated Smad proteins can activate or interact with proteins from other signaling pathways. Interestingly, Smads have been implicated in the posttranscriptional processing of microRNAs (miRNA), which participate in the regulation of messengerRNA (mRNA). Smads bind to the DROSHA microprocessor subunit p68 to facilitate processing of primary miR-21 (pri-miR-21) into precursor miR-21 (pre-miR-21) thereby leading to an increased expression of miR-21 [37]. Imoto et al. reported in 2003 that Smad7 interacts with PIASy, a protein inhibitor of activated STAT in Hep3B cells [38]. In summary, non-canonical TGF-β signaling is highly complex and diverse, and many of its interactions are still not set in any context. However, it is probable that these interactions may contribute to the cancer-related effects of TGF-β signaling in a Smad-dependent or Smad-independent manner [39] [30].

2.2.3 TGF-β-induced apoptosis and growth inhibition

TGF-β-induced apoptosis and growth inhibition play a central role in liver tissue development and homeostasis. Due to the several different mechanisms of Smad-dependent or independent TGF-β signaling, TGF-β-induced apoptosis and/ or growth inhibition can be mediated via different mechanisms depending on cell type and context. Upon canonical Smad signaling several transcribed genes are responsible for TGF-β-induced apoptosis/ growth inhibition, e.g. phospholipid phosphatase SHIP [40], death-associated protein kinase (DAPK) [41], TGF-β-inducible early response gene 1 (TIEG1) [42], and pro-apoptotic protein BIM [43]. Induction of cyclin-dependent kinase inhibitors (CDKIs) like p21 and p15 lead to inhibition of cell cycle progression in the G1 phase [44] [45]. TGF-β also represses the transcription factor c-myc, which is responsible for cell proliferation [46], and decreases the levels of anti-apoptotic Bcl-x_L [47]. Smad-dependent expression of growth arrest and DNA-damage-inducible, beta (GADD45β) does not only lead to activation of apoptosis but also to a delayed activation of p38 MAP kinase pathways. In pancreatic carcinoma cells, this in turn leads to expression of thrombospondin-1 (TSP-1), which is involved in suppression of tumor cell growth and angiogenesis [48]. Another mechanism of TGF-β-induced apoptosis is mediated by MAPKs, like JNK and p38. The Daxx-JNK pathway mediates TGF-β-induced apoptosis upon binding of Daxx to TβRII. Homeodomain-interacting protein kinase 2 (HIPK2) phosphorylates Daxx which leads to the activation of MAP kinases MKK4/7 which then activate JNK, triggering apoptosis in AML12 hepatocytes [49] [50]. Yamashita et al. 2008 reported that in HEK 293T cells TRAF6 becomes activated upon constitutively binding to TβRI and subsequent formation of the TβRI-TβRII-complex. This in turn activates the MAP kinase kinase kinase TAK1 in addition with recruitment of TAB2. Activated TAK1 then phosphorylates and activates MKK3 or MKK6, leading to activation of p38, whereby Smad7 functions as a scaffold protein facilitating this pathway. Furthermore, this signal transduction is independent of R-Smads and the kinase activity of TβRI. Hence, TβRI is able to activate either the canonical Smad pathway, or the pathway TRAF6-TAK1-p38/JNK [51] [52]. However, in Hep3B cells, Chen et al. 1998 reported that the survival pathway PI3K/ Akt is able to protect against TGF-β-induced apoptosis upon blocking TGF-β-induced activation of caspase-3 without affecting Smad phosphorylation and nuclear translocation [53]. In 2004, Conery et al. showed, that TGF-β-induced apoptosis is also dependent on the crosstalk with Akt/PKB serine/threonine

kinase in Hep3B cells. Akt is able to interact with unphosphorylated Smad3 in the cytoplasm, preventing its phosphorylation and translocation to the nucleus. Hence Smad3-dependent gene transcription important for TGF-β-induced apoptosis is inhibited. Interestingly, the interaction of Smad3 and Akt is independent of Akt kinase activity, but dependent on the ratio of Smad3 to Akt [54] [55]. Contrary, Song et al. 2006 reported that Akt suppresses Smad3 activation in an Akt kinase-dependent manner by means of the downstream kinase mammalian target of rapamycin (mTOR) in a prostatic epithelial cell NRP-152 [56]. Seoane et al. 2004 described that Akt phosphorylates transcription factor FoxO, thereby inhibiting its nuclear translocation in neuroepithelial and glioblastoma cells. However, FoxO is needed for Smad3 transcriptional activity to induce p21 expression [57]. A lot of other groups had shown that Smad3 is the main driver responsible for TGF-β-induced apoptosis and growth inhibition. For example, Liu et al. 1997 reported that Smad3 phosphorylation and activation is required for TGF-β-induced growth inhibition and transcriptional activation of the PAI-1 promoter in epithelial cells [58]. Wildey et al 2003 showed that Smad3 overexpression increases BIM expression and subsequently apoptosis upon TGF-β treatment in WEHI 231 B lymphocytes [59]. In summary, the induction of apoptosis and growth arrest by TGF-β is dependent on cell type and context, and the state of differentiation. However, there is no evidence that the different mechanisms are restricted to only a specific cell type or state of differentiation. Hence, this may explain the different outcomes upon TGF-β treatment of hepatocytes.

2.3 HBV

HBV has been discovered in 1970 as a member of the *Hepadnavirus* family [60]. Two billion people worldwide have been infected with the virus, of which more than 240 million have chronic (long-term) liver infections, and about 600 000 people die every year due to the consequences of hepatitis B (WHO, July 2012). Although, most adults clear the infection spontaneously [61], a vaccination against HBV is available since 1982 protecting for at least 20 years. Over one billion doses of hepatitis B vaccine have been used worldwide resulting in a significant reduction of HBV infection (WHO, July 2012). Unfortunately, vaccination and treatment therapies are barely available in developing countries and many people will still be infected. It is of major importance to elucidate the

underlying molecular mechanisms in more detail which lead to the development of HCC in chronic HBV infection [62]. Therapy treatment with antiviral drugs, like lamivudine, entecavir, or immune system modulators like pegylated interferon-alpha (IFN-α) cannot clear the viral infection, but can decrease viral replication [63]. Unfortunately, studies on HBV, its impact on cell transformation and the immune system, have been hampered, because HBV has a very strong tropism for liver parenchymal cells of humans, chimpanzees, woodchucks, or ducks. Since correlation of the immune system of woodchucks and ducks to the human immune system is not really reliable, and trials with chimpanzees are not always feasible, HBV is mostly investigated in cell culture models. Since HBV infection is restricted to differentiated cells, only PHHs can be infected, supporting HBV replication for several weeks [64] [65]. Some hepatoblastoma cell lines, like HepG2, do support HBV replication after transfection of HBV DNA, but impact on the host cell upon initiation of infection of HBV is not considered [66] [67]. However, Gripon et al. 2002 could develop the cell line HepaRG, which is susceptible to HBV infection, as they express several liver-specific receptors needed for viral entry [68].

2.3.1 HBV particle

HBV is a small enveloped DNA virus (42nm Dane particle) with a relative small relaxed circular, partially double-stranded genome of around 3.2kb length with 4 overlapping open reading frames (ORF) (Figure 4). The pre-S/S ORF encodes the three viral surface proteins named large (L), middle (M) and small (S) surface protein. The pre-C/C ORF encodes the e antigen (HBeAg) and the core antigen (HBcAg). The P ORF encodes the terminal protein (TP) and the viral polymerase. The X gene encodes a small protein (HBx) that is essential for virus replication [69] [70]. HBV mutations, due to errors in viral reverse transcription, especially in the surface ORF, are important to escape the antiviral defense of the immune system. According to their genomic sequence variations, HBV has been divided into eight genotypes [71]. Further, based on antigenic epitopes presented on its envelope proteins HBV is also divided into four major serotypes (adr, adw, ayr, ayw) [72]. Interestingly, it has been argued that viral genotypes have different courses of HBV infection in terms of persistence, viral load, resistance to therapy, and HCC development [73]. Since HBV is a DNA virus, HBV DNA integration into the hepatocyte genome has been detected in around 80% of HCC from HBV-positive

patients [74] [75]. DNA integration is supposed to be a mechanism associated with HBV-induced HCC development. Although this integration step is not obligatory and not necessary for viral replication, it allows persistence of the viral genome [76]. HBV DNA integration occurs often in genes encoding proteins crucial for cell proliferation and apoptosis [77]. Modification of its expression (e.g. *cis*-activation) with impact on carcinogenesis has been controversial [78]. Nevertheless, the HBx gene is the most commonly integrated and expressed protein found in HCC tissue [79]. Interaction of HBx with cellular proteins has also been reported. HBx has been investigated to interact with epidermal growth factor receptor, c-myc, c-jun, AP-1, SP-1, p53, and NFκB, among others [80]. These interactions may hold another mechanism of HBV-induced HCC development.

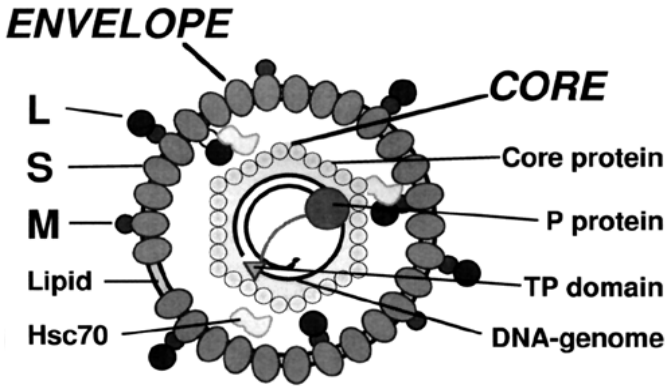

Figure 4: The HBV viron is around 42nm in diameter. The envelope is a lipid bilayer containing viral surface proteins L, M, and S. The preS1 domain of the L protein can interact with cellular heat shock protein Hsp70. This is probably responsible for the dual function of preS1 domain in mediating contact between virus and host cell, and viral envelope and capsid [81]. The inner nucleocapsid consists of core protein and encloses the partially double-stranded circular DNA of around 3.2kb, of which the 5'-end of the complete (-)-DNA strand is covalently linked to the TP domain of P protein (taken from [69]).

2.3.2 HBV and TGF-β

Since TGF-β plays an important role in liver fibrosis [82], many studies have attempted to investigate the role of TGF-β in the course of HBV infection and whether it is usable as a marker in disease progression and severity. Flisiak et al. 2005 reported an upregulation of plasma TGF-β in acute viral hepatitis B, but not in hepatitis C. During the four-week follow-up TGF-β plasma levels decreased, although the levels were still

significantly higher than normal. Furthermore, they observed that the concentration of TGF-β at the beginning of the severe form of hepatitis B doubled in value from that of the mild form subgroup. Here as well, they could observe in the following weeks a decline in TGF-β levels of the severe form down to the concentrations found in the mild form subgroup. They state, that this higher release in TGF-β is due to more damaged hepatocytes during acute liver disease, but not due to its mechanism, and that this is different from chronic liver disease associated with the activation of hepatic stellate cells and fibrosis [83]. In line, Guo et al. 2009 showed that the HBx-expressing liver cell line QSG7701 grown in a co-culture system induced TGF-β expression in the hepatic stellate cell line LX-2 [84]. The group of Dong et al. 2008 investigated the levels of TGF-β expression in livers, with respect to HBV replication, as determined by HBV DNA. In contrary to Flisiak et al, they reported, that hepatic TGF-β expression can be correlated with HBV replication and the degree of HCC differentiation [85]. *In vitro* studies by Yoo et al. 1996 showed, that HBx *trans*-activates the TGF-β promoter through the Egr-1 binding sites in transfected HepG2 cells [86]. In line, Pan et al. 2004 could show in Mv1Lu cells stably expressing HBx higher TGF-β activity due to upregulation of TGF-β and downregulation of α_2-macroglobulin [87]. Furthermore, TGF-β-sensitive Mv1Lu cells transfected with HBx were less responsive to TGF-β-induced apoptosis as determined by ^{3}H thymidine incorporation [88]. In 2000, Shih et al could show that in TGF-β-sensitive Hep3B cells stably expressing HBx, HBx was able to block TGF-β-induced apoptosis, but did not affect TGF-β-induced activation of the PAI-1 gene. Obviously, HBx is able to inhibit only the cytostatic branch of TGF-β signaling. Moreover, Akt phosphorylation levels were induced in HBx expressing cells. Deactivation of Akt by the inhibitor LY294002 could rescue TGF-β-induced apoptosis [89]. In contrary, Lee et al. 2000, reported that HBx enhanced transcriptional activity upon TGF-β through direct interaction with Smad4 together with components of the basic transcriptional machinery [90].

In summary, it is still not clarified whether HBV infection results in an upregulation of TGF-β and the cellular source responsible for TGF-β release. There is incidence that HBx could inhibit tumor-suppressive functions of TGF-β, however, this not proven in regard to full HBV yet.

2.4 HCV

HCV has been discovered in 1989 as a member of the *Flaviviridae* family [91]. Around 3% of the worldwide population is infected by HCV, of which only a fraction is able to clear the virus spontaneously, whereas 80% become chronically infected [92]. 20% of chronically HCV-infected patients progress to cirrhosis and 1-3% will develop HCC [93]. Standard therapy treatment is a combination of pegylated IFN-α and ribavirin. Unfortunately, only 20% of patients are cured by this long-lasting and costly medication (approximately 35,000 $/ year). Furthermore this therapy is accompanied by severe side effects like, anemia, depression and flu-like symptoms [94]. However, new developments in therapy have been made recently. Bocepravir and telaprevir are direct antiviral drugs, which inhibit the NS3/4A proteases; both compounds progressed into phase III trials. Combination of both compounds together with standard therapy of peginterferon α and ribavirin increased sustained virologic response rates in treatment-naïve genotype 1 patients from 38-44% to 66-75% [95].

2.4.1 HCV particle

HCV is an RNA virus, with a genome of around 9,600kb. It is organized in one open reading frame encoding a 3,000aa polyprotein, which is cleaved into at least 10 proteins: the non-structural proteins NS2, NS3, NS4A, NS4B, NS5A and NS5B are released from the precursor polyprotein upon cleavage by virus-encoded proteases and assist in viral replication and assembly. The structural proteins core, E1, E2, p7 are released from the precursor polyprotein upon cleavage by cellular proteases and compose the viral particle [96] (Figure 5). HCV is divided into 6 genotypes (1-6), which are further split into 30 subtypes (1a, 1b, 3a...). Within the host, several quasispecies develop due to the high error rate of the RNA-Polymerase. This prolific and error-prone replication often leads to rapid emergence of point mutations that confer drug resistance [94] and allows the virus to escape from the host immune system and to establish a chronic infection (hcspFACTsheet, 2006). Interestingly, a switch from acute to chronic infection has been associated with a wider variety of quasi-species [97]. According to different tissue sub-localizations, like tumor and non-tumor regions, different viral variants have been isolated suggesting that they may contribute to HCV-induced carcinogenesis [98] [99]. However, HCV is not able to integrate into the host genome. Nevertheless, it is assumed

that viral proteins like core, NS3, and NS5A interact with host proteins and cellular structures causing transformations due to oxidative stress, apoptosis, ER stress, and dysregulated signal transduction [100]. Since Lohmann et al. 1999 established an HCV subgenomic replicon system in a human hepatoma cell line, investigation of HCV replication, influence on cellular signaling pathways, and efficacy measurement of antiviral components was possible [101]. Recently, Bandaudha et al. were able to develop a culture system of primary human hepatocytes that support productive replication of infectious HCV genotypes 1a, 1b, and 2a [102]. These were striking news for the study of host response to HCV infection and progressive liver disease. Ever since, research groups especially focused on elucidating the rendered signaling pathways involved in HCV-induced HCC development, e.g. the Janus kinase (JAK), MAPK, tumor necrosis factor (TNF-α), sphingolipid, insulin, oxidative stress, and the TGF-β signal transduction pathway have been found to be influenced at least [92] [103].

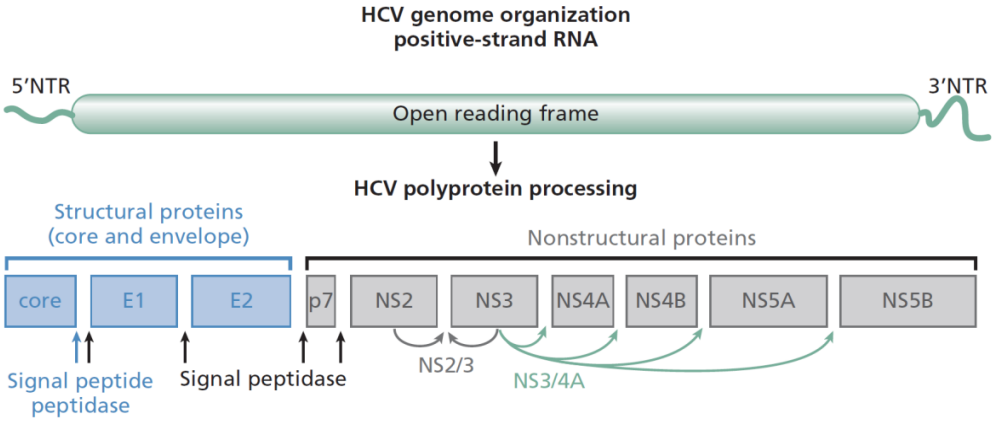

Figure 5: Organization of the HCV genome. The viral RNA contains 3'- and 5'-untranslated regions (UTR) that are required for viral replication. The 5'-UTR also contains an internal ribosomal entry site (IRES) that directs translation of a viral polyprotein, which is further proteolytically processed into 3 structural and 7 nonstructural proteins by viral enzymes (NS2/3 and NS3/4A) and cellular enzymes (signal peptidase and signal peptide peptidase) (taken from [104]).

2.4.2 HCV and TGF-β

Several publications showed that chronic inflammation as caused by HCV is accompanied by increased oxidative stress [105] [106] [107]. A role of reactive oxygen species (ROS) in carcinogenesis has been shown in many cases. Thus, ROS

downstream signaling components MAPKs, are reported to be involved in TGF-β/ Smad and integrin-mediated tumor metastasis [108]. Under healthy conditions, ROS are essential mediators of apoptosis involved in TGF-β-induced apoptosis. Interestingly, in Huh7 cells HCV induces TGF-β1 expression through a ROS-dependent activation of p38 MAPK, JNK, and ERK pathways [109]. In respect thereof, Wilson et al studied the effect of hypoxia inducible factor-1α (HIF-1α) in the lifecycle of HCV and hepatoma migration. They found an increase in HIF-1α expression in HepG2 cells expressing HCV glycoproteins and in Huh7.5 cells permissive for HCV infection, which resulted in higher cell migration and reduced cell polarity as assessed by enumerating MRP-2 positive BC/100 nuclei and tight junction integrity. The increase in HIF-1α led to an upregulation of the downstream effectors VEGF and TGF-β. Inhibiting either the VEGF or TGF-β of HIF-1α itself restored cell polarity and migration capacity, and additionally, had also a negative effect on HCV replication [110].

However, research using complete and infectious HCV virus is limited due to safety issues. Nevertheless, in order to further elucidate HCV impact on liver disease and HCC progression in more detail, several *in vitro* studies using individual viral proteins have been performed investigating their impact on cell behavior. Especially the HCV core protein attracted attention and was characterized to be involved in cell growth, apoptosis and carcinogenesis. Within the cell, it is often found on ER membranes, on the surface of lipid droplets, on the mitochondrial outer membrane, and to some extent in the nucleus [111] [112] [113]. Overexpression of HCV core protein in HepG2 cells resulted in enhanced cell proliferation concomitant with increased activity of JNK, Erk, and p38 MAP kinases [114]. In regard to its effect on cell survival, core protein lead to secretion and autocrine stimulation of HB-EGF, thereby activating the Akt mediated anti-apoptotic pathway through Ras/PI3K signaling [115]. Several groups reported the influence of HCV core expression on the TGF-β-dependent cell cycle control, resulting in down-regulation of cyclin-dependent kinase inhibitor p21 in HepG2 and in murine fibroblast NIH 3T3 cells, respectively. Mechanistic background of this inhibitory effect was later elucidated by Cheng et al, showing decreased DNA binding abilities of Smad3 due to interaction with HCV core protein (for more detail see below) [116] [117]. In line, Kwun and Jung published in 2003 that HCV core protein may regulate transcription of p21, depending on cell type and status in opposite manners. In HepG2 and Hep3B cells, p21 is upregulated, whereas in primary hepatocytes and NIH3T3 cells, p21 is

downregulated. As possible mechanisms stabilization of p53 and balance between TGF-β and sodium butyrate signaling pathways was suggested (the HCV core responsive region within the p21 promoter overlaps with the TGF-β/ Smad and the sodium butyrate responsive elements) [118]. The ability of HCV core to regulate transcription factors was also investigated. Shrivastava et al reported constitutive activation of Ap-1 by core, which correlated with the activation of JNK and MAPK [119]. Similarly, Cheng et al found that promoters containing Sp-1 or SBEs are not activated, while promoters which contain Ap-1-binding elements are [120]. Several investigations consistently found that overexpression of HCV core protein in hepatoma cells results in an upregulation of TGF-β1 protein by activation of MAPK signaling pathways [121] [122] [123]. Although TGF-β1 expression obviously is upregulated, its cytostatic/ proapoptotic signaling branch was often found to be abrogated. For example, Cheng et al investigated the TGF-β1 signaling pathway in Huh7 cells and revealed that overexpressed HCV core protein may also directly interact with the MH1 domain of Smad3, thereby blocking TGF-β/ Smad3-mediated transcriptional activation through interference with the DNA-binding ability of Smad3, but not with its nuclear translocation ability. These biochemical interactions lead to repression of TGF-β/Smad3-mediated apoptosis as investigated by TGF-β-induced p21 promoter activation. Further, overexpression of Smad3 increased the sensitivity of the Huh7 cells to TGF-β-induced apoptosis, whereas expression of dominant-negative-Smad3 enhanced survival [120]. Pavio et al. in 2005 supported the direct impact of HCV core on TGF-β/ Smad3 signaling. They isolated Hepatitis C virus core variants from liver tumor but not from adjacent non-tumor tissue which interact with Smad3 and inhibit the TGF-β pathway in HepG2 cells [124]. In a follow-up study of the same group, Battaglia et al published that this liver cancer-derived HCV core protein switches TGF-β growth inhibitory effects to tumor-promoting responses in regard to components implicated in EMT by decreasing Smad3 activation [125]. Using an in vitro co-culture system with primary HSCs isolated from rats, and a stable HepG2-HCV core cell line which had been transfected with HCV core gene, HCV core protein promoted liver fibrogenesis via up-regulation of CTGF and TGF-β1 in HepG2 cells [122]. CTGF has been linked to TGF-β pathways in fibroproliferative diseases [24] [25]. Hence, Kovalenko et al. investigated the role of CTGF upregulation and its suitability for the assessment of liver fibrosis in HCV-infected patients. They could show that HCV infected patients had significantly higher serum CTGF levels than healthy controls and that CTGF correlated with the histological degree of liver fibrosis [126]. Another recent publication by Wu et al.

2012 on HCV-induced fibrosis investigated the effects of HCV core protein in a completely new experimental setup. They observed the impact of secreted HCV core protein on hepatic stellate cells and found increased expression of α-SMA, procollagen α2(1) and TGF-β [127].

In summary, HCV core protein has been associated to interact with Smad3 and to interfere with TGF-β induced apoptosis. In regard to this, there are still discrepancies, e.g. about the regulation of p21. Furthermore, it is not clarified yet, whether CTGF upregulation is dependent on TGF-β in this context. Most importantly, results obtained about HCV core protein, are still to be proven in a full HCV model.

2.5 Project aim

Chronical HBV and HCV infection often lead to liver inflammation, fibrosis and finally to HCC. TGF-β is pivotal in liver cell signaling upon liver damage and during carcinogenesis TGF-β may turn from tumor suppressor to tumor promoter. The aim of this project was to elucidate the impact of viral infection on TGF-β dependent signaling pathway, signaling outcome and initial triggers for the progression of chronic liver disease to HCC.

(i) HBV is able to cause HCC although it is a noncytopathic virus causing few gene aberrations. To elucidate the role of TGF-β signaling in the cause of HBV induced HCC, this study questioned whether HBV is able to change the outcome of TGF-β signaling from being a tumor suppressor towards being a tumor promoter. Therefore, cDNA microarrays were generated from freshly isolated primary human hepatocytes (PHHs) which were infected with HBV and treated with TGF-β *in vitro*. It was discriminated between early (1h) and late (24hrs) expression signatures and compared infected versus uninfected cells. To verify the microarray data results, HepG2.2.15 cells were analyzed for canonical TGF-β signaling, like Smad phosphorylation and transcriptional activation, and TGF-β induced apoptosis.

(ii) HCV has been reported to negatively interfere with canonical TGF-β signaling, but the question whether TGF-β signaling changes from being a tumor suppressor towards a tumor promoter upon HCV has not been investigated in detail yet. The aim of this study was to verify functional effects of inhibition of TGF-β signaling like Smad phosphorylation and transcriptional activation, TGF-β induced apoptosis, and TGF-β induced EMT-like characteristics in transfected Huh7 cells, which overexpress HCV core protein, and in Huh7.5 cells, which are highly permissive for full HCV replication.

3 MATERIALS AND METHODS

3.1 Materials

3.1.1 General technical equipment and devices

Analytical balance	Sartorius (Göttingen, Germany)
Agarose gel electrophoresis system	Bio-Rad Laboratories (Munich, Germany)
Blotting chamber	Invitrogen (Karlsruhe, Germany)
Centrifuge for Eppendorf tubes Biofuge	Eppendorf (Hamburg, Germany)
Centrifuge	Heraeus (Hanau, Germany)
CO_2 Incubator	Kendro (Langenselbold, Germany)
Confocal microscope	Leica (Solms, Germany)
Electrophoresis Powersupply	Gibco BRL (Eggenstein, Germany)
Geltray DNA gel	Bio-Rad Laboratories (Munich, Germany)
Gene Pulser system	Bio-Rad Laboratories (Munich, Germany)
Ice mashine	Scotsman Ice Systems (IL, USA)
Laminar Flow	Heraeus (Hanau, Germany)
Light microscope	Leica (Solms, Germany)
Luminometer Lumat LB9507	Berthold (Freiburg, Germany)
Magnetic stirrer	Heraeus (Hanau, Germany)
Microlitre pipettes	Eppendorf (Hamburg, Germany)
Microwave	Sharp (Hamburg, Germany)

Molecular Imaging System ChemiDoc	Bio-Rad Laboratories (Munich, Germany)
Microplate reader Tecan	Tecan (Crailsheim, Germany)
Neubauer hemacytometer	Hecht (Sondheim, Germany)
Pasteur pipettes	WU (Bamberg, Germany)
PCR mashine	Bio-Rad Laboratories (Munich, Germany)
pH electrode	WTW (Weilheim, Germany)
pH meter	WTW (Weilheim, Germany)
PipetBoy	Integra Instruments (Hamburg, Germany)
Real-time PCR	Stratagene (Waldbronn, Germany)
Refrigerator	Liebherr (Ochsenhausen, Germany)
SDS-Page Mini Protean 3 Cell gel chambers	Bio-Rad Laboratories (Munich, Germany)
Thermomixer	Eppendorf (Hamburg, Germany)
Ultra low temperature freezer	New Brunswick Scientific GmbH (Nürtingen, Germany)
UV-Table	iNTAS (Göttingen, Germany)
Vacuum pump	Vacuubrand GmbH & Co KG (Wertheim, Germany)
Vortex	Heidolph (Kelheim, Germany)
Water-purification system Milli-Q	Millipore (Eschwege, Germany)
Waterbath with termostat	VWR (Bruchsal, Germany)

3.1.2 Disposable Material

Blotting paper	Whatman (Dassel, Germany)
Cell Culture T-flasks (25, 75, 175 cm^2)	Greiner GmbH (Frickenhausen, Germany)
Cover slides	R.Langenbrinck (Teningen, Germany)
Cryotubes	Greiner GmbH (Frickenhausen, Germany)
Microscope glass slides	R. Langenbrinck, Emmendingen
Nitrocellulose Transfer membrane	Whatman (Dassel, Germany)
One-way pipette (2-50ml)	Greiner GmbH (Frickenhausen, Germany)
Parafilm	American National Can (WI, USA)
Pasteur pipettes	Poulten & Graf (Wertheim, Germany)
PCR thin wall reaction tubes	Eppendorf (Hamburg, Germany)
Reaction tubes (1.5 and 2.0ml)	Eppendorf (Hamburg, Germany)
Pipette Tips (10-1000µl)	Eppendorf (Hamburg, Germany)
Pipette Filter Tips (10-1000µl)	Eppendorf (Hamburg, Germany)
Polypropylentubes (15 and 50ml)	Greiner GmbH (Frickenhausen, Germany)
Scalpel	Feather Safety Razor (Osaka, Japan)
Tissue Culture dishes (Ø10cm)	Greiner GmbH (Frickenhausen, Germany)
96-, 48-, 24-, 12-, and 6-well Plates	Greiner GmbH (Frickenhausen, Germany)
96-Well plates for UV measurement	Greiner GmbH (Frickenhausen, Germany)
96-Well plates for Fluorescence measurement	Greiner GmbH (Frickenhausen, Germany)

3.1.3 Chemicals

Acetic Acid	Sigma-Aldrich (Munich, Germany)
Acetone	Merck (Darmstadt, Germany)
Acrylamide/ bis-acrylamide, 30% solution	Serva (Heidelberg, Germany)
Agarose	Serva (Heidelberg, Germany)
Ammonium persulfate (APS)	Sigma-Aldrich (Munich, Germany)
Bacto-Agar	Life Technologies (Darmstadt, Germany)
Bromphenol blue, sodium salt	Baaklab (Schwerin, Germany)
Bovine serum albumin (BSA)	Merck (Darmstadt, Germany)
1M $CaCl_2$ solution	Sigma-Aldrich (Munich, Germany)
ρ-coumaric acid	Sigma-Aldrich (Munich, Germany)
DAPI	Roche (Mannheim, Germany)
Deoxycholic acid	Serva (Heidelberg, Germany)
Dimethyl sulfoxide (DMSO)	Sigma-Aldrich (Munich, Germany)
3-[4,5-dimethylthiazol-2-yl]-2,5-diphenyltetrazolium bromide (MTT)	Sigma-Aldrich (Munich, Germany)
Draq5	Alexis Biochemicals
EDTA, disodium salt	Merck (Darmstadt, Germany)
Ethanol 100%	Merck (Darmstadt, Germany)
Ethidium bromide (10mg/ml)	AppliChem (Darmstadt, Germany)
Fluorescein sodium salt	Promega (Mannheim, Germany)
G418 (Neomycin)	Sigma-Aldrich (Munich, Germany)

Glycerol	Sigma-Aldrich (Munich, Germany)
Glycin	Merck (Darmstadt, Germany)
Hydrogen peroxide solution 30 % (w/w) in H_2O	Sigma-Aldrich (Munich, Germany)
Isopropanol	Merck (Darmstadt, Germany)
Luminol (3-aminophtolhydrazide)	Sigma-Aldrich (Munich, Germany)
LY294002	Sigma-Aldrich (Munich, Germany)
β-Mercaptoethanol	AppliChem (Darmstadt, Germany)
Methanol	Merck (Darmstadt, Germany)
1M $MgCl_2$ solution	Sigma-Aldrich (Munich, Germany)
Mycophenolic acid (MPA)	Gift of S.Urban, University of Heidelberg
NaOH	Merck (Darmstadt, Germany)
Nonidet™ P40 substitute (NP-40)	Roche (Mannheim, Germany)
Paraformaldehyde (PFA)	Sigma-Aldrich (Munich, Germany)
PD98059	Sigma-Aldrich (Munich, Germany)
Phalloidin	Invitrogen (Karlsruhe, Germany)
Phosphatase Inhibitor Cocktail 2	Sigma-Aldrich (Munich, Germany)
Polybrene	Sigma-Aldrich (Munich, Germany)
Polyethylene glycol 8000	Sigma-Aldrich (Munich, Germany)
Ponceau S Red	Sigma-Aldrich (Munich, Germany)
Protease inhibitor, complete, EDTA-free	Roche (Mannheim, Germany)
SB203580	Sigma-Aldrich (Munich, Germany)

SB431542	Sigma-Aldrich (Munich, Germany)
Sodium dodecyl sulfate (SDS)	Roth (Karlsruhe, Germany)
SP600125	Sigma-Aldrich (Munich, Germany)
N,N,N',N'-tetramethylethylenediamine (TEMED)	Sigma-Aldrich (Munich, Germany)
Tris base	Roth (Karlsruhe, Germany)
Triton X-100	Sigma-Aldrich (Munich, Germany)
Trypan blue	Sigma-Aldrich (Munich, Germany)
Tween-20	Bio-Rad Laboratories (Munich, Germany)
U0126	Sigma-Aldrich (Munich, Germany)

3.1.4 Solutions and Buffers

4% PFA (w/v) (pH 7.4)	Heat 500 ml PBS to 80 ℃ + 4 % (w/v) Paraformaldehyde + 0.2mM 1M $CaCl_2$ stock solution + 0.2mM 1M $MgCl_2$ stock solution
ECL solution	10ml 0,1 M TRIS buffer (pH = 8,5) 50µl Luminol (250mM) 22µl ρ-coumaric acid (90mM) 3µl hydrogen peroxide solution 30 % (w/w) in H_2O
Cytomix	120mM KCl 0.15mM CaCl2 10mM potassium phosphate buffer (pH 7.6) 25mM Hepes (pH 7.6) 2mM EGTA 5mM MgCl2, pH 7.6 (KOH) freshly added: 2mM ATP (pH 7.6) 5mM glutathione
Luciferase assay buffer	25mM glycyl-glycin (pH 7.8) 15mM potassium phosphate buffer (pH 7.8) 15mM MgSO4 4mM EGTA freshly added: 1mM DTT and 2mM ATP

Luciferase lysis buffer	1 % (w/v) Triton X-100 25mM glycyl-glycin (pH 7.8) 15mM MgSO4 4mM EGTA freshly added: 1mM DTT
Renilla luciferase substrate solution	luciferase assay buffer without DTT and ATP freshly added: coelenterazine solution 1:700
MTT staining solution	PBS + 5mg/ml MTT
MTT stop solution	DMSO + 10% SDS + 0.6% acetic acid
DNA loading buffer	35% Glycerol 1x TAE buffer Spatula tip bromphenol blue
50x TAE buffer	242g Tris base 57.1ml Glacial Acetic Acid 18.6g EDTA, sodium salt Add 1l distilled H_2O
RIPA buffer	1.815g Tris base 4.383g NaCl 6ml Nonidet P40 0.279g EDTA, sodium salt 0.3g SDS 1.6g Deoxycholic acid, sodium salt Add 300ml distilled water, adjust to pH 7.2 pre-working solution: 50ml RIPA + 1tablet of Complete Protease Inhibitor →aliquot it to 5ml working solution: 5ml RIPA (with Complete) + 50µl Phosphatase Inhibitor Cocktail
10x TBS	12.1g Tris base 87.66g NaCl Add 1l distilled water, adjust to pH 7.6
TBST	1x TBS 10ml 10% Tween-20 Add 1l distilled water

10x Lämmli	144g Glycin (192 mM) 30.34g Tris base (125mM) 100ml 10% SDS Add 1l distilled water
5x Protein loading buffer	2,5ml β-Mercaptoethanol (12,5%) 2g SDS (10%) 10mg Brom Phenol Blue 6ml 1M Tris HCl pH6,8 (0,3M) 200µl 500mM EDTA (5mM) or 1ml of 100mM EDTA 10ml 99%Glycerin (50%) 1,3ml H_2O add 20ml distilled wáter
10x Transfer buffer	144g Glycine (192 mM) 60.72g Tris base (250 mM) Add 1l distilled water
1x Transfer buffer	100ml 10x Transfer buffer 200ml Methanol (20%) Add 1l distilled water
Blocking buffer	1% BSA (w/v) in PBS
Permeabilization buffer	0,3% (v/v) Triton-X 100 in PBS
Stripping buffer	0.2M NaOH

3.1.5 Reagent and Biological Kit

Biorad Protein Assay kit	Bio-Rad (munich, Germany)
Competent E.coli One Shot TOP 10	Invitrogen (Karlsruhe, Germany)
Dulbecco's Modified Eagle's Medium (DMEM) With high glucose, w/o L-glutamine	Lonza Group Ltd. (Cologne, Germany)
DNA Ladder	AppliChem (Darmstadt, Germany)
FastStart Polymerase	Roche (Mannheim, Germany)
Fetal Calf Serum (FCS)	Invitrogen (Darmstadt, Germany)
Fluorescent Mounting Medium	DakoCytomation (Hamburg, Germany)
Hank’s Buffered Salt Solution (HBSS)	PAA Laboratories (Cölbe, Germany)

Lipofectamine 2000	Invitrogen (Darmstadt, Germany)
L-glutamine 200mM	PAA Laboratories (Cölbe, Germany)
Mini-/ Maxi-Plasmid Extraction Kit	Qiagen (Hilden, Germany)
Opti-MEM® I reduced serum medium	Invitrogen (Karlsruhe, Germany)
Penicillin/streptomycin 10,000U/10,000µg/ml	PAA Laboratories (Cölbe, Germany)
Prestained Protein Ladder	Fermentas (St.Leon-Rot, Germany)
RNAiMax	Invitrogen (Karlsruhe, Germany)
Reporter Lysis buffer	Promega (Mannheim, Germany)
RNeasy Mini Kit	Qiagen (Hilden, Germany)
RNeasy QuantiTect Reverse Transcription Kit	Qiagen (Hilden, Germany)
TaqMan® Universal PCR Master Mix	Applied Biosystems (CA, USA)
10x Trypsin-EDTA	PAA Laboratories (Cölbe, Germany)
Venor®GeM Mycoplasma PCR Detection Kit	Minerva Biolabs (Berlin, Germany)

3.1.6 Media

Huh7 Growth Medium	DMEM + 10% FCS + 2mM Glutamine + 100U/ml resp. 100g/ml Penicillin/Streptomycin
HepG2/2.15 Growth Medium	William E medium + 10% heat-inactivated FCS + 2mM Glutamine + 100µM non-essential amino acids + 100U/ml resp. 100g/ml Penicillin/Streptomycin
PHH1 Medium	William E medium + 25mM hydrocortisone + 2.5µg of insulin/ml + 2mM glutamine + 10% FCS + 2% dimethyl sulfoxide

PHH2 Medium	William E medium + 25mM hydrocortisone + 2.5µg of insulin/ml + 2mM glutamine + 0.5% dimethyl sulfoxide
LB Medium	1% (w/v) NaCl 1% (w/v) Yeast extract 0.5% (w/v) Trypton
LB agar	1.5% Bacto-agar in LB medium (autoclave and add antibiotics)

3.1.7 Cells

HepG2

HepG2 cells were derived from a 15-year-old white male from Argentina with differentiated hepatocellular carcinoma by the group of Aden et al. in 1979. HepG2 cells are epithelial-like and grow as monolayers and in small aggregates [128]. HepG2 cells are completely resistant to TGF-β-induced apoptosis [129].

HepG2.2.15

HepG2.2.15 cells were derived from HepG2 cells by Sells et al. in 1987. HepG2 cells were stably transfected with a plasmid carrying the gene that confers resistance to G418 and four 5'-3' tandem copies of the HBV genome. HepG2.2.15 cells support the assembly and of the replicative intermediates of HBV DNA and of Dane-like particles [67]. It should be noted that the transfection of HepG2 cells to create HepG2.2.15 cells occurred when HepG2 cells were already transformed and thus may not directly reflect the development of HCC in hepatocytes that have been naturally infected with HBV [130]. All experiments with these cells were performed in the S2 laboratories of S.Urban (Department of Virology, University of Heidelberg) due to safety issues.

Huh7

Huh7 cells were derived from a 57-year-old Japanese male with a well differentiated hepatocellular carcinoma by the group of Nakabayashi et al. in 1982. Huh7 cells are epithelial-like and grow in monolayers [131]. Huh7 cells are sensitive to TGF-β-induced apoptosis [47] [132].

Huh7.5

Huh7.5 cells were derived from Huh7 cells by Blight et al. in 2002. Huh7 cells transfected with subgenomic HCV replicons were cured of HCV RNA by prolonged treatment with IFN-α. Cured Huh7 cells were electroporated with subgenomic RNA replicons and selected by G418, resulting in the Huh7.5 cell line, which is highly permissive for HCV replication [133]. All experiments with these cells were performed by Daniel Rupp in the S3 laboratories of R.Bartenschlager (Department of Virology, University of Heidelberg) due to safety issues.

Primary human hepatocytes

Primary human hepatocytes from liver resections were obtained from patients undergoing partial hepatectomy. Experimental procedures were performed according to Human Tissue and Cell Research Foundation guidelines. Informed patient consent was approved by the Ethical Committee of the University of Munich (Munich, Germany). PHHs were isolated, as previously described [134] and seeded at 1×10^5 cells/cm^2 in 12-well plates. After arrival of PHHs, cells were put on PHH1 medium supplemented with 10% FCS and 2% dimethyl sulfoxide (DMSO), prior to infection with HBV. Experiments with HBV-infected PHHs were performed in the S2 laboratories of S.Urban (Department of Virology, University of Heidelberg) due to safety issues.

HEK293A

Human embryonic kidney cells which are transformed by sheared human adenovirus type 5 DNA. These cells are used as packaging system for the expansion of adenovirus and were obtained from Invitrogen (Karlsruhe, Germany).

3.1.8 Plasmids

HCV core

pBICEP-CMV-2 (bicistronic expression vector used for stable transfection from Sigma-Aldrich, Munich, Germany) plasmid encoding HCV core protein isolated from tumor liver tissue of a patient with HCV-related HCC (kindly provided by S.Battaglia, Inserm, Unite´ 785, Villejuif, France).

β-Gal plasmid

β-galactosidase expression vector (pCR3lacZ) (Invitrogen, Karlsruhe, Germany).

CAGA reporter plasmid

pGL3 basic plasmid (Promega, Mannheim) encoding 9 repetitions of the CAGA sequence (Smad-binding-sites SBE from the PAI-I promoter) in the promoter region of a firefly luciferase [135].

Smad7 promoter reporter plasmid (-1280)

pGL3-Basic Vector encoding a firefly luciferase under control of the mouse Smad7 promoter (region -1276 to +41) [136].

HCV viral construct pFK-RLuc-2A-core-Jc1 (JcR-2A)

monocistronic full length reporter virus; RLuc is fused in-frame to the N-terminal 16 aa of the core protein with the foot-and-mouth disease virus (FMDV) 2A peptide to trigger proteolytic removal between the luciferase and the following complete Jc1 open reading frame

3.1.9 Polyacrylamide gels

Compounds for 2 mini gels	4% stacking gel	10% resolving gel
30% Acrylamide	0.83ml	6.7ml
Tris pH 8.8	-	5ml
Tris pH 6.8	0.63ml	-
10% SDS	50µl	200µl
H_2O	3.4ml	7.9ml
10% APS	50µl	200µl
TEMED	5µl	8µl

3.1.10 Primer

TaqMan® Real Time PCR

TGF-β1 (Hs00171257_m1)	Applied Biosystems (CA, USA)
rS18 (Hs03003631_g1	Applied Biosystems (CA, USA)

Conventional PCR

Protein (product size bp)	Sequence 5' → 3'
p15 (299/422 bp)	For: TTTCGGGAGGCGCGCGAT Rev: GCTGGGGAACCTGGCGTCAG
GADD45β (290bp)	For: AGGATCGCCTCACAGTGG Rev: CCGCACGATGTTGATGTC
HCV core (264bp)	For: TTACCTGTTGCCGCGCAGGG Rev: GACCTACGCCGGGGGTCAGT
Bim (130bp)	For: TAAGTTCTGAGTGTGACCGAGA Rev: GCTCTGTCTGTAGGGAGGTAGG
c-myc (381bp)	For: AGCAGCTCGAATTTCTTCCA Rev: GAAACTTTGCCCATAGCAGC
β2MG (290bp)	For: CTCACGTCATCCAGCAGAGA Rev: CAAACCTCCATGATGCTGC

3.1.11 Antibodies

Akt (#9272)	Cell Signaling (Frankfurt, Germany)
Bcl-2 (#2870)	Cell Signaling (Frankfurt, Germany)

Bcl-xL (#2764)	Cell Signaling (Frankfurt, Germany)
Cleaved PARP (#9542)	Cell Signaling (Frankfurt, Germany)
CTGF (#14939)	Santa Cruz (Heidelberg, Germany)
E-Cadherin (#610181)	BD Bioscience (Heidelberg, Germany)
hepatitis B core antigen (HBcAg)-specific polyclonal antibody (H363)	kind gift from S.Urban, Department of Virology, University of Heidelberg, Germany
p21 (#P1484)	Sigma-Aldrich (Munich, Germany)
p38 (#9212)	Cell Signaling (Frankfurt, Germany)
Phospho-p38 (#4631S)	Cell Signaling (Frankfurt, Germany)
Phospho-Akt (#4060P)	Cell Signaling (Frankfurt, Germany)
Phospho-c-jun (#9261S)	Cell Signaling (Frankfurt, Germany)
pErk (#7383)	Santa Cruz (Heidelberg, Germany)
Phospho-Smad1/3 (#1880-1)	Epitomics/ Biomol
Phospho-Smad2 (#3101)	Cell Signaling (Frankfurt, Germany)
Smad3 (#51-1500)	Invitrogen (Karlsruhe, Germany)
Smad7 (#11392)	Santa Cruz (Heidelberg, Germany)
Tubulin (#4074-100)	Abcam (Cambridge, UK)
Vimentin (#20346)	Abcam (Cambridge, UK)
ZO-I (#40-2200)	Invitrogen (Karlsruhe, Germany)
goat anti-rabbit IgG-HRP	Santa Cruz (Heidelberg, Germany)
goat anti-mouse IgG-HRP	Santa Cruz (Heidelberg, Germany)

donkey anti-goat IgG-HRP	Santa Cruz (Heidelberg, Germany)
AlexaFluor 488 (green), 555 (red), 633 (far red) 2' AB	Invitrogen (Karlsruhe, Germany)

3.1.12 Adeno-/ Lentivirus

AdLacZ	Adenovirus expressing bacterial β-galactosidase under the control of a CMV promoter (kindly provided by C.H.Heldin, Department of Medical Sciences, Clinical Chemistry, Uppsala, Sweden)
AdSmad7	Adenovirus encoding human Smad7 cDNA fused with the Flag epitope sequence under the control of a CMV promoter (kindly provided by C.H.Heldin, Department of Medical Sciences, Clinical Chemistry, Uppsala, Sweden)
AdSmad3	Adenovirus encoding human Smad3 cDNA fused with the Flag epitope sequence under the control of a CMV promoter (kindly provided by C.H.Heldin, Department of Medical Sciences, Clinical Chemistry, Uppsala, Sweden)
Leshp38	Lentivirus expressing shRNA targeting sequences in the MAPK p38 (kindly provided by S.Urban, Department of Virology, University of Heidelberg, Germany)
Leshcontr-1	Lentivirus expressing shRNA predesigned from Dharmacon, containing at least four mismatches to all known human genes (kindly provided by S.Urban, Department of Virology, University of Heidelberg, Germany)

3.1.13 Cytokines

Human recombinant TGF-β1	Peprotech (Hamburg, Germany)

3.1.14 siRNA

Smad3 siRNA	Qiagen (Hilden, Germany)
Control siRNA	Qiagen (Hilden, Germany)
p38 MAPK shRNA	5`-GGAAUUCAAUGAUGUGUAUUU-3
Control shRNA	Dharmacon (Waltham, USA)

3.2 Methods

3.2.1 Cell Culture

Maintenance of Cells

For maintenance of cell lines, cells were grown at 37℃ and 5% CO_2 in a humid atmosphere in T-flasks containing DMEM growth medium until cells reached a confluence of about 80%. In order to adjust the media prior usage, growth medium was adapted to 37℃. Medium was removed from the cells and cells were washed with room tempered HBSS, in order to remove left medium, which may negatively influence the effect of subsequent trypsinization. After washing, Trypsin/EDTA (1x) solution was added to the cells and the flask was put back into the incubator. The Trypsin/EDTA is needed to disrupt the Ca^{2+}-dependent cell-cell-contacts and to obtain a single cell suspension. The enzymatic reaction was stopped when cells detached by adding medium containing 10% FCS. Corresponding to a seeding density of around 30%, part of the cell suspension was plated out in a T-flask and placed back into the incubator. Every 3-4 days, conditioned medium was replaced by fresh room tempered growth medium until cells reached 80% confluence.

Determination of Cell Number

For experiments which require a defined cell number, cells were counted by means of a Neubauer hemacytometer. Therefore, cells were trypsinized and cell suspension was collected in a Falcon tube. Then, 20µl of this suspension were mixed with 20µl of 0.05% trypan blue in PBS (ratio 1:2). 10µl of this suspension were filled into each side of the

Neubauer hemacytometer and the viable unstained cells were counted immediately under the microscope. Cells were counted by the following calculation:

Viable cell count / number of squares * dilution factor * 10^4 = viable cells/ ml

Cell Harvest and Lysis

For cell harvest culture dishes were plated on ice. The medium was removed and the cells were washed with cold HBSS. An appropriate volume of RIPA cell lysis buffer was added onto the wells and the culture dish was frozen immediately at -80℃ for 1h in order to break cell walls. Subsequently, cell suspension was scraped and collected in a 1.5ml Eppendorf tube. Cell debris were pelleted by centrifugation for 10min at 13,000rpm and 4℃ in a biofuge. Supernatant was tra nsferred into a new Eppendorf tube and stored at -80℃ until usage.

Thawing of Cells

The vial containing the cryopreserved cells was placed into a 37℃ waterbath and rotated gently until the content was completely thawed. Immediately, cells were transferred into a T-flask with growth medium in a seeding density of 5500 cells/cm^2 and placed into the incubator at 37℃ and 5% CO_2. After 4h of cultivation, cells had attached to the Bottom of the T-flask. Conditioned medium was replaced by fresh growth medium to remove the residual DMSO and unattached cells. The medium was then changed every 3-4 days thereafter, until the culture was approximately 80% confluent and subculturing of the cells had to take place.

Freezing of Cells

Cells were frozen in a concentration of $1x10^6$ cells/ml. Briefly cells were suspended in freezing medium and transferred into a cryotube, which was placed into the ultra-low freezer at -80℃ in an isopropanol-freezer-box. The next day, cryotubes were put into liquid nitrogen for infinite storage.

Kill Curve

For determination of the appropriate amount of antibiotic G418, which leads to cell death, the cells were plated on a 12-well plate (70% confluence) in 1ml medium one day prior to antibiotic treatment. The next day, cells were treated with different

concentrations of G418 (0 - 1000µg/ml). After 2 days, cells were regarded under the microscope and number of dead cells in comparison to viable cells was estimated roughly. Subsequently, fresh medium was applied to the cells with appropriate concentration of selective antibiotic and plates were incubated again for 2 days until second estimation of cell numbers could be performed. This was repeated, until lowest concentration of G418 was determined which results in death of all cells.

Transduction of Cells

For transduction, cells were plated in 12-well plates in a seeding density appropriate to the duration of the corresponding experiment in growth medium. Transduction took place the next day. Adenovirus was added in a concentration of 50ifu/cell and incubated for 2h. For transduction with Lentivirus, cells were incubated with virus particles in the presence of polybrene (8µg/ml) for 24h. After incubation, cells were washed with HBSS once and starvation medium was added. Proper overexpression/ downregulation of the protein was proven after 2-3 days cultivation.

Transfection of Cells

For transient transfection of Cell lines with 10nM/24-well siRNA or 1µg/24-well plasmid DNA, respectively, cells were plated with the appropriate cell number in growth medium w/o antibiotics one day before transfection. The transfection was carried out as follows: siRNA or plasmid DNA was mixed with Opti-MEM® I reduced-serum medium in a concentration according to the manufacturers' protocol. Then RNAiMax or Lipofectamine 2000, respectively, was added at an amount to obtain a suitable ratio of siRNA or plasmid DNA to transfection reagent (e.g. 2:6, 2:8), mixed and incubated for 20min at room temperature. The medium of the cells was exchanged for fresh medium containing no FCS and no antibiotics. The transfection mix was added dropwise to the cells and swayed gently to disperse the mixture. Six hours after transfection the medium was replaced again. In case of plasmid DNA transfection, Transfection efficiency was checked by cotransfection of ß-Gal plasmid via expression of ß-galactosidase under control of a CMV promoter. For investigation of proper transfection of siRNA, cells were harvested 72 hours after transfection and silencing of the respective gene product was detected by means of western blot analysis.

Selection of stably transfected cells

At 48hrs after transfection of cells with the plasmid of interest containing a resistance gene against neomycin, cells were put on medium containing 400µg/ml neomycin. Medium was changed every 2-3 days and selection was performed for at least 21 days.

HBV Infection of PHHs

HBV infection of PHHs was done in 12-well plates. PHHs were kept in PHH1 medium. Inoculation was with 500µl of medium containing 4% PEG 8000 and 10µl of the concentrated HBV virus stock for 16 hours at 37℃. The next day, PHHs were washed 3 times with PBS and further cultivated for 8 days with PHH-2 medium (Figure 3.1). Medium was refreshed every second day.

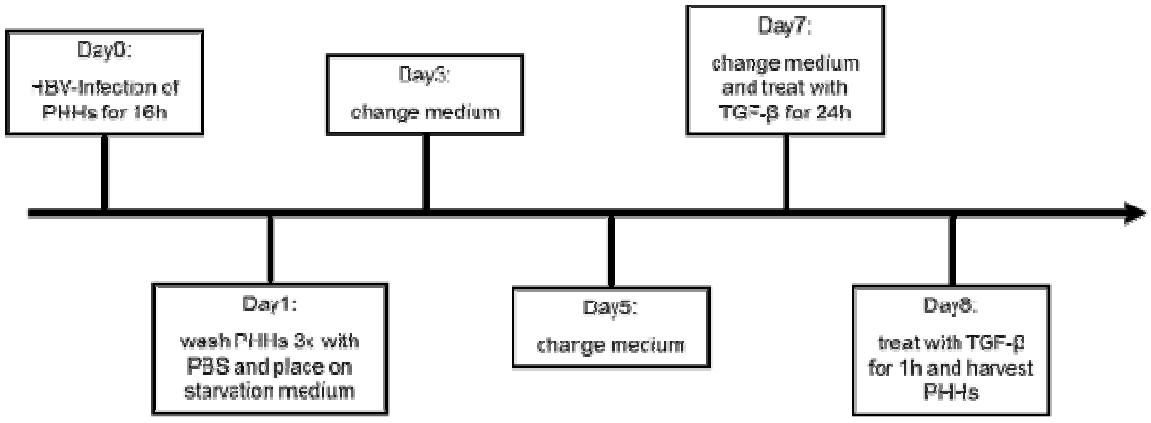

Figure 3.1: Experimental setup of HBV infection of PHHs with subsequent TGF-β treatment (5ng/ml). Immediately upon receipt of PHHs, cells were infected with HBV for 16hrs. The next day, cells were washed with PBS and cultivated for 8 days. Medium was refreshed every second day and samples of the supernatant for HBsAg and HBeAg measurements were taken. TGF-β treatment for 24hrs was performed on day 7, treatment for 1h on day 8 until all samples were harvested. The experiments were performed three times independently, each experiment with PHHs of another donor. RNA was isolated and subjected to microarray analysis at the core facility of the Medical Faculty Mannheim, University Heidelberg.

Electroporation of Huh7.5 cells with HCV RNA

Cells were washed once with PBS, trypsinized and sheared by pipetting up and down through a 1,000µl tip to get single-cell suspensions. After washing once with DMEM complete (5min at 700 rpm) and once with 50ml PBS (5min at 700 rpm) Huh7.5 cells were resuspended at 1.5 x 10^7 cells per ml in Cytomix. 10µg of in vitro transcribed RNA

were mixed with 400µl cell suspension and electroporated in a cuvette with a gap width of 0.4cm (Bio-Rad) at 975µF and 270V. Cells were immediately transferred to 19ml DMEM complete and plated with 2ml per 6-Well. After 16h electroporation complete DMEM was exchanged by serum-free DMEM. The next day, cells were treated with 5ng/ml TGF-β for 0, 1, and 24h. Then cells were harvested for Luciferase Assay to determine viral replication and for Western Blot analysis and RNA extraction, respectively.

Immunofluorescence

The expression of several cell markers was proven by immunofluorescence staining. Therefore, cells were grown on cover slips in 12-well plates. Medium was aspirated and washed with PBS. Fixation of cells was performed with 4% PFA for 20min at room temperature with subsequent treatment by 0.3% Triton X-100 for 5min. Afterwards, cells were blocked using 1% BSA in PBS for 1h to inhibit unspecific binding of the primary antibody. Incubation with first antibody diluted in 0.2% BSA in PBS was performed in the dark overnight at 4℃. The next day, cover slips we re washed 3 times with PBS and subsequently incubated with a mixture of secondary antibody (1:300 in 0.2% BSA in PBS) and Draq5 (1:5000) for 1h in the dark at room temperature. Afterwards, cover slips were washed with PBS (3 times) and placed up-side-down into mounting medium on an object slide. Slides were dried and stored in the dark at 4℃ until microscopy.

Immunofluorescence analyses of HBcAg expression in infected cells.

At 8 days post-infection, HBV-infected PHHs were washed with PBS, fixed with 4% paraformaldehyde for 20min, and treated with permeabilization buffer for 30min.Afterwards, cells were washed and HBcAg-specific polyclonal antibody H363 was added (1:1,000 dilution in PBS containing 5% skim milk powder). After 2h of incubation at 4℃, the cells were washed 3-times and incubated in the dark for 1h at room temperature with 1:500-diluted Alexa Fluor 488-conjugated secondary mouse anti-rabbit antibody in PBS containing 5% skim milk powder. Cells were washed 3-times with PBS, incubated for 30min with 1µg DAPI and finally washed again 3-times with PBS. Images were acquired by means of confocal microscopy.

Phalloidin staining

The formation of stress fibers was studied by Phalloidin staining. Therefore, cells were grown on cover slips in 12-well plates. Medium was aspirated and washed with PBS. Fixation of cells was performed with 4% PFA for 20min at room temperature with subsequent treatment by 0.3% Triton X-100 for 5min. Phalloidin was diluted 1:400 concomitant with Draq5 (1:5000) in blocking buffer. The mixture was added onto the cover slips and incubated for 1h at room temperature in the dark. Afterwards, cover slips were washed with PBS 5min (3 times) and placed up-side-down into mounting medium on an object slide. Slides were dried and stored in the dark at 4℃ until microscopy.

Renilla-Luciferase assay

Quantification of luciferase reporter activity (Renilla-Luciferase) was used to determine transient HCV RNA replication of the full-length virus construct JCR2a. Infected cells were harvested at the appropriate time points (see individual experiment description) by washing once with PBS and addition of ice-cold luciferase lysis buffer (350µl per 6-well, 200µl per 12-well and 100µl per 24-well). Cells were frozen immediately and after thawing lysates were resuspended by pipetting.

For measurement of cells out of 6-wells 100µl lysate were mixed with 360µl Renilla-Luciferase substrate solution and measured for 10 sec in a luminometer.

Promoter Reporter Assay

For promoter reporter assays, cells were seeded in 24-well plates with an appropriate cell concentration. Cells were transfected (as described above) with plasmid containing the promoter of interest followed by the luciferase gene. 24h post-transfection, cells were treated with the substance of interest and incubated for another 24h. Then, cells were washed with PBS and 50µl of 2x Reporter Lysis Buffer was added to the wells. The plate was frozen at -80℃ in order to disrupt cells. Afterwards, 20µl of cell lysate was transferred into a white 96-well plate and 50µl of Luciferase Assay Reagent was added. Luminescence was measured immediately in a microplate reader.

β-Gal assay

For measurement of β-Gal expression as e.g. an indicator for transfection efficiencies, cells were seeded in 24-well plates with an appropriate cell concentration. Cells were

transfected (as described above) with plasmid containing the LacZ gene. β-Gal Assay was performed using the β-Galactosidase Assay Kit from Promega according to the manufacturers protocol with slight modifications. Briefly, 48-72h post-transfection, wells were washed with PBS and 50µl of 2x Reporter Lysis Buffer was added to the wells. The plate was frozen at -80°C in order to disrupt cells. Afterwards, 20µl of cell lysate was transferred into a transparent 96-well plate and 20µl of Assay 2x Buffer was added. The plate was covered and incubated for 30min at 37°C until a yellow color had developed. The reaction was stopped by adding 60µl of 1M Sodium Carbonate and absorbance was measured at 420nm in a microplate reader.

MTT Assay

For proliferation studies of cells, cells were seeded in 24-well plates with a seeding density of 5,000 cells/ well. After cell attachment, medium was changed to starvation medium w/o FCS and incubated overnight (37°C, 5% CO_2). The next day, cells were treated with TGF-β for 48h. Then, 5mg/ml MTT solution was added to each well (final concentration 500µg/ml) and incubated for 4h, to allow metabolization of yellow MTT to purple formazan. MTT is a pale yellow colored substance, which is converted into a blue formazan crystal by a dehydrogenase enzyme located in the mitochondrion of viable cells. The blue formazan crystals accumulate within the cells and its amount can be quantified. Therefore, supernatant of each well was removed carefully without disrupting cells and MTT solvent was added to resolve formazan crystals. The plate was shaken in the dark for 2h at room temperature till measurement of absorbance at a wavelength of 560nm against a reference wavelength of over 650nm. MTT solvent was used as negative control.

LDH Assay

Upon cell death, triggered by necrosis or apoptosis, cell membrane becomes permeable which leads to release of lactate dehydrogenase into the supernatant. This enzyme converts lactate into pyruvate thereby converting NAD^+ into $NADH+H^+$. The LDH assay utilizes the $NADH+H^+$ for conversion of tetrazolium into formazan. Formazan is measured photometrically allowing conclusion on LDH activity and in turn on cell death rate.

Cells were seeded in 96-well plates (100µl) and starved overnight until treatment with TGF-β (5ng/ml) for at least 24h. At the end of the experiment, 50µl of the supernatant

was transferred into a transparent 96-well plate and mixed with 50µl reagent from the Cytotoxicity Detection Kit from Roche. The plate was incubated in the dark and measured with a Tecan reader at 490nm. For determination of relative cell death rate, LDH release in the supernatant was measured only. For determination of absolute cell death rate, remaining viable cells of the control well were lysed in 100µl Triton X-100 (1%). Fifty µl of this cell lysate were transferred and measured as well.

LDH (supernatant) / (LDH (supernatant) + LDH (lysed cells)) * 100 = absolute cell death (%)

The reagent of the Cytotoxicity Detection Kit was mixed immediately prior to usage, composed of catalyst and dye solution in a ration 1:45. 1% Triton X-100 and medium served as negative control.

Migration Assay

Effects of TGF-β on cell migration were determined by means of Transwell assays. Therefore, cells were grown on Ø10cm dishes one day prior in medium containing 1% BSA. The next day, cells were trypsinized and centrifuged (5min, 500g) and resuspended in 1 or 2ml medium (1% BSA) and counted. The frame wells of the Transwell Assay plate were filled with PBS (1.5ml) to prevent dehydration effects. For the lower wells (750µl/well) medium (1%BSA) was prepared containing either PBS (control) or 5ng/ml TGF-β. Then, transwells were placed into the wells. For the upper wells, 25,000 cells/well in medium (1% BSA) were suspended and PBS or TGF-β was added. The plate was incubated for 24h. The next day, cells of the upper and the lower wells were collected carefully by trypsinization in 200µl and transferred into a white 96-well plate. The plate was centrifuged (10min, 10,000rpm) and supernatant was discarded. ATP solution (40µl) was added to the cells and luminescence was measured.

3.2.2 Microbiological Methods

Transformation of bacteria

In order to amplify plasmid DNA, competent bacteria were transformed with the plasmid of interest. Therefore, 1µg purified plasmid DNA was added to the transformation mix. The procedure was then performed as described in the manual provided by the

manufacturer (Invitrogen). Briefly, after incubation of the transformation mix for 30min on ice, heat-shock was performed for 40sec at 42℃. After another 3min on ice the transformation mix was incubated with S.O.C medium for 1h at 37℃ in a shaker at 220rpm. Then 50µl of bacterial suspension was plated on agar plates consisting of 1% bacto-agar, LB-Medium and the appropriate antibiotic. The added antibiotic allowed only such bacteria to grow, which had taken up the plasmid of interest containing the resistence gene. The plates were then incubated at 37℃ for at least 16h, but not longer than 20h, in order to obtain single colonies. Individual colonies were then picked for subsequent bacterial culture.

Bacterial culture of transformed bacteria

To obtain the plasmid DNA in an adequate amount, a single colony was picked from a plate to inoculate LB-Medium containing the appropriate selective antibiotic. For subsequent miniprep, 5ml of LB-Medium was inoculated. For maxiprep 200ml LB-medium were inoculated with 100µl of the 5ml culture used for miniprep. The culture was then incubated in a bacteria shaker for 20h at 37℃ and 220rpm.

Plasmid DNA extraction (mini-/maxiprep) from bacteria

For miniprep 1ml bacteria culture was transferred into a 1.5ml-Eppendorf tube and centrifuged for 5min at 4000 rpm in a biofuge. The supernatant was discarded and plasmid DNA was extracted from the bacteria pellet as described in the Qiagen miniprep manual. This method is based on adsorption of the DNA to a matrix. For maxiprep 200ml of bacterial culture were centrifuged for 5min at 6000rpm and then DNA extraction was performed as described in the manual.

The concentration of purified DNA was determined by optical density (OD) measurement. For this, the samples were diluted 1:20 in Millipore water and measured at wavelengths of 260nm and 280nm by means of a UV spectrophotometer against H_2O as a blank. Thereby, 50ng/µl of double stranded DNA correspond to one unit of absorbance at 260nm (OD_{260}=1). By the means of the formula

$$\text{DNA } (\mu g/ml) = OD_{260nm} \times \text{dilution factor} \times 50$$

The DNA concentration was calculated using the software of the spectrophotometer.

3.2.3 Biochemical Methods

Determination of Protein Concentration

The determination of the protein concentration was performed in a 96-well plate by using the DC Protein Assay Kit® from Bio-Rad which is based on the Lowry method. For each sample triplicates were performed. The assay was carried out as follows: 20µl reagent A' (freshly made from 1ml reagent A and 20µl reagent S) and 200µl reagent b were added to 2µl of the sample and incubated for 15min at room temperature. A standard curve made out of bovine serum albumin (BSA) solutions in the same buffer with known concentrations (0, 1, 2, 4, 8, and 10mg/ml) served as reference. The OD at 690nm was measured using Tecan multiplate reader and protein concentrations in the samples were calculated by the according software.

3.2.4 Immunoblot Analysis

SDS polyacrylamide gel electrophoresis (SDS-PAGE)

The samples with cell lysates were mixed with Lämmli loading buffer (5x). Denaturation of proteins with this buffer leads to a negative charge of proteins, which allows separation by electrophoresis. A defined amount of protein (e.g. 30µg) in 20µl lysis buffer was mixed with 5µl 5x Lämmli loading buffer and heated for 5min at 95℃. The samples were then ready for loading on a gel, or were stored at -20℃ in the freezer until used. Then the polyacrylamide gel consisting of the resolving gel and the stacking gel was prepared (Sambrook and Russel). First, the compounds needed for the resolving gel were mixed. APS and TEMED were added last shortly before casting the gel into the chamber, because the two components initiate polymerisation within a few minutes. Immediately after casting the resolving gel, it was covered with isopropanol in order get rid of bubbles and to produce a smooth layer. After 15min the polymerization was completed and the isopropanol was washed off well with MilliQ water. Water remaining on the gel was removed with Whatman-paper without touching or disrupting the gel. Afterwards, the compounds for the stacking gel were mixed and APS and TEMED were added finally. A comb generating either 15 or 10 pockets was introduced into the stacking gel and the gel was allowed to polymerize for at least 30min. After polymerization the comb was taken out of the chamber and the pockets formed were

rinsed with MilliQ water in order to remove remaining acrylamide. The chamber was then placed into the electrophoresis system and filled with electrophoresis running buffer. The initial current was 50V in order to concentrate the probes at the border of the resolving gel. Once they entered the resolving gel, voltage was increased to 110V. The run of the gel was finished when the pre-stained protein marker was well separated and the loading dye reached the bottom of the gel.

Blotting

Immediately after terminating gel electrophoresis, the transfer of the separated proteins onto a protein-binding membrane made out of nitrocellulose occurred. Proteins transfer from the negative pole to the positive pole according to the charge of the proteins. Therefore, the gel was placed on 3 sheets of Whatman-paper in the sandwich cassette and the membrane was placed on top of the gel and covered with at least 3 sheets of Whatman-paper. It was important not to trap air bubbles between the membrane and the gel, as this would result in a diminished protein transfer. The stack of gel, membrane and Whatman-paper was placed into the blotting chamber filled with transfer buffer and run at 180mA for 3h. After blotting the membrane was washed 3× for 5min with TBST and was ready for further treatments.

Incubation with antibodies

The membrane was incubated for 30min in 5% milk in order to block unspecific binding sites of the antibodies. Afterwards, the membrane was washed 3× for 5min with TBST and was then incubated with the primary antibody o/n at 4℃. The next day the membrane was washed 3× for 5min with TBST and incubated for 1h at room temperature with a secondary antibody. Thereafter the membrane was washed 3× for 15min with TBST and the immunoreactive bands were detected by means of the ECL solution and an Immunoblot Imaging System.

Stripping of membranes

If another protein had to be detected on the same membrane, it was necessary to remove the bound antibodies and ECL solution. Therefore, the membrane was washed with ddH_2O and stripped with 0.2M NaOH for 5min. Subsequently, the membrane was washed again withddH_2O, followed by TBST. Then the membrane was ready for incubation with another antibody.

3.2.5 Molecular Biological Methods

Production, purification, and quantification of HBV particles

HBV particles were provided by the lab of Prof Urban, Molecular Virology, University of Heidelberg. Production of HBV virus was performed as described previously [137]. Briefly, Medium of HepG2.2.15 or HepAD38 cells was collected between days 3 and 8. Precipitation of viral particles from cell culture supernatants was performed overnight at 4℃ with 6% polyethylene glycol 8000 (PEG 8000; Sig ma) and concentrated by centrifugation (12,000 × *g*, 60 min, 4℃). After suspension in 1/100 of the vo lume of PBS-10% fetal calf serum (FCS), the particle composition and the viron concentration were quantified by analytical cesium chloride density gradient centrifugation and DNA dot blot analysis [138]. Aliquots were stored at -80℃.

Adenovirus preparation and quantification

For amplification of human recombinant E1-deleted adenoviral vectors, HEK293A cells were grown in T175-flasks until 80% confluence. Cells were infected with 3x10*6 ifu and further cultivated for 3-4 days until cells had started to detach and die. This cytopathic effect is due to the production of adenovirus. To harvest the adenovirus, medium was aspirated and 5ml PBS was put on the cells. The falsk was frozen and thawed 3-times to break cells and release adenovirus. Finally, the supernatant was centrifuged to get rid of cell debris and 1ml aliquots were frozen at -80℃ u ntil usage.

Lentivirus preparation and quantification

Lentivirus preparation was previously reported (Hepatology, 2012, 56, 9-16). In brief, shRNA, targeting p38 MAPK was subcloned into LeGO-G lentiviral vectors. Cell-free viral supernatants were generated by transient transfection of HEK293T packaging cells using the third generation packaging plasmids pMDLg, pRSV-Rev, and the envelope plasmid pVSV-G.

In vitro transcription

For production of in vitro transcripts of the individual constructs first 10µg of the respective plasmid DNA had to be linearized to prepare “run off” transcripts of the correct length. Constructs carrying the genomic ribozyme of hepatitis δ (δg) downstream

of the 5"-end of the RNA were additionally digested with MluI, which cuts directly after the ribozyme sequence, in a reaction volume of 100µl. For purification, plasmid DNA was mixed with 20µl 3M sodium acetate (pH 6.0) in a total volume of 200µl and extracted twice with 200µl TE saturated phenol and once with 200µl chloroform. At each step, the sample was first mixed with a vortex and then centrifuged (5min, 13,000rpm) for proper separation of the organic and aqueous phases and the upper aqueous phase was transferred to a new Eppendorf tube. To precipitate the DNA, 2.5vol 100% ethanol were added and the sample was left at -20°C for at least 30 min. After centrifugation for 20min at 13,000rpm at 4°C, the pellet was washed once with 200µl 70% ethanol (3min, 13,000rpm), air-dried briefly and dissolved in 60µl RNase-free H_2O.

For in vitro transcription, 20µl 5 x RRL transcription buffer, 12.5µl 25mM rNTPs, 2.5µl RNasin (40U/µl) and 4µl T7 RNA polymerase (19U/µl) were added to the purified DNA. After incubation for 2 h at 37°C, again 2 µl of T7 RNA polymerase were added, followed by 2h incubation at 37°C. Transcription was terminated by addition of 6µl of RNase-free DNase (1U/ml)) for 30min at 37°C. For purification of the RNA, 60µl 2M sodium acetate (pH4.5), 440µl H_2O and 400µl water-saturated phenol were added. The sample was mixed with a vortex, left on ice for 10min and centrifuged at 4°C for 10min at 13,000rpm. The supernatant was transferred to a new Eppendorf tube and extracted again with 1vol chloroform (vortex, 5min at 13,000rpm). RNA was subsequently precipitated with 0.7vol isopropanol (15min at 13,000rpm), washed once with 70% ethanol (3min at 13,000rpm) and dissolved in 50µl RNase-free H_2O. Agarose gel electrophoresis was used to check RNA integrity and the concentration was determined by measurement of the optical density at 260nm.

Mycoplasma Assay

The Venor GeM Mycoplasma Detection Kit was used for the detection of a mycoplasma contamination. Therefore, cells were grown until they had reached 100% confluence. Conditioned growth medium (500µl) was centrifuged for 5min at 1200rpm and supernatant (100µl) was heated for 5min at 95°C prior to a second centrifugation of 5sec at 13000rpm. For the following PCR, 2µl of the supernatant was used.

Cycles	Temperature (℃)	Time (sec)
1x	94	120
	94	30
39x	55	30
	72	30
	4	for ever

Mastermix:

Reagent	Amount (1×) (µl)
PCR grade H_2O	15.3
10× Reaction Buffer	2.5
Primer/Nucleotide Mix	2.5
Internal Control DNA	2.5
Polymerase (5U/µl)	0.2
Probe	2
Total volume	23

Photometrical Determination of Nucleic Acid Concentration

The concentration of purified DNA was determined by optical density (OD) measurement. For this, the samples were measured at wavelengths of 260nm and 280nm by means of a Tecan microplate reader against H_2O as a blank. Thereby, 50ng/µl of double stranded DNA correspond to one unit of absorbance at 260nm (OD_{260}=1). By the means of the formula

DNA (µg/ml) = OD_{260nm} × dilution factor × 50

The DNA concentration was calculated using Microsoft Excel.

RNA Extraction

In order to extract total RNA, medium was removed and the cells were rinsed with PBS. Cell lysis with subsequent RNA extraction was performed according to the RNeasy Mini Kit protocol from Qiagen. The concentration of RNA was measured as described above. RNA was considered to be of high purity if the ratio of the $OD_{260/280}$ was higher than 2. The samples were then stored at -80℃.

Synthesis of first strand DNA by reverse transcription

For the first strand DNA synthesis up to 1µg of each RNA sample was transcribed using the QuantiTect® Reverse Transcription Kit from Qiagen. In order to remove genomic DNA, 1µg RNA in 12µl H_2O was incubated with 2µl "genomic DNA wipeout" for 2min at 42℃. Then, the reaction mixture, set up as describ ed in the following table, was added and incubated for 1h at 42℃.

Reagent (conc.)	Amount (µl)
5x RT-Puffer [µl]	4
dNTP-Mix 5 mM each (0,5mM) [µl]	1
Polymerase [µl]	1
Template RNA 1µg in H_2O + genomic DNA wipeout	14
total ad 20µl H_2O [µl]	20

Polymerase chain reaction (PCR)

For amplification of cDNA, primers specific for the gene of interest were designed by means of the program Primer-BLAST from NCBI and ordered from Eurofins MWG Operon. Primers were diluted 1:10 and a mastermix was set up (see following table):

Reagent (conc.)	Amount (µl)
10x PCR Buffer [µl]	2
dNTP-Mix 10 mM each (200 µM) [µl]	0.4
Primer forward + reverse (0,2 µM)	1
H2O ad 20µl	14.5
FastStart (2,5 U / rct)	0.1
cDNA (max 20ng)	2

The PCR conditions were as follows:

Step	Temperature (℃)	Time (min)
1	95	3:00
2	94	0:45
3	51 - 74	1:00
4	72	1:00
5 go to step 2→ × (27-36)		
6	72	5:00
7	4	forever

Transcripts of a housekeeping gene, like of ß2MG, were quantified as an endogenous control. For the linear range of ß2MG amplification cycle number 28 was determined to be most suitable.

PCR products were loaded on a 1.5% agarose gel and evaluated under UV light. The results were quantified by densiometry using Image J (National Institutes of Health).

Quantitative real-time polymerase chain reaction

Expression levels of TGF-β were determined by means of Taqman Real Time PCR. Therefore, 2ng cDNA was used, however, for rS18 (housekepping gene) only 10pg were used. The final reaction volume was 20µl containing 10x TaqMan® Universal PCR Master Mix, 1µl gene specific Taqman probes, the appropriate amount of cDNA, filled up with ddH_2O. The PCR conditions were as followed: 10min, 95℃ → 40cycles 15s, 95℃ → 1min, 60℃.

The obtained results were evaluated by the corresponding software in order to subtract the background fluorescence signal and to obtain a baseline. The PCR cycle number at which fluorescence reaches a threshold value of 10 times the standard deviation of baseline emission is used for quantitative measurement. This cycle number is called the cycle threshold C(t) and its value is inversely proportional to the initial amount of target cDNA. Since both the amount of total RNA added to each reverse transcription reaction tube (based on wavelength absorbance) and its quality (i.e., degradation) are no reliable parameters to estimate the amount of the respective mRNA in the RNA preparation used for RT-PCR, transcripts of a housekeeping gene are quantified as an endogenous

control. A housekeeping gene is involved in basic functions needed for the maintenance of the cell. Housekeeping genes are constitutively expressed (they are always turned ON), and it is postulated that the expression is similar in all cells. The amplification efficiencies of target and reference genes have to be determined in advance, to ensure that primer binding sites differ only to a low extent. Quantification is then performed using the ddC(t) method. For each experimental sample, the C(t) value of the housekeeping gene is subtracted from the C(t) value of the gene of interest resulting in the dC(t) value. The dC(t) value of the sample of treated cells is then subtracted from the dC(t) value of the sample referring as control, e.g., untreated cells, resulting in the ddC(t) value. This ddC(t) value is then transformed by the equation Exp=2-ddC(t), leading to the decrease or increase of mRNA levels respective to the sample.

Agarose gel electrophoresis

For evaluation of amplified cDNAs, agarose gel electrophoresis was performed using a 1.5% agarose gel. For this, agarose was dissolved in TAE buffer by heating in the microwave. After dissolving the solution was cooled to ~60℃, Ethidiumbromide (10,000X) was added and the gel was cast in a tray with a comb. After gelling, the gel chamber was filled with TAE buffer and 20µl of PCR amplification mix was pipetted into the pockets. The gel chamber was then connected to a power supply and run at 100V for the appropriate time. Finally, the gel was photographed under UV light.

Measurement of HBsAg and HBeAg secretion

For quantification of expressed and secreted HBsAg and HBeAg, supernatants of infected PHHs were collected between days 3 and 7 and measured quantitatively (ARCHITECT, IU/mL; Abbott) at the core facility of the Universitätsklinikum Heidelberg, Analytical Laboratories. HBsAg levels were measured in IU/ml and HBeAg in relative light units (RLU).

3.2.6 Microarray analysis

Microarray Hybridization

RNA extraction was performed as described above using the RNeasy kit from Qiagen.
The 28S/18S ratios of total RNA samples were assessed with the Bioanalyzer 2100

(Agilent) to ensure that quality was comparable between samples. Of each sample, 150ng of total RNA were used to prepare cDNA according to the Ambion WT Expression Kit. Following cDNA-Cleanup, 5.5µg ssDNA were fragmented, labeled (WT Terminal Labeling and Controls Kit, Affymetrix) and hybridized for 17h at 45℃. GeneChip Human Gene 1.0 ST Arrays (Affymetrix) were washed and stained in the Affymetrix Fluidics Station 450. Fluorescence intensities of the hybridized arrays were acquired with the GeneChip Scanner 3000 and the operating software AGCC (Affymetrix).

Microarray Data Analysis

Microarray raw data were pre-analyzed and normalized, respectively, by the core facility of the Universitätsklinikum Mannheim. Genomic data were analysed by encapsulated R application [139]. In brief, from the pre-analyzed data, probesets with low variability were filtered out by means of median absolute deviation (MAD). Remaining probesets were further processed, only if the p-value of a statistical test (Student's *t*-test, Wilcoxon signed-rank test) was be below a certain threshold ($p < 0.05$) and second, the fold-change of groups compared were greater than a value specified (>1.3-fold or <−1.3-fold). The list of significant altered genes were assigned to their corresponding pathways by means of KEGG or GO. Subsequently, significantly affected pathways were identified by applying a statistical test to a contingency table.

3.2.6 Confocal Microscopy

Confocal imaging was performed with a Leica laser scanning spectral confocal microscopy (model DM IRE2) equipped with an oil objective (HCX PL Apo 40x/1.32), an argon laser (488nm), a krypton laser (568nm), and a helium/neon laser (633nm). Images were developed with a TCS SP2 scanner and Leica Confocal software (Version 2.5).

3.2.7 Statistical Analysis

All experiments were performed independently and at least three times. Obtained results are represented in means ± SE. Significant difference of results was determined by means of Student's *t*-test and indicated with *$p<0.05$ and **$p<0.02$.

4 RESULTS

4.1 Impact of HBV infection on TGF-β signaling in human hepatocytes

HCC is a heterogeneous disease regarding etiology as well as biologic and clinical behavior. Chronical HBV infection leads to fibrosis and often ends in HCC [140, 141]. TGF-β is a profibrotic cytokine playing a pivotal role in cell signaling in liver upon liver damage. However, a direct role of HBV mediated changes on TGF-β signaling outcome towards oncogenicity has yet to be determined. To address this question, two approaches were made. To study the effects of HBV infection and TGF-β on the transcriptome, PHHs were infected with HBV and treated with TGF-β. Isolated RNA was subjected to microarray chips and results were evaluated by encapsulated R application. HepG2.2.15 cells are stably transfected with the HBV genome and produce HBV particles, thereby mimicking effects induced by HBV proteins after HBV infection. For verification of microarray results, HepG2.2.15 cells were investigated regarding the functional impact of HBV on TGF-β signaling pathway.

4.1.1 HBV infection impairs TGF-β signaling in primary human hepatocytes

Most of the reported studies investigating the mechanisms of HBV induced HCC have concentrated on cell culture systems expressing HBV or if PHHs were used, infection efficiency with HBV was only up to 50%. However, the infection protocol established in the group of Prof Urban, results in infection efficiency of nearly 100% [142], and presents an advantage in comparison to other investigational models established before.
cDNA microarrays are powerful tools to identify disease related gene expression profiles in biological samples, as well as interactions between pathogenic organisms and their host cells.

To provide new insight into the molecular mechanisms of HBV and to improve our understanding of TGF-β signaling in the pathogenesis of HBV infection, I performed a

cDNA microarray of PHHs infected with HBV or not upon TGF-β treatment (5ng/ml) and compared the alterations in the gene expression profiles comprehensively.

4.1.1.1 HBV infection and TGF-β treatment of PHHs

PHHs were infected with HBV as described in 3.2.1. The efficiency of HBV infection of PHHs was shown by immunofluorescence staining of HBV core antigen (green) on day 8 post-infection. Nearly 100% of PHHs were infected with HBV (Figure 4.1)

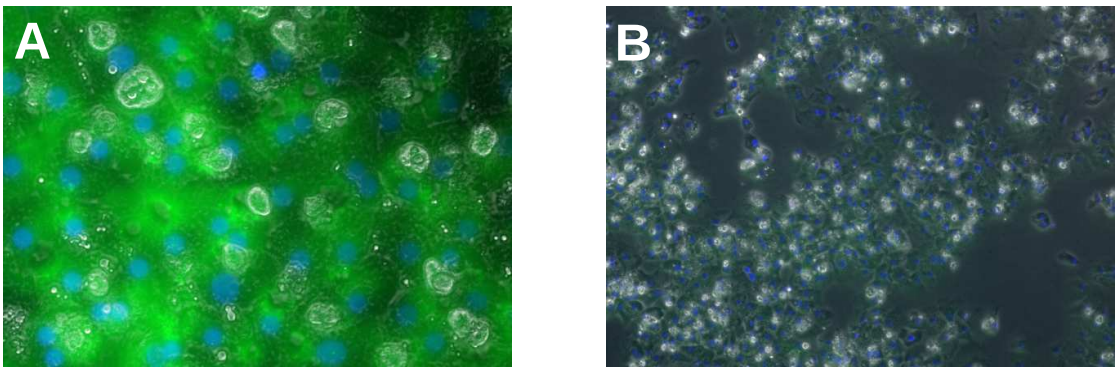

Figure 4.1: IF staining of HBV core antigen (green). Nuclear staining was done by DAPI (blue). (A) HBV infected hepatocytes on day 8 post-infection (magnification 400x). (B) Uninfected PHHs (magnification 100x). One shown as representative.

To verify HBV replication, the supernatant of HBV infected PHHs was collected every second day and HBsAg and HBeAg levels were measured. HBsAg and HBeAg levels increased steadily during the cultivation time, indicating that PHHs were infected with HBV and supported its replication. HBsAg levels were only slightly different in the three donors (Figure 4.2 A); ranging from 30IU/ml on day 3 up to 420IU/ml on day 7 post-infection. HBeAg values (Figure 4.2 B) ranged from 50 on day 3 up to 6600 (donor #1), 3000 (donor #2), 500 (donor #3) on day 7. HBeAg values differed within the donors, which might be due to individual patient dependent differences influencing HBV infection and replication.

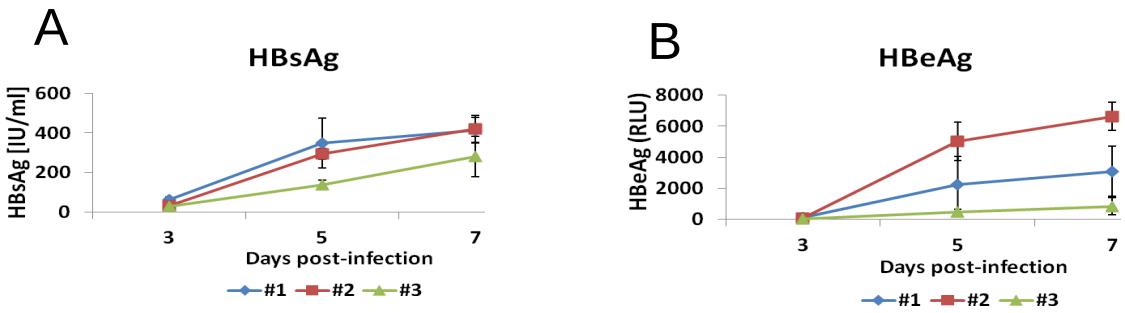

Figure 4.2: HBsAg and HBeAg levels of HBV infected PHHs. To observe HBV replication, HBV antigens were measured quantitatively in duplicates in the supernatant of HBV infected PHHs every second day. (A) HBsAg and (B) HBeAg levels of the three donors #1, #2, #3.

4.1.1.2 Microarray analysis and statistics

To ensure that experiments are performed on PHHs of the same age, HBV infected PHHs were treated with TGF-β for 0 and 1h on day 8 post-infection and for 24 h already on day 7 post-infection, respectively. On day 8 post-infection, cells were then harvested, mRNA was isolated and microarray hybridization was performed according to the manufacturers' protocol. After pre-analyzation and normalization of microarray raw data by the in-house core facility ZMF, genomic data were evaluated by encapsulated R application [139], including unspecific filtering, followed by statistical tests and pathway analysis (Figure 4.3).

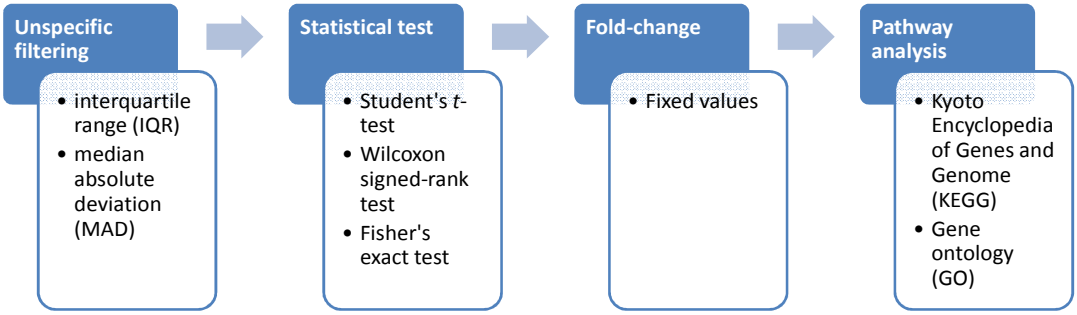

Figure 4.3: Encapsulated R application of genomic data. Steps applied to microarray data (solid boxes). The respective alternative procedures are shown in outline boxes below. Difference of expression values of comparison groups was set at >1.3-fold and <-1.3-fold. Significant difference of a Student's t test between the comparison groups was set $p<0.05$ (taken from [139]).

Heat Map analysis of the genomic data obtained (Figure 4.4), reflects gene expression values of the different donors upon their different treatment and revealed three major results.

Firstly, each donor displayed different basal gene expression signatures, unexpectedly significant. As already indicated by the different HBV antigen levels, HBV infection and replication had different impact on gene regulation of each donor, probably due to individual physiologic backgrounds. However, this study is focused on gene regulations common in all donors, as they might be general happenings in the course of HBV infection. Individual, donor specific alterations need to be addressed in a further study.

Secondly, HBV had only a minor impact on gene regulation of PHHs. This was not surprising, as HBV is a noncytopathic virus causing only few gene alterations. Progression towards HCC is mainly due to the immunologic reactions as ongoing elimination of HBV from infected hepatocytes results in constant inflammation of the liver [143] [65]. Nevertheless, those gene aberrations which are triggered by HBV might give additional triggers for oncogenic potential of HBV infected cells and the liver.

Thirdly, HBV infected PHHs remained sensitive towards long term TGF-β treatment. Interestingly, TGF-β treatment for 24hrs in HBV infected PHHs resulted mainly in similar gene alterations in all donors. However, expression of some genes seemed to be influenced by HBV infection. For this study, it was of main interest, whether these different expressed genes render the outcome of TGF-β signaling in HBV infected PHHs, e.g. from a normal cytostatic response towards a tumorigenic response.

When interpreting the following results, it has to be considered, that microarray analysis can yield false-negative results because of its limited sensitivity. HBV proteins might modulate other genes and it is possible that the modulation in this microarray study was underestimated. Nevertheless, even a relatively small difference in the array analysis could be physiologically significant.

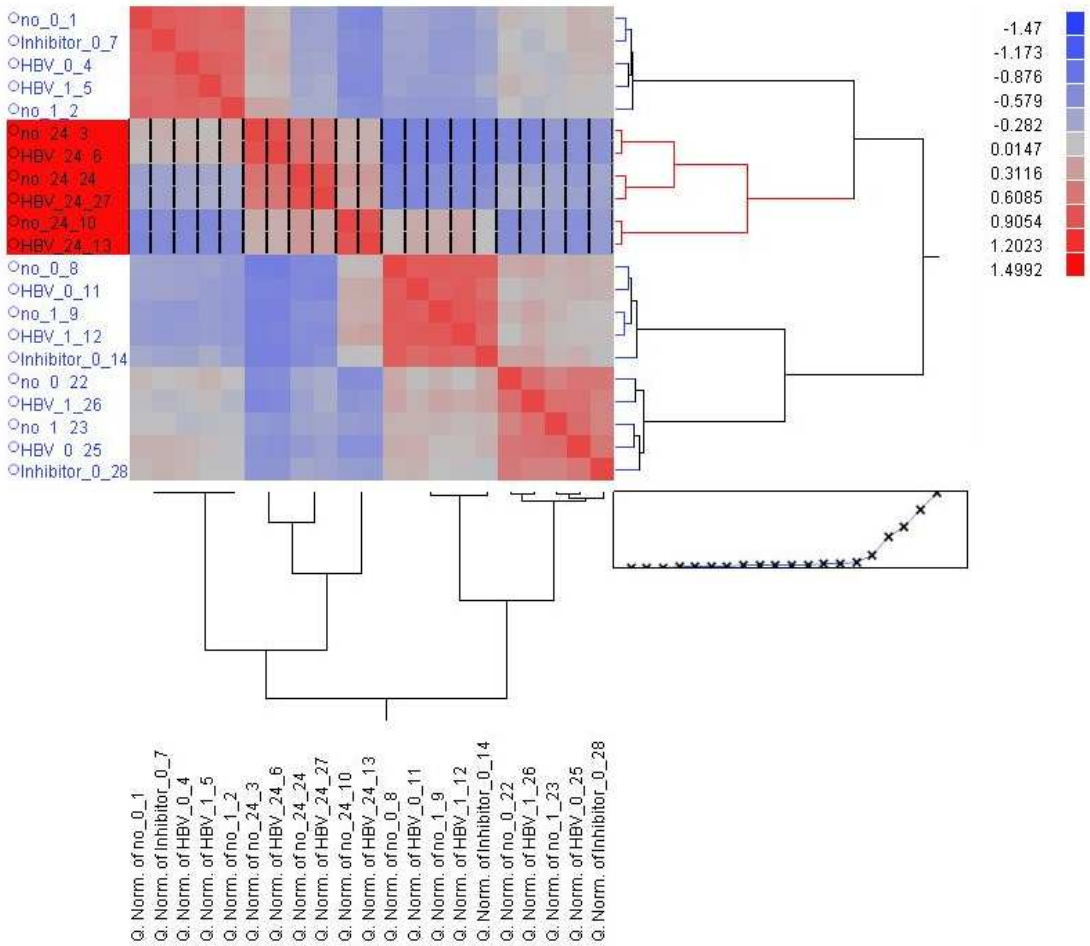

Figure 4.4: Heat map representation of expression analysis of the microarray data of HBV infected PHHs showing all gene expression clusters. The heat map is hierarchically ordered from left to right by whole-transcriptome expression.

“HBV/or not TGF-β (h) _Sample number”
Donor #1 (Sample number 1-7), donor #2 (Sample number 8-14), donor #3 (Sample number 22-28).

4.1.1.3 HBV has only a minor impact on gene regulation of PHHs

Current literature shows, that HBV is a noncytopathic virus causing only less aberration in gene expression of the host cell [143]. It is thought that HCC development is due to the immune system, which tries to eliminate infected hepatocytes, thereby leading to a constant inflammation of the liver [144] [145]. However, some infected cells escape the immune system due to cellular transformations. These cells may be the beginning of HCC development. The first aim of this study was to elucidate common and solid influences of HBV infection on TGF-β signaling, which may have an oncogenic potential

and might be one reason for HCC development upon HBV infection. To investigate general mechanisms of HBV induced HCC, only gene alterations which were identical in all three donors were taken into account; donor specific regulations, which might be important nonetheless, were disregarded. In compliance with these requirements only 12 genes were found to be regulated upon HBV infection (Figure 4.5 A). Of these genes, 10 genes were slightly up- and 2 genes were slightly downregulated. According to the literature, most of the regulated genes have already been investigated in the context of carcinogenesis. KEGG pathway analysis was performed for the search of ontological biological processes. Significantly rendered pathways were defined by statistical tests to a contingency table, as described in material and methods. As expected from single gene knowledge, most pathways regulated were formally assigned to pathways associated to glioma, chronic myeloid leukemia, bladder cancer, melanoma, and prostate cancer.

Note: For understanding and simplicity reasons, I will discuss single genes regulated in my analysis right in the results section. A more general discussion of the array results will be placed in the discussion section of this thesis. The gene MDM2 is upregulated by HBV in PHHs, which is involved in the p53 signaling pathway [146]. p53 signaling regulates cell cycle arrest, cell death, cell differentiation, senescence, DNA repair and neovascularization [147]; its deregulation can lead to impaired apoptosis and increased cell proliferation. The MDM2 protein is a transcription factor, which forms a complex with p53. This complex inhibits p53 transcriptional activity with subsequent ubiquitination and degradation of p53. A reduction in p53 protein levels results in a downregulation of its target gene p21, a negative regulator of cell cycle progression at G1 phase [148]. Hence, disruption of p53 signaling pathway by an upregulation of MDM2 has an oncogenic potential and can lead to increased proliferation, which was already investigated in glioma [149], chronic myeloid leukemia [150], bladder cancer [151], melanoma [152], and prostate cancer [153].

The most upregulated gene identified in this analysis is Thymidylate synthase (TYMS), which encodes the rate limiting enzyme in the production of dTTP, required for DNA synthesis [154]. Recently, it has been associated to liver cancer proliferation and progression, respectively, and drug resistance [155] [156]. TYMS is induced by the transcription factor LSF (Late SV40 Factor). Compared to normal hepatocytes and liver, a LSF overexpression was detected in human HCC cell lines and in HCC patients LSF

expression levels correlated with the stages and grades of the disease. Stable overexpression of LSF in less aggressive Hep3B cells resulted in significant increase in proliferation, colony formation, soft agar growth and Matrigel invasion [157].

The spermatogenesis-associated gene, SPATA18, regulates the quality of mitochondria, mediating the repairing or degradation of unhealthy mitochondria [158]; mitochondrial dysfunction has been implicated in cancer [159]. In response to mitochondrial damage, SPATA18 was recently discovered as a novel transcriptional target of p53 and p63 [160]; Bornstein et al reported that p63 induces SPATA18 and suggested that p63 can compensate for a loss of p53 activity due to their homology. Since p53 signaling might be impaired in HBV infected PHHs, cell homeostasis might be maintained by p63.

A

HBV vs Ø	
Gene	**log2**
TYMS	0,58439
PGA5	0,53731
SPATA18	0,50189
ARVP6125	0,45511
DDB2	0,44591
CYGB	0,44422
MDM2	0,43708
LOC286359	0,42086
CNGA3	0,40719
GPR109B	0,39675
ABCB11	-0,42879
SNORD116-21	-0,59567

B

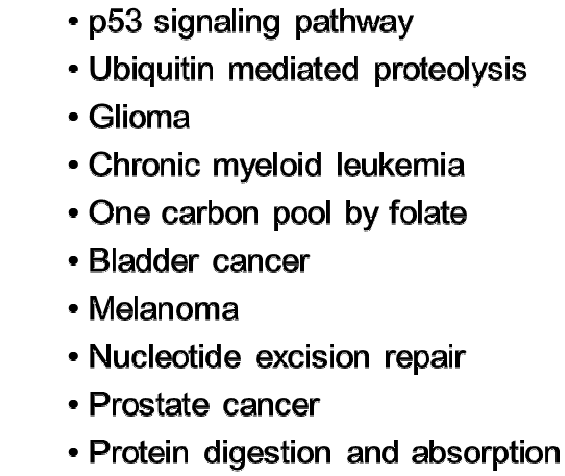

Figure 4.5: Gene regulation upon HBV infection common in all donors. (A) List of genes regulated upon HBV infection. Values are given in log2. (B) Pathways regulated upon HBV infection.

4.1.1.4 HBV infection decreased the number of TGF-β regulated target genes in PHHs

As it was shown before, that HBV infection influences TGF-β signaling [88] [89], I was now interested how HBV infection changes TGF-β dependent gene transcription in detail. Comparison of the total number of genes regulated in the microarray analysis described above revealed differential regulation of only a few genes: HBV infected hepatocytes versus uninfected hepatocytes after 1h (20 genes in uninfected PHHs vs 7

genes in HBV infected PHHs) and after 24hrs (501 genes in uninfected PHHs vs 213 genes in HBV infected PHHs) TGF-β treatment (Figure 4.6). In total, 1h TGF-β treatment regulated around 28 genes in uninfected PHHs and 15 genes in HBV infected PHHs. After 24hrs TGF-β treatment, 1566 genes were regulated in uninfected PHHs versus 1278 genes in HBV infected PHHs. This indicates that HBV reduced the impact of TGF-β on cell signaling.

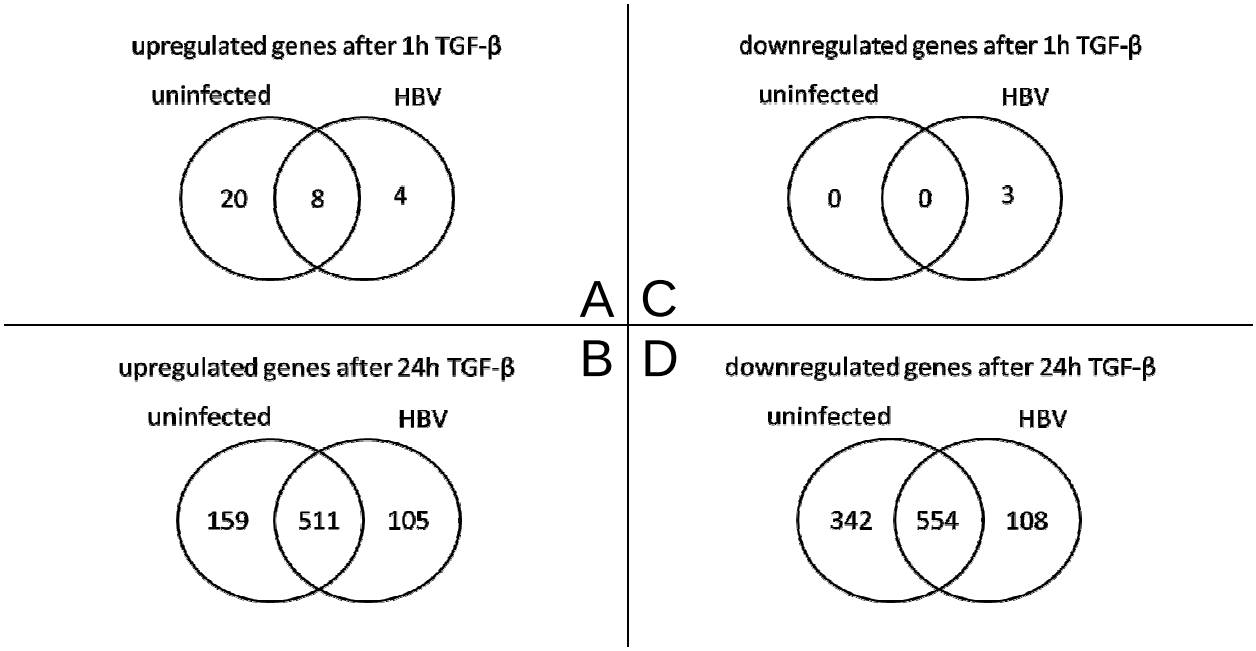

Figure 4.6: Number of TGF-β regulated genes. Amount of upregulated genes in uninfected or HBV infected PHHs upon TGF-β treatment (5ng/ml) for (A) 1h and (B) 24hrs. Amount of downregulated genes in uninfected or HBV infected PHHs upon TGF-β treatment (5ng/ml) for (C) 1h and (D) 24hrs.

4.1.1.5 HBV infection inhibits regulation of the TGF-β signaling pathway in PHHs after 1h TGF-β treatment

As just described, HBV infection of PHHs reduced the total number of TGF-β regulated target genes. As it was shown before, that HBx protein was able to block TGF-β induced apoptosis in Hep3B cells [89], I next analyzed which genes were differentially regulated after HBV infection of TGF-β treated PHHs and whether these can be assigned to cytostatic or tumorigenic TGF-β effects.

After 1h treatment typical early TGF-β target genes, like negative feedback inhibitor Smad7, plasminogen activator inhibitor PAI-1 (Serpine1), the cell cycle arrest protein

p21 (CDKN1A), or the DNA-binding protein inhibitor Id-1 (ID1) were found to be upregulated in uninfected PHHs (Figure 4.7 A). Interestingly, upregulation of these typical TGF-β target genes was not found in HBV infected PHHs (Figure 4.7 B). In HBV infected PHHs, only 4 genes were upregulated (PPP1R3B, GUSBL1, NAT8, CEBPB) and 3 genes were downregulated (LOC100506959, RPL7A, MIR122).

CEBPB (CCAAT/enhancer-binding protein beta) is a transcription factor and involved in regulation of immune and inflammatory responses. In detail, it was reported to bind to the IL-1 response element in the IL-6 gene, to regulatory regions of several acute-phase and cytokine genes, and to the promoter of the collagen type I gene [161] [162]. Further, it was reported that CEBPB is involved in the transcription of HBV genes [163] [164]. Xu et al. investigated the role of TGF-β in the survival of the myelo-monocytic leukemia cell line U937 co-cultured with bone marrow (BM)-derived mesenchymal stem cells (MSC). TGF-β inhibited spontaneous and cytarabine-induced apoptosis in U937 cells, increased pro-survival phosphorylation of Akt, and induced significant upregulation of CEBPB gene and protein expression. Although, the observations of Xu et al are obtained in a different cellular setup, their results may suggest a novel role of CEBPB in TGF-β induced cell survival arguing for its tumorigenic potential [165].

The PPP1R3B gene encodes the catalytic subunit of the serine/ threonine phosphatase, protein phosphatase-1 (PP-1), which is involved in regulation of hepatic glycogen metabolism [166]. TGF-β has been shown to stimulate the motility of endothelial cells, keratinocytes, fibroblasts, as well as cancer cells [167] [168]. Walsh et al. reported that endothelial cell motility is induced by TGF-β in a PP-1 dependent manner. Although these investigations of Walsh et al. have been performed in endothelial cells, it might be true for other cell types responsive for TGF-β induced motility [169].

MIR122 downregulation was recently reported to enhance interferon-α signaling in the liver through regulation of SOCS3 promoter methylation [170]. Interferon-α is a cell response after recognition of viral or bacterial nucleic acids.

Regulated genes which were identified in both, uninfected and HBV infected PHHs had similar expression levels (Figure 4.7 C). Among these genes were typical TGF-β target genes like GADD45B, BHLHE40, and RND1. GADD45B is induced upon environmental stress and is an effector of TGF-β induced apoptosis [171]. BHLHE40 is involved in the regulation of apoptosis and cell proliferation and was recently discovered to play a promotive role in TGF-β induced EMT [172]. RND1, a member of the Rho GTPase family, regulates the organization of the actin cytoskeleton in response to TGF-β [173].

A

Ø (1h TGF-β)	
Gene	**Ø**
KLF10	1,5285
SMAD7	1,5213
SERPINE1	1,4553
HES1	1,2280
ID1	1,1690
ANGPTL4	0,9867
ELF3	0,9205
SLC25A25	0,8804
SIK1	0,8356
HAMP	0,7639
ADM	0,7127
EFNA1	0,6356
HMOX1	0,6178
CEBPA	0,5982
MIDN	0,5823
CYR61	0,4704
CDKN1A	0,4630
ARRDC2	0,4546

B

HBV (1h TGF-β)	
Gene	**HBV**
PPP1R3B	0,5585
GUSBL1	0,5498
NAT8	0,4613
CEBPB	0,3936
LOC100506959	-0,4449
RPL7A	-0,4938
MIR122	-0,7580

C

overlay of genes (1h TGF-β)		
Gene	**Ø**	**HBV**
BHLHE40	1,2664	1,0914
DDIT4	1,8258	1,6785
DUSP1	0,7954	0,6785
GADD45B	1,5872	1,4734
GADD45G	0,9618	0,9324
RND1	0,6897	0,6737
TRIB1	0,4325	0,3996
ZFP36	1,0061	0,9251

Figure 4.7: Gene regulation upon 1h TGF-β. Regulated genes in (A) uninfected (Ø) and (B) HBV infected PHHs after 1h TGF-β treatment (5ng/ml). (C) Shows the genes which were regulated in both uninfected and HBV infected PHHs. All values are given in log2.

To assign deregulated genes in the context of cell signaling pathways, KEGG pathway analysis was performed, and significantly rendered pathways were defined by statistical tests to a contingency table, as described in material and methods. TGF-β treatment for 1h of uninfected PHHs induced the regulation of pathways involved in metabolism, like porphyrin and chlorophyll metabolism, and pathways involved in development, like axon guidance (Figure 4.8). Interestingly, TGF-β treatment led to the regulation of the TGF-β signaling pathway in uninfected PHHs only, but not in HBV infected PHHs. In contrast, in HBV infected hepatocytes p53 and mTOR signaling pathway were activated, the latter one being a downstream target of Akt survival pathway. Although, several pathways associated to cancer were regulated in uninfected PHHs upon 1h TGF-β, these pathways were not regulated upon 24hrs TGF-β treatment anymore (Figure 4.11).

1h TGF-β (5ng/ml)					
uninfected PHHs			**HBV-infected PHHs**		
Pathway	Number of genes		Pathway	Number of genes	
	upregulated	downregulated		upregulated	downregulated
Cell Cycle	3	0	Cell Cycle	2	0
MAPK signaling pathway	3	0	MAPK signaling pathway	3	0
TGF-β signaling pathway	2	0	p53 signaling pathway	2	0
Axon guidance	2	0	mTOR signaling pathway	1	0
Maturity onset diabetes of the young	1	0	Circadian rhythm - mammal	1	0
Glioma	1	0			
Chronic myeloid leukemia	1	0			
Acute myeloid leukemia	1	0			
Bladder cancer	1	0			
Circadian rythm - mammal	1	0			
Melanoma	1	0			
Porphyrin and chlorophyll metabolism	1	0			

Figure 4.8: Pathway regulation upon 1h TGF-β. List of significantly regulated pathways upon 1h TGF-β treatment (5ng/ml) of uninfected and HBV-infected PHHs. Signaling pathways only found in either group are highlighted in red.

4.1.1.6 HBV infection inhibits regulation of the TGF-β signaling pathway in PHHs after 24hrs TGF-β treatment

Differential expression of the 20 most upregulated genes upon TGF-β treatment for 24hrs in uninfected and HBV-infected PHHs, as well as genes found to be upregulated in both, are listed in Figure 4.9. The 20 most downregulated genes are listed in Figure 4.10.

A

Ø up (24h TGF-β)	
Gene	**Ø**
ATF5	1,0410
RDH16	0,9999
HNF1B	0,8874
JMJD1C	0,8544
NA	0,8303
GRHL1	0,7940
MEGF6	0,7777
CLDN14	0,7585
BTBD11	0,7421
TMPRSS9	0,7382
TBX15	0,7168
LOC338799	0,7079
ENKUR	0,6962
VSIG10L	0,6827
DGAT2	0,6718
SLC7A1	0,6680
RNU2-2	0,6517
G3BP2	0,6478
RAP1GAP	0,6237
NEDD9	0,6182

B

HBV up (24h TGF-β)	
Gene	**HBV**
CRYAB	1,2742
TLE2	1,2506
IER3	1,1104
TGFB2	1,1063
ARHGEF5	1,0614
GLIPR1	1,0453
HMOX1	1,0052
HSD11B2	0,9977
SPON2	0,9972
LIMCH1	0,9668
HAL	0,9611
C5orf24	0,9075
SH2D4A	0,8746
KIAA1147	0,8604
ADCY5	0,7497
GPER	0,7489
LOC402778	0,7285
MSN	0,6974
MAFK	0,6907
ALOX5	0,6888

C

overlap up (24h TGF-β)		
Gene	**Ø**	**HBV**
FAM20A	0,3834	0,4070
ATP13A2	0,3857	0,4196
LIMS1	0,3874	0,3848
TOR1B	0,3891	0,5027
STK38	0,3949	0,4177
KIAA1804	0,3976	0,3983
DBI	0,3976	0,4196
FAM102B	0,3981	0,6108
TJP1	0,4000	0,4557
HIVEP2	0,4002	0,4979
ARID5A	0,4037	0,3852
RNFT1	0,4079	0,7694
ARID2	0,4106	0,4172
FAM113B	0,4114	0,4720
WWC3	0,4153	0,3853
REEP3	0,4242	0,4512
LYSMD4	0,4245	0,4708
SLC30A1	0,4257	0,4781
CDC34	0,4266	0,4056
MVD	0,4273	0,4182

Figure 4.9: Upregulated genes upon 24h TGF-β. List of the 20 most upregulated genes in (A) uninfected (Ø) and (B) HBV infected PHHs after 24hrs TGF-β treatment (5ng/ml). (C) Genes which were upregulated in both uninfected and HBV-infected PHHs. All values are given in log2.

A

Ø down (24h TGF-β)	
Gene	**Ø**
CYP7A1	-2,9241
SLC2A14	-1,3274
GPRC5B	-1,2700
SLC6A12	-1,2681
KLF15	-1,2610
UGT1A9	-1,1384
CBS	-1,1087
LIPG	-1,1017
GLYCTK	-1,0453
ASB13	-1,0175
HSD17B13	-0,9834
LAMA3	-0,9792
AKR1D1	-0,8275
C14orf105	-0,8033
SEPX1	-0,7850
TCEA2	-0,7648
PCYT2	-0,7502
DEFB1	-0,7488
MYRIP	-0,7274
AHSG	-0,7104

B

HBV down (24h TGF-β)	
Gene	**HBV**
GPX2	-1,1954
CYP4A11	-1,0598
SOAT2	-1,0266
CITED2	-1,0214
ADRA1A	-0,9596
FSTL1	-0,8815
CYP2A7	-0,8156
RSC1A1	-0,8084
FLVCR2	-0,7886
ELF3	-0,7857
TMEM140	-0,7807
RORC	-0,7585
MYC	-0,7350
ADCK3	-0,7177
ACSM5	-0,7065
BTN3A1	-0,6977
HSD17B2	-0,6675
TBC1D8	-0,6341
UGT1A10	-0,6282
CNNM1	-0,6259

C

overlap down (24h TGF-β)		
Gene	**Ø**	**HBV**
SULT2A1	-2,6561	-2,5265
HLF	-2,3367	-2,4098
TDO2	-2,2251	-2,2700
GYS2	-2,2206	-1,8480
FABP1	-2,1885	-1,9388
SLC6A1	-2,0948	-2,0833
PCK1	-2,0395	-1,9637
ACOT12	-2,0344	-1,7925
GNMT	-2,0311	-1,7818
ADH1B	-2,0177	-2,1255
BBOX1	-1,8964	-1,7890
PAH	-1,8528	-1,9035
CREB3L3	-1,8413	-1,9998
LBP	-1,8360	-1,7871
ADH1A	-1,7776	-1,7384
HAO1	-1,7733	-1,6251
AKR1C4	-1,7620	-1,5969
VNN1	-1,7396	-1,7904
CYP2E1	-1,7396	-1,7313
BHMT	-1,7386	-1,7249

Figure 4.10: Downregulated genes upon 24h TGF-β. List of the 20 most downregulated genes in (A) uninfected (Ø) and (B) HBV infected PHHs after 24hrs TGF-β treatment (5ng/ml). (C) Shows the genes which were downregulated in both uninfected and HBV-infected PHHs. All values are given in log2.

As they are so many, regulated genes upon 24h TGF-β treatment cannot be discussed in detail here. Therefore, special attention is laid on the analysis of regulated signaling pathways. Upon 24hrs TGF-β treatment in HBV infected PHHs, only a few metabolic pathways, but more cancer associated pathways were regulated (Figure 4.11). According to the ontology of KEGG pathway analysis, this includes e.g. colorectal cancer, bladder cancer, melanoma, acute myeloid leukemia, and basal cell carcinoma among others. Further, insulin signaling pathway, an important pathway for cell homeostasis, was regulated in HBV infected PHHs. Disturbance of insulin signaling in concert with HBV infection has already been reported [174] [175] [176]. As described for 1h TGF-β treatment results, the TGF-β signaling pathway was only regulated in uninfected PHHs after 24hrs of TGF-β treatment, but not in HBV infected PHHs. This shows that TGF-β signaling pathway sensitivity might be impaired in hepatocytes upon HBV infection.

24h TGF-β (5ng/ml)					
uninfected PHHs			**HBV-infected PHHs**		
Pathway	Number of genes		Pathway	Number of genes	
	upregulated	downregulated		upregulated	downregulated
Acute myeloid leukemia	7	0	ABC transporters	6	3
Adherens junction	10	5	Acute myeloid leukemia	7	0
Adipocytokine signaling pathway	3	7	Adherens junction	8	6
Alanine, aspartate and glutamate metabolism	2	8	Adipocytokine signaling pathway	4	6
Aldosterone-regulated sodium reabsorption	3	3	Aldosterone-regulated sodium reabsorption	5	3
alpha-Linolenic acid metabolism	3	2	Arachidonic acid metabolism	3	7
Arginine and proline metabolism	2	13	Arginine and proline metabolism	2	10
Ascorbate and aldarate metabolism	0	9	Ascorbate and aldarate metabolism	0	8
Biosynthesis of unsaturated fatty acids	6	3	Axon guidance	13	4
Bladder cancer	5	1	Base excision repair	2	5
Butanoate metabolism	0	8	beta-Alanine metabolism	0	5
Caffeine metabolism	0	4	Bladder cancer	7	1
Drug metabolism - other enzymes	2	7	Butanoate metabolism	1	7
ErbB signaling pathway	9	4	Caffeine metabolism	0	5
Ether lipid metabolism	2	6	Drug metabolism - other enzymes	2	8
Fat digestion and absorption	5	3	ErbB signaling pathway	10	4
Glycerolipid metabolism	4	10	Fat digestion and absorption	4	2
Glycerophospholipid metabolism	5	11	Glioma	4	1
Glycolysis / Gluconeogenesis	1	13	Glycerolipid metabolism	4	6
Glycosaminoglycan biosynthesis - keratan sulfate	1	4	Glycerophospholipid metabolism	6	6
GnRH signaling pathway	4	3	Glycolysis / Gluconeogenesis	1	12
Lysine degradation	3	10	Glycosaminoglycan biosynthesis - keratan sulfate	2	2
Mismatch repair	1	4	Glyoxylate and dicarboxylate metabolism	2	6
Nitrogen metabolism	0	7	GnRH signaling pathway	4	3
One carbon pool by folate	1	4	Insulin signaling pathway	11	6
Other types of O-glycan biosynthesis	5	8	Long-term depression	3	2
Pancreatic cancer	4	2	Lysine degradation	2	6
Pantothenate and CoA biosynthesis	0	5	MAPK signaling pathway	17	13
Pentose and glucuronate interconversions	0	10	Mucin type O-Glycan biosynthesis	3	2
Phenylalanine metabolism	0	7	Nitrogen metabolism	1	6
Propanoate metabolism	0	7	One carbon pool by folate	1	4
Purine metabolism	6	18	Osteoclast differentiation	8	7
Pyruvate metabolism	2	9	Other types of O-glycan biosynthesis	4	7
Retinol metabolism	1	6	Pancreatic cancer	6	2
Starch and sucrose metabolism	0	11	Pantothenate and CoA biosynthesis	0	6
Sulfur metabolism	0	4	Pathways in cancer	22	5
Synthesis and degradation of ketone bodies	1	3	Pentose and glucuronate interconversions	0	9
T cell receptor signaling pathway	7	3	Phenylalanine metabolism	0	7
TGF-β signaling pathway	16	3	Phototransduction	1	2
Ubiquinone and other terpenoid-quinone biosynthesis	0	3	Primary bile acid biosynthesis	1	5
VEGF signaling pathway	5	5	Propanoate metabolism	1	7
Vitamin B6 metabolism	1	2	Prostate cancer	7	1
			Proximal tubule bicarbonate reclamation	1	4
			Pyruvate metabolism	3	7
			Renal cell carcinoma	6	0
			Starch and sucrose metabolism	0	11
			Terpenoid backbone biosynthesis	4	0
			Vascular smooth muscle contraction	6	8
			Vitamin B6 metabolism	1	2
			Vitamin digestion and absorption	1	4

Figure 4.11: Pathway regulation upon 24h TGF-β. List of significantly regulated pathways upon 24hrs TGF-β treatment (5ng/ml) of uninfected and HBV infected PHHs. Signaling pathways only found in either group are highlighted in red.

In total, 27 genes related to Cancer Pathways were regulated, of which 22 genes were up- and 5 genes were downregulated (Figure 4.1). The highest upregulated gene was EGLN3 and its overexpression was identified in renal cell carcinoma before [180]. E2F3 a member of the transcription factor family E2F was also found to be upregulated. E2F3 upregulation is involved in cellular transformation [181]. c-myc, which induces genetic instability [182] was downregulated upon HBV infection, confirming the results obtained by Ryu et al. 2006 [183].

HBV (24h TGF-β)			
Pathways in Cancer			
upregulated genes		downregulated genes	
Gene	fold-induction	Gene	fold-induction
EGLN3	3,449	BIRC3	0,488
ITGAV	3,343	MYC	0,601
PDGFA	3,124	FZD4	0,622
FGF2	3,024	CDK4	0,686
SMAD3	2,635	PLD1	0,708
CEBPA	2,308		
RARA	2,258		
RUNX1	2,134		
CDKN1A	1,996		
FN1	1,752		
PPARD	1,697		
VEGFA	1,682		
ERBB2	1,606		
EPAS1	1,547		
VEGFB	1,499		
LAMA5	1,477		
STAT3	1,415		
E2F3	1,390		
TCEB1	1,380		
FZD6	1,371		
TGFA	1,345		
FOXO1	1,303		

Figure 4.12: Regulated genes associated to cancer. List of regulated genes belonging to pathways in cancer in HBV infected PHHs upon 24hrs TGF-β treatment (5ng/ml).

In this study, regulation of the TGF-β signaling pathway was abrogated in HBV infected PHHs. Interestingly, Smad3, as a member of the canonical TGF-β signaling pathway was upregulated by TGF-β in HBV infected PHHs. Honda et al. 2006 performed a microarray study comparing tissue of patients with chronic hepatitis B or chronic hepatitis C. They identified an upregulation of Smad3 in chronic HBV but independent of TGF-β. Honda et al. hypothesized that pro-apoptotic and DNA repair responses are predominant upon HBV infection [184]. Microarray results of this study point that pro-apoptotic TGF-β signaling pathway is abrogated and Smad3 upregulation might be associated to another function, e.g. it is thought to play a role in the regulation of carcinogenesis, like in prostate cancer, due to regulation of angiogenic molecule expression [185].

Next, the different significantly regulated signaling pathways were assigned to biologically functional categories. In general, HBV infection had a major impact on the

cell, highlighted in the broad variety of functional categories affected and the great impact towards the outcome of TGF-β treatment. In detail, the assignment revealed, that most regulated pathways in uninfected PHHs upon 24hrs TGF-β treatment belonged to metabolism processes, like metabolism of cofactors and vitamins, lipid metabolism, amino acid metabolism, nucleotide metabolism, and energy metabolism (Figure 4.13); whereas less metabolic pathways were regulated in HBV infected PHHs. This suggests that HBV deplets cellular resources probably needed for its replication and propagation process.

24h TGF-β (5ng/ml)			
uninfected		**HBV infected**	
Funcional Category	**Pathways**	**Funcional Category**	**Pathways**
Amino Acid Metabolism	4	Amino Acid Metabolism	3
Biosynthesis of other secondary metabolites	1	Biosynthesis of other secondary metabolites	1
Cancers	3	Cancers	7
Carbohydrate Metabolism	7	Carbohydrate Metabolism	8
Cell Communication	1	Cell Communication	1
Digestive System	1	Circulatory System	1
Endocrine System	2	Development	1
Energy Metabolism	2	Digestive System	2
Excretory System	1	Endocrine System	3
Glycan Biosynthesis and Metabolism	2	Energy Metabolism	1
Immune System	1	Excretory System	1
Lipid Metabolism	6	Glycan Biosynthesis and Metabolism	2
Metabolism of Cofactors and Vitamins	5	Lipid Metabolism	4
Nucleotide Metabolism	1	Membrane Transport	1
Replication and Repair	1	Metabolism of Cofactors and Vitamins	3
Signal Transduction	3	Metabolism of other Amino Acids	1
Xenobiotics biodegradation and metabolism	1	Metabolism of Trepenoids and Polyketides	1
		Nervous System	1
		Replication and Repair	1
		Sensory System	1
		Signal Transduction	2
		Xenobiotics biodegradation and metabolism	1

Figure 4.13: Regulated functional categories upon 24h TGF-β. Amount of pathways regulated within the functional categories of uninfected and HBV infected PHHs treated for 24hrs with TGF-β (5ng/ml).

4.1.1.7 HBV infection inhibits Smad3 phosphorylation upon TGF-β treatment in PHHs

The microarray results of this study indicate that HBV impairs the sensitivity of PHHs towards exogenous TGF-β stimulation. As suggested by p21 downregulation in TGF-β treated HBV infected PHHs compared to uninfected PHHs, HBV might inhibit TGF-β induced apoptosis in hepatocytes, probably to assure virus survival. In epithelial cells as

haptocytes, cytostatic TGF-β signaling is mainly mediated via the canonical Smad3 pathway [186]. To validate the hypothesis, that HBV inhibits TGF-β signaling via Smad3, PHHs of 3 other donors were infected with HBV or not. One donor displayed an impaired phosphorylation of Smad3 upon 48h TGF-β treatment (Figure 4.14). Although this was found only once out of three different donors, this finding might support the hypothesis, that HBV infection is able to inhibit the activation of TGF-β signaling via Smad3, which can lead to decreased apoptosis.

Availability of PHHs is limited, nevertheless, screening of a greater set of donors is urgently needed to elucidate the sigificance of this finding and should be considered for further investigations.

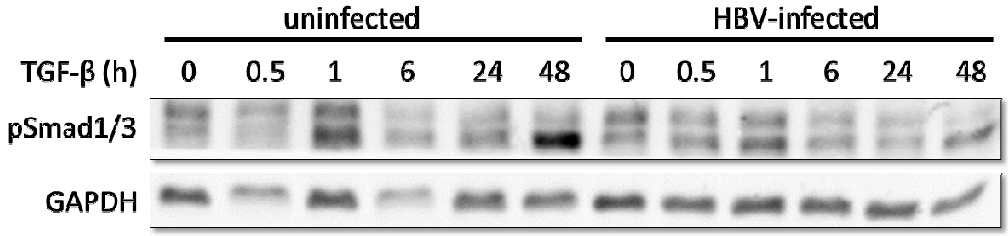

Figure 4.14: HBV infection inhibits Smad3 phosphorylation in HBV infected PHHs. PHHs were infected with HBV or not. Four days post-infection, PHHs were treated with TGF-β for 48hrs. PHHs were harvested on day 6 post-infection. Protein lysates were subjected to immunoblot analysis of pSmad3. GAPDH served as loading control.

In summary, cDNA microarray of HBV infected PHHs vs. uninfected PHHs revealed that HBV is a noncytopathic virus causing few gene aberrations. Secondly, TGF-β treatment for either 1h or 24hrs of HBV and uninfected PHHs showed, that the number of TGF-β regulated target genes is decreased upon HBV infection. Thirdly, HBV infection was able to inhibit TGF-β effects related to regulation of the TGF-β signaling pathway, e.g. Smad7 regulation and TGF-β target genes, like p21, which is involved in TGF-β induced apoptosis and growth arrest. This was supported by an abrogated Smad3 phosphorylation in HBV infected hepatocytes upon TGF-β treatment. Fourthly, global characteristics of gene expression profiles upon 24hrs TGF-β treatment support the hypothesis of current literature, that the process of HBV replication limits cellular resources needed for proper metabolism, thereby causing a deregulation of cell signaling which can be responsible for cell transformation.

4.1.2 Akt deactivation sensitizes HepG2.2.15 cells for TGF-β induced apoptosis

Gene expression analysis presented in this study revealed inhibition of the canonical TGF-β signaling pathway by HBV infection confirmed by abrogation of Smad7 induction, and the abrogation of p21 induction (Figure 4.7). The latter possibly causes inhibition of TGF-β induced apoptosis/ growth arrest. Inhibition of Smad3 phosphorylation in HBV infected PHHs (Figure 4.14) supported the hypothesis of an impaired TGF-β signaling. To verify these results and analyze its underlying mechanism in more detail, the cell line HepG2.2.15 was used. These cells are derived from the parental cell line HepG2, stably transfected with a plasmid containing full HBV DNA [67]. As HepG2.2.15 cells produce infectious HBV particles, they are able to reveal effects induced by HBV proteins after HBV infection. Further, HepG2.2.15 cells present a purified liver cell model, disregarding the *in vivo* effects of other cells of the liver or the immune system. Hence, HepG2.2.15 cells are a valuable model for investigating the effects of HBV proteins on host cells [187].

4.1.2.1 TGF-β dependent Smad3 transcriptional activity is reduced and Smad3 phosphorylation level is more transient

As described above, HBV infection impaired TGF-β induced gene expression of TGF-β signaling components and reduced Smad3 phosphorylation in PHHs. To investigate the underlying mechanism, HepG2.2.15 cells and the parental cell line HepG2 were treated with TGF-β in a time course from 0 to 24hrs. Smad3 expression levels were equal in both cell lines as confirmed by Immunoblot analysis (Figure 4.15). HBV replication reduced Smad3 phosphorylation levels from prolonged in HepG2 to transient in HepG2.2.15 cells. No changes were seen in Smad2 phosphorylation levels at any time points.

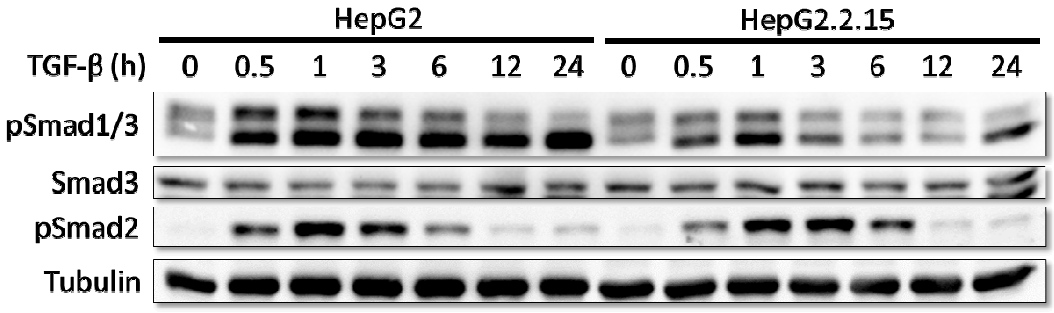

Figure 4.15: HBV reduced Smad3 phosphorylation levels in HepG2.2.15 cells. HepG2 and HepG2.2.15 cells were starved overnight prior to treatment with TGF-β (5ng/ml) for the indicated time points. Protein lysates were subjected to immunoblot analysis of pSmad3, Smad3, and pSmad2. Tubulin served as loading control.

CAGA reporter assay was performed to investigate the impact of impaired Smad3 phosphorylation on its transcriptional activity. As expected, reduced Smad3 dependent transcriptional activity was detected upon TGF-β treatment in HepG2.2.15 cells compared to HepG2 control cells (Figure 4.16) already after 3hrs.

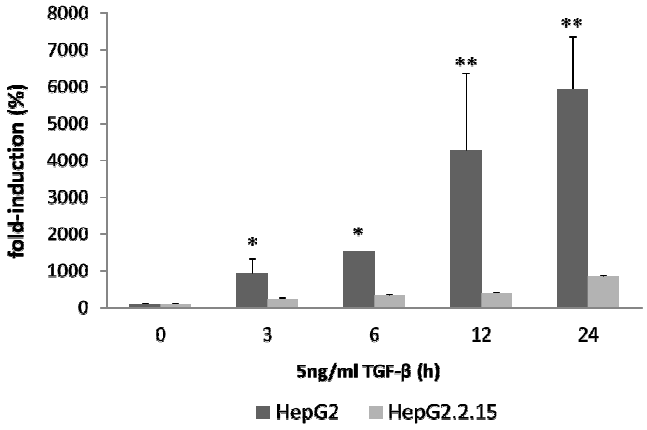

Figure 4.16: Smad3 transcriptional activity is reduced in HepG2.2.15 cells. HepG2 and HepG2.2.15 cells were cotransfected with plasmids encoding β-Gal and the CAGA sequence, respectively, using Lipofectamine 2000 for 4hrs. Cells were starved overnight prior to treatment with TGF-β (5ng/ml) for the indicated time points. *p<0.05 and **p<0.02.

4.1.2.2 TGF-β has no impact on cell death

Microarray results of HBV infected PHHs indicated that stimulated TGF-β signaling and Smad3 phosphorylation is impaired. In line one typical TGF-β target gene p21, involved in cell cycle arrest, was not induced by TGF-β treatment in HBV infected PHHs. Further, Smad3 signaling known to mediate TGF-β induced apoptosis [58], was also impaired in HepG2.2.15 cells. These results suggest that TGF-β induced apoptosis might be

impaired upon HBV infection. To investigate this hypothesis, HepG2.2.15 cells were treated with TGF-β and a LDH assay was performed. TGF-β treatment had no significant impact on apoptosis in HepG2.2.15 (Figure 4.17). However, HepG2 cells were insensitive towards TGF-β induced apoptosis as well, in line with previous reports [129].

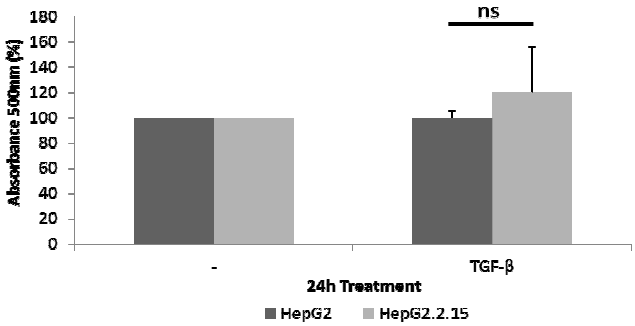

Figure 4.17: HepG2.2.15 and HepG2 cells are insensitive to TGF-β induced apoptosis. HepG2 and HepG2.2.15 cells were starved overnight prior to treatment with TGF-β (5ng/ml) for 24hrs. LDH release was measured in the supernatant. ns = not significant

4.1.2.3 HBV induced pAkt levels independently of TGF-β

Although resistance against TGF-β induced apoptosis was monitored in both, HepG2 and HepG2.2.15, I asked, whether there are different regulation mechanisms responsible maybe via different / additional impact of HBV on apoptosis resistance of HepG2.2.15 cells. It was reported before, that viruses induce activation of cell survival pathways to inhibit death of cells they infect [89] [188] [189] [190] [191]. Accordingly, an increase in Akt activation has been reported to be associated with HBV infection [192] [193] and pro survival Akt signaling antagonizes apoptotic pathways like TGF-β signaling [194]. Therefore, Akt activation was analyzed for its capability to influence the resistance of HepG2 and/or HepG2.2.15 cells against TGF-β induced apoptosis.

Investigation of Akt phosphorylation by immunoblot analysis revealed higher Akt activation in HepG2.2.15 cells replicating HBV compared to HepG2 cells (Figure 4.18). However, Akt phosphorylation was independent of TGF-β treatment.

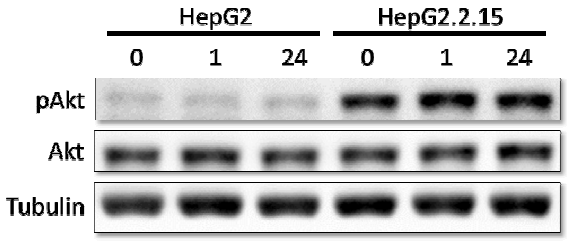

Figure 4.18: HBV induced pAkt independent of TGF-β. HepG2 and HepG2.2.15 cells were starved overnight prior to treatment with TGF-β (5ng/ml) for 1h and 24hrs. Protein lysates were subjected to Immunoblot analysis of pAkt and Akt. Tubulin served as loading control.

4.1.2.4 Akt deactivation sensitizes HepG2.2.15 cells for TGF-β induced apoptosis

To investigate whether the elevated levels of phosphorylated Akt are responsible for the inhibition of TGF-β induced apoptosis in HepG2.2.15 cells, cells were treated with Akt inhibitor LY294002 (20µM) for 2hrs prior to TGF-β treatment for 24hrs. To proof proper inhibition of Akt inhibitor LY294002, cell lysates were investigated by Immunoblot analysis, showing that Akt phosphorylation was completely abolished by usage of LY294002 (Figure 4.19 A). Upon deactivation of Akt and concomitant TGF-β treatment, HepG2.2.15 showed increased cell death (Figure 4.19 B) as measured by LDH assay. In contrast, HepG2 cells were completely insensitive towards TGF-β induced cell death after treatment with Akt inhibitor. Treatment of HepG2.2.15 cells with either TGF-β or Akt inhibitor alone had no significant impact on cell death. In line, PARP cleavage showed that treatment of HepG2.2.15 cells with Akt inhibitor sensitized those for TGF-β induced apoptosis.

In order to test whether autocrine TGF-β effects would have any impact on apoptosis or Smad phosphorylation, type I TGF-β receptor inhibitor SB431542 (5µM) was used. However, there was no difference in apoptosis or Smad3 phosphorylation compared to DMSO treated cells, indicating no significant role of autocrine TGF-β signaling in this context.

Overall, basal Smad3 phosphorylation levels in HepG2.2.15 cells were low compared to HepG2 cells.

This result suggests that HBV infection increases Akt activation, which in turn might be responsible for impaired responsiveness towards TGF-β induced apoptosis in the cell line.

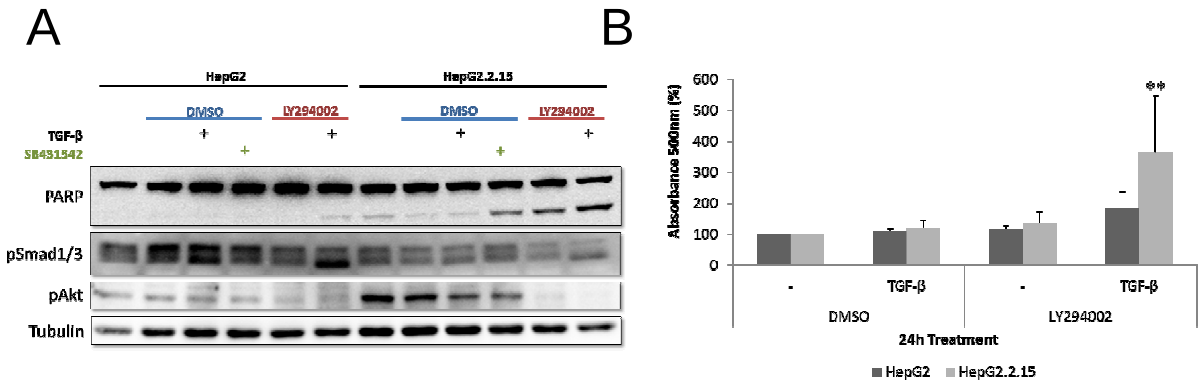

Figure 4.19: Akt deactivation sensitizes HepG2.2.15 cells for TGF-β induced apoptosis. HepG2 and HepG2.2.15 cells were starved overnight and treated for 2h with Akt inhibitor LY294002 (20µM) or with type I TGF-β receptor inhibitor SB431542 (5µM) prior to treatment with TGF-β (5ng/ml) for 24hrs. (A) LDH release was measured in the supernatant. (B) Protein lysates were subjected to Immunoblot analysis of PARP, Smad3, and pAkt. Tubulin served as loading control. **p<0.02

Taken together these results suggest that regulation of the crosstalk between TGF-β signaling, Akt signaling and other proapoptotic and pro survival pathways is influenced by HBV infection. However, the exact interplay and all players remain to be elucidated

4.1.2.5 Smad7 overexpression does not abrogate TGF-β induced apoptosis upon Akt deactivation in HepG2.2.15

Canonical Smad signaling is mainly responsible for mediation of TGF-β induced apoptosis [40] [41] [43]. As Smad3 phosphorylation and activation is reduced in HBV replicating cells, TGF-β induced apoptosis after Akt inhibition might be mediated by Smad independent signaling. To proof this hypothesis, the negative feedback inhibitor of canonical TGF-β signaling Smad7, was overexpressed by adenovirus infection. Smad7 overexpression was confirmed by Immunoblot analysis and reduced Smad3 phosphorylation proved functionality of overexpressed Smad7 (Figure 4.20 A). Adenovirus infection in combination with DMSO or TGF-β treatment had no impact on cell death in HepG2 and HepG2.2.15 cells (Figure 4.20 B). However, adenovirus infection in combination with inhibitor treatment had an impact on cell death in HepG2.2.15 cells observed by an increase in LDH release, but there was no increase in cleaved PARP. Upon Smad7 overexpression and Akt inhibition no decrease in TGF-β induced apoptosis could be observed.

In summary, Smad7 overexpression by adenovirus infection suggests, Smad independent TGF-β induced apoptosis upon Akt inhibition. However, as an effect of control adenovirus infection had significant impact on apoptosis in LY294002 treated cells this question needs to be analyzed by different means to allow conclusive interpretation. Therefore, knock-down of Smad3 was used as an alternative approach to address this question.

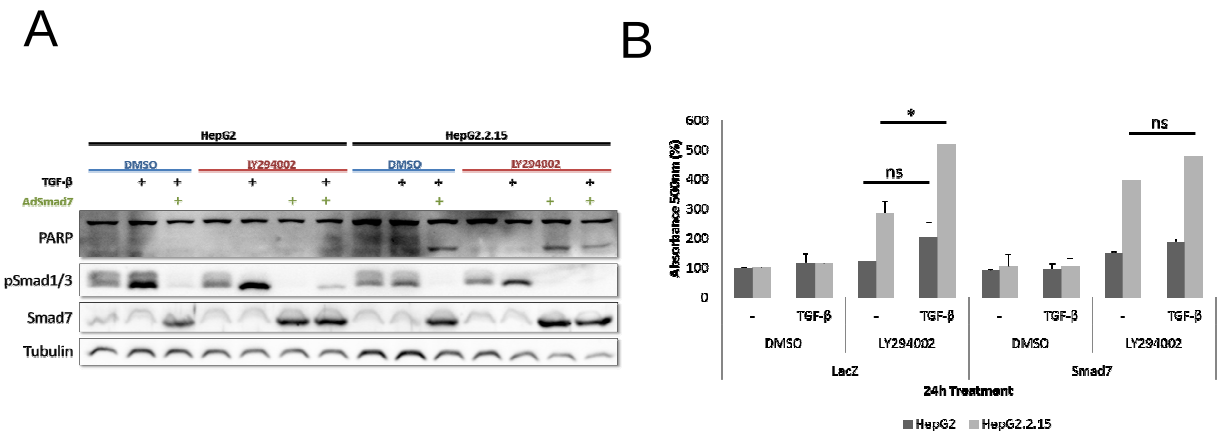

Figure 4.20: Smad7 overexpression had no decreasing effect on TGF-β induced apoptosis upon Akt deactivation. HepG2 and HepG2.2.15 cells were transduced with AdLacZ or AdSmad7 for 2hrs and kept on starvation medium for 48hrs. Cells were treated with Akt inhibitor LY294002 (20µM) for 2hrs prior to treatment with TGF-β (5ng/ml) for 24hrs. (A) LDH release was measured in the supernatant. (B) Protein lysates were subjected to Immunoblot analysis of PARP, Smad3, and Smad7. Tubulin served as loading control. ns = not significant. *p<0.02

4.1.2.6 TGF-β induced apoptosis upon Akt deactivation is potentially Smad3 independent in HepG2.2.15 cells

To clarify, whether TGF-β induced apoptosis in HepG2.2.15 cells treated with Akt inhibitor is independent of Smad signaling, Smad3, the main driver mediating TGF-β induced apoptosis in epithelial cells [58] [59], was downregulated by RNA interference. Due to the low detection specificity of the Smad3 antibody available, downregulation of Smad3 was investigated indirectly by a downregulation of phospho-Smad1/3 (Figure 4.21 A). In contrast to adenoviral control infection, control siRNA did not induce apoptosis of Akt inhibitor treated cells allowing straight forward interpretation of the results obtained. Smad3 downregulation did not reduce apoptosis in LY294002 and

TGF-β treated HepG2.2.15 as measured by LDH assay, indicating that TGF-β induced apoptosis upon Akt deactivation is independent of Smad3 signaling (Figure 4.21 B). However, an increase of PARP cleavage upon Smad3 downregulation and TGF-β treatment in HepG2.2.15 cells was demonstrated. These different results might be explained by different sensitivity of LDH assay and PARP cleavage assay. Further, LDH measures apoptosis and secondary necrosis, while PARP is a more specific marker for caspase mediated apoptosis.

In summary, the results shown do not allow a final interpretation of the role of Smad3 for TGF-β mediated apoptosis in LY294002 treated HepG2.2.15 cells.

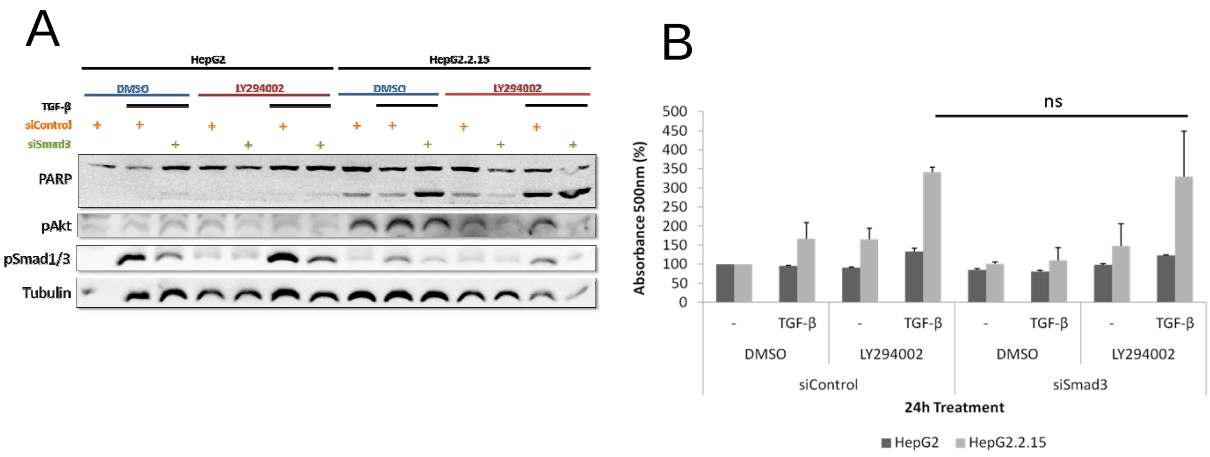

Figure 4.21: Downregulation of Smad3 has no decreasing effect on TGF-β induced apoptosis upon Akt deactivation. HepG2 and HepG2.2.15 cells were transfected with siControl or siSmad3 for 6hrs, respectively, and starved for 48hrs. Cells were treated with Akt inhibitor LY294002 (20µM) for 2hrs prior to treatment with TGF-β (5ng/ml) for 24hrs. (A) LDH release was measured in the supernatant. (B) Protein lysates were subjected to immunoblot analysis of PARP, pAkt, and Smad3 (B). Tubulin served as loading control. ns = not significant.

4.1.2.7 Smad3 overexpression does not increase TGF-β induced apoptosis upon Akt deactivation in HepG2.2.15 cells

It was reported before by Conery et al. that Akt is able to interact with unphosphorylated Smad3 in the cytoplasm, preventing its phosphorylation and translocation to the nucleus, thereby inhibiting TGF-β induced apoptosis in Hep3B cells [54]. This observation raised the question, whether the elevated Akt activation in HepG2.2.15 cells

might inhibit Smad3 signaling by this mechanism in HepG2.2.15 cells. It was analyzed, whether Smad3 overexpression can rescue functional Smad3 signaling and whether concomitant Akt inhibition can elevate TGF-β induced apoptosis in HepG2.2.15 cells. Smad3 was overexpressed as confirmed by Immunoblot analysis (Figure 4.22 A) (Note: As ectopic expressed Smad3 has a flag-tag, its molecular weight is heavier and runs higher on the immunoblot as endogenous Smad3). Although the amount of adenovirus used for Smad3 overexpression was equal in HepG2 and HepG2.2.15 cells, expression levels were higher in HepG2 cells. This might be due to interference of HBV and adenovirus in HepG2.2.15 cells. However, nothing has been reported towards this observation before. An increase in Smad3 phosphorylation level upon treatment with LY294002 and TGF-β, compared to treatment with TGF-β alone was observed in HepG2 and HepG2.2.15 cells. This may confirm the results of Conery et al., described above, that Akt prevents phosphorylation of Smad3. Adenovirus infection had no impact on LDH release in HepG2 and HepG2.2.15 cells allowing straight forward interpretation of the results obtained (Figure 4.22 B). Smad3 overexpression and Akt inhibition had no increasing effect on TGF-β induced apoptosis in HepG2 and HepG2.2.15 cells as determined by LDH release. Results observed on PARP cleavage nicely fit to the results of LDH assay. PARP cleavage and low levels of total PARP were observed upon treatment with TGF-β and Akt inhibitor in HepG2.2.15 cells, but were independent of Smad3 overexpression. In contrast to purified Adenovirus, which was used for Smad7 overexpression, adenovirus soup, which was used for Smad3 overexpression, had no impact on apoptosis in combination with Akt inhibitor.

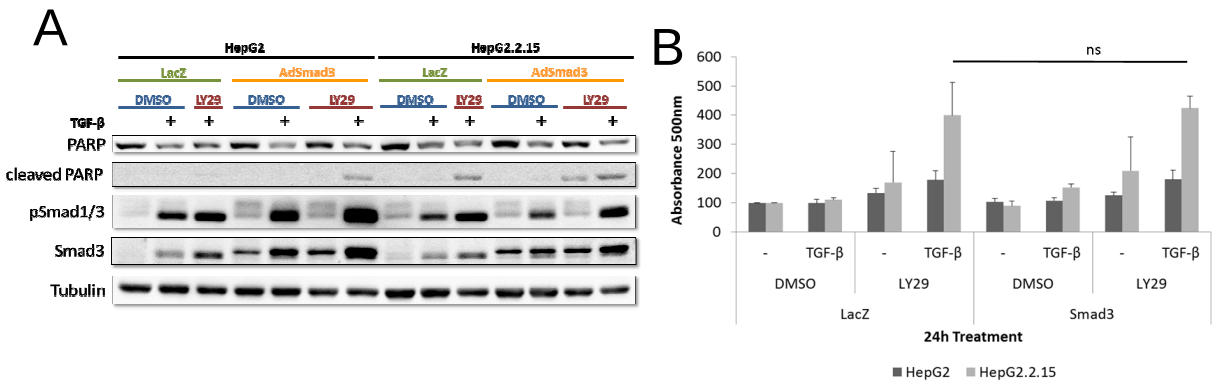

Figure 4.22: Smad3 overexpression does not increase TGF-β induced apoptosis upon Akt deactivation. HepG2 and HepG2.2.15 cells were transduced with AdLacZ or AdSmad3 for 2hrs, respectively, and starved for 48hrs. Cells were treated with Akt inhibitor LY294002 (20µM) for 2hrs prior to treatment with TGF-β (5ng/ml) for 24hrs. (A) LDH release was measured in the supernatant. (B) Protein lysates were subjected to immunoblot analysis of PARP, pSmad3, and Smad3 (B). Tubulin served as loading control. ns = not significant.

In summary, Smad3 downregulation and Smad3 overexpression had no significant impact on LDH release in TGF-β induced apoptosis upon Akt deactivation. However, PARP cleavage revealed contradictory results compared to LDH assay after Smad3 knock down and TGF-β treatment.

Taken together, results obtained by Smad7 overexpression, Samd3 overexpression and Smad3 knockdown suggest that TGF-β mediated apoptosis is probably independent of Smad3 signaling after Akt inhibition in HBV replicating HepG2.2.15 cells.

4.1.2.8 SB203580 reduces TGF-β induced apoptosis upon Akt deactivation in HepG2.2.15 cells

It has been reported before, that TGF-β induced apoptosis can be mediated independent of Smad signaling by MAPKs, JNK, and p38 signaling pathways [49], [50], [51] [52]. Since TGF-β induced apoptosis upon Akt inhibition was probably independent of Smad3 signaling in HepG2.2.15 cells, impact of these crosstalking pathways was analyzed. Cells were treated with different inhibitors of these pathways: PD98059 (20µM) for MEK1 inhibition, U0126 (10µM) for MEK1/2 inhibition, SP600125 (20µM) for

JNK inhibition and SB203580 (5µM) for p38 inhibition. Treatment with the inhibitors alone did not induce cell death, except for U0126 in HepG2 cells (Figure 4.23). Inhibition of MAPK pathway by either PD98059 or U0126 strongly induced cell death in HepG2 cells upon TGF-β treatment, but only moderately in HepG2.2.15 cells. Concomitant treatment with Akt inhibitor, MAPK pathway inhibitors, and TGF-β, induced strong cell death in both, HepG2 and HepG2.2.15 cells. This suggests that in cells not replicating HBV, activation of MAPK pathway is highly needed to counteract TGF-β induced apoptosis.

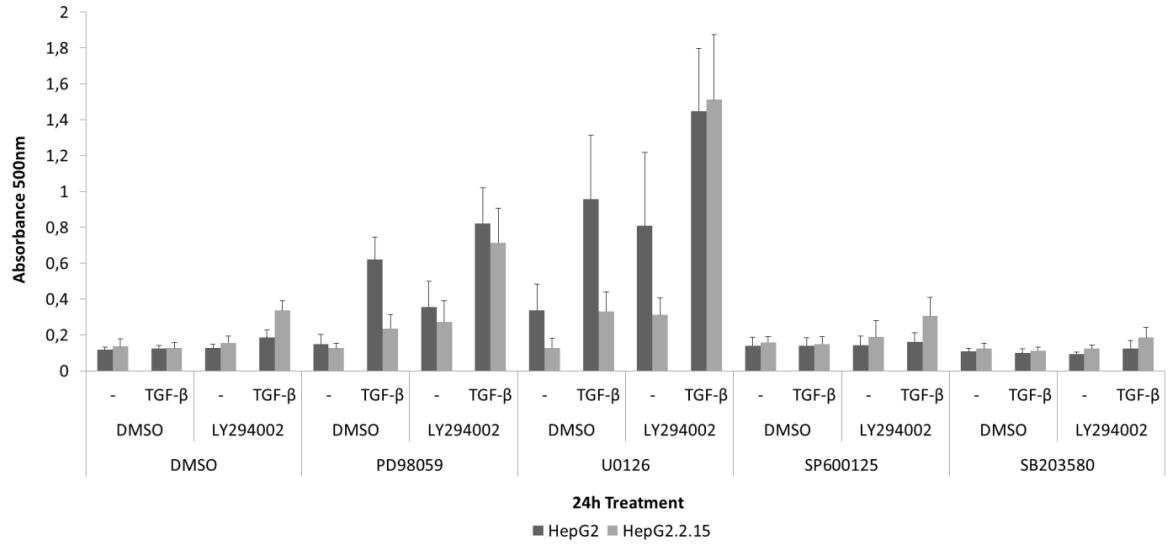

Figure 4.23: Signaling pathway involved in the mediation of TGF-β induced apoptosis upon Akt deactivation. HepG2 and HepG2.2.15 cells were starved overnight and treated for 2h with Akt inhibitor LY294002 (20µM), MEK1 inhibitor PD98059 (20µM), MEK1/2 inhibitor U0126 (10µM), JNK inhibitor SP600125 (20µM), and p38 inhibitor SB203580 (5µM) prior to treatment with TGF-β (5ng/ml) for 24hrs. LDH release was measured in the supernatant.

Treatment with JNK inhibitor did not change apoptotic levels in HepG2 nor in HepG2.2.15 cells. Treatment with p38 inhibitor SB203580 (5µM) decreased TGF-β induced apoptosis upon Akt deactivation in HepG2.2.15 cells (Figure 4.23 and 4.24 A). No impact on LDH release was observed in HepG2 cells upon treatment with SB203580 and Akt inhibitor and TGF-β, respectively (Figure 4.23 and 4.24 A). In summary, only usage of inhibitor SB203580 could reduce TGF-β induced apoptosis upon Akt inhibition in HepG2.2.15 cells.

Immunoblot analysis of protein lysates revealed that treatment with SB203580 reduced Smad3 phosphorylation levels in both, HepG2 and HepG2.2.15 cells (Figure 4.24 B). Strong PARP cleavage was investigated in HepG2.2.15 samples treated with Akt inhibitor and TGF-β, but were reduced upon additional treatment with SB203580. Interestingly, reduced p38 activation by SB203580 was not detectable. Specificity of p-p38 antibody was proven in Huh7 lysate (Figure 4.24 C) suggesting low levels of p-p38 in HepG2 and HepG2.2.15 below antibodies sensitivity. p38 expression levels were equal in both cell lines independent of treatment.

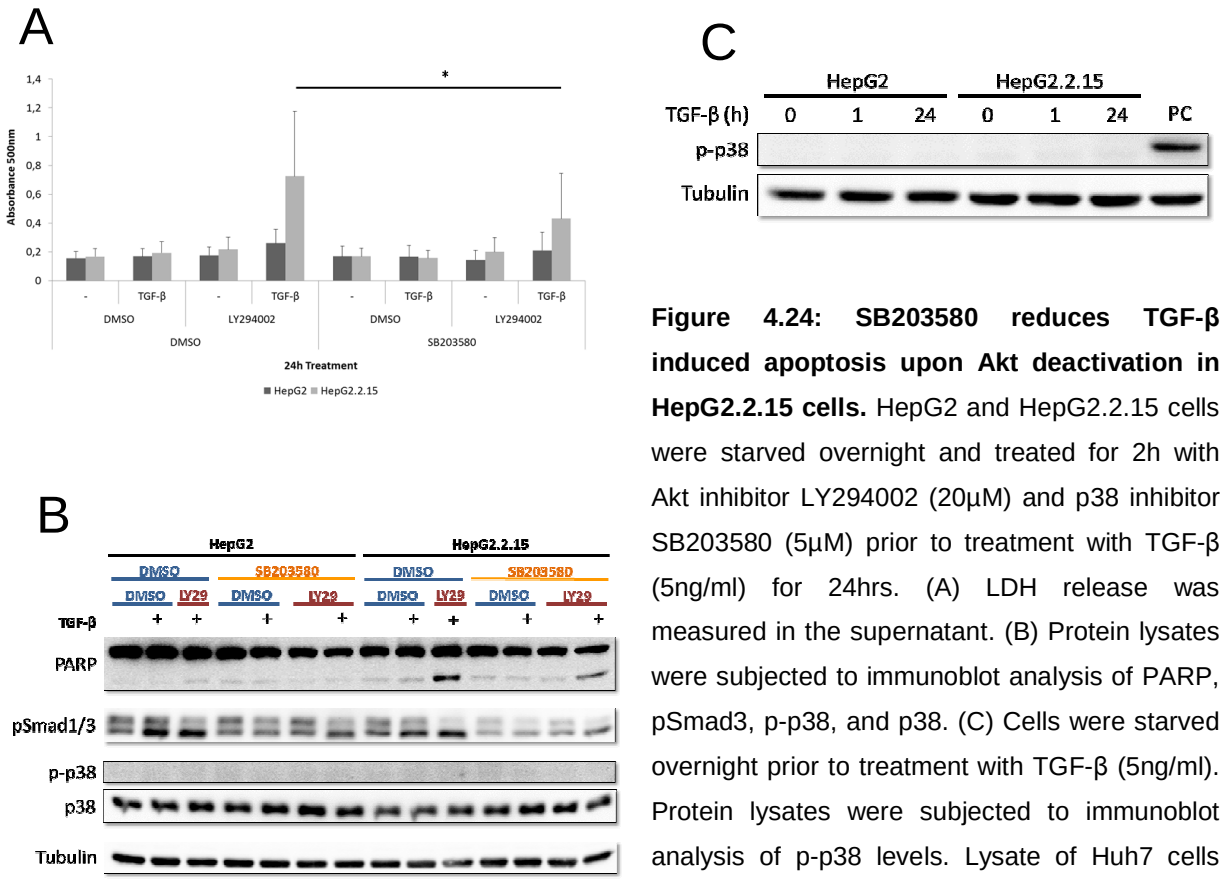

Figure 4.24: SB203580 reduces TGF-β induced apoptosis upon Akt deactivation in HepG2.2.15 cells. HepG2 and HepG2.2.15 cells were starved overnight and treated for 2h with Akt inhibitor LY294002 (20µM) and p38 inhibitor SB203580 (5µM) prior to treatment with TGF-β (5ng/ml) for 24hrs. (A) LDH release was measured in the supernatant. (B) Protein lysates were subjected to immunoblot analysis of PARP, pSmad3, p-p38, and p38. (C) Cells were starved overnight prior to treatment with TGF-β (5ng/ml). Protein lysates were subjected to immunoblot analysis of p-p38 levels. Lysate of Huh7 cells served as positive control (PC). Tubulin served as loading control.

4.1.2.9 Knock-down of p38 does not impair TGF-β induced apoptosis upon Akt inhibition

In line with my result above, it was reported recently [195], that HepG2.2.15 cells do not show basal p38 phosphorylation. Hence, the impact of SB203580 on the reduction of TGF-β induced apoptosis upon Akt deactivation in this study is probably not caused by p38 activation inhibition. To clarify this, cells were transduced with lentivirus carrying siRNA against p38. LDH assay revealed, that there was no reduction in cell death as observed upon usage of SB203580 (Figure 4.25 A). However, as a complete downregulation of p38 was not achieved by siRNA repetition of the experiments (Figure 4.25 B), for future experiments usage of a stable knock out cell line would give more information. Furthermore, it has to be considered, that the SB203580 charge used is not specific for p38 as indicated.

In summary the results presented here do not delineate p38 involvement in TGF-β dependent apoptosis of LY294002 treated HepG2.2.15 cells.

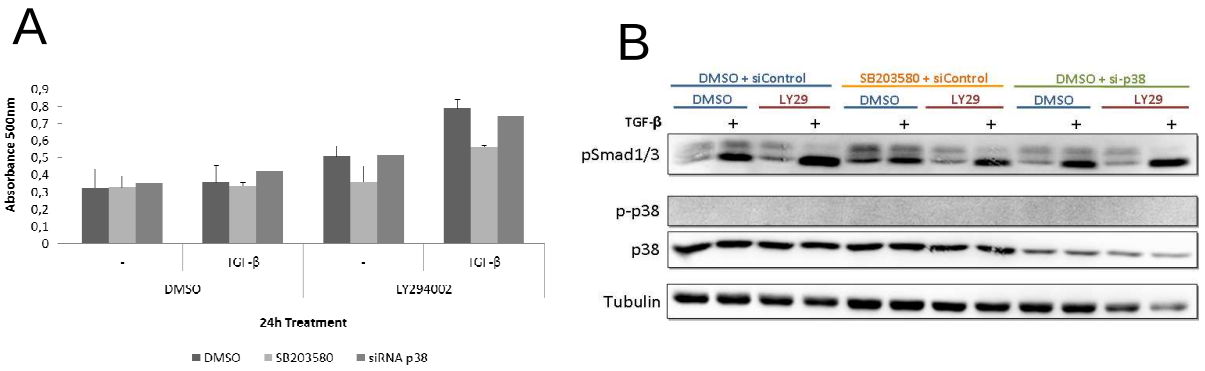

Figure 4.25: p38 knock-down does not impair TGF-β induced apoptosis in HepG2.2.15 cells. HepG2.2.15 cells were transduced with AdLacZ or AdSmad3 for 2hrs, respectively, and starved for 48hrs. Cells were treated with Akt inhibitor LY294002 (20µM) for 2hrs prior to treatment with TGF-β (5ng/ml) for 24hrs. (A) LDH release was measured in the supernatant. (B) Protein lysates were subjected to immunoblot analysis of PARP, pSmad3, and Smad3 (B). Tubulin served as loading control.

4.1.2.10 SB203580 has no negative influence on HBV replication

Viral infection and replication is reported to induce cell stress which might lead to an increase in cell apoptosis [196]. Reducing HBV replication may improve cell stability and viability, turning them more resistant against usage of pro-apoptotic agents like TGF-β. In this study, p38 inhibitor SB203580 decreased TGF-β induced apoptosis upon Akt inhibition in HepG2.2.15 cells. However, a decrease in p38 activation could not be proven. Furthermore, knockdown of p38 had no comparable effect. This raised the question, whether SB203580 has a negative impact on HBV replication itself, which in turn might be responsible for the decrease of TGF-β induced apoptosis upon Akt activation in HepG2.2.15 cells. To investigate this hypothesis, cells were treated with SB203580 and TGF-β, respectively. After 24h, supernatant of cells were investigated for changes in HBsAg secretion, as an indicator of HBV replication. There were no significant changes detectable in secreted HBV antigens (Figure 26). This indicates that SB203580 has no negative impact on HBV replication.

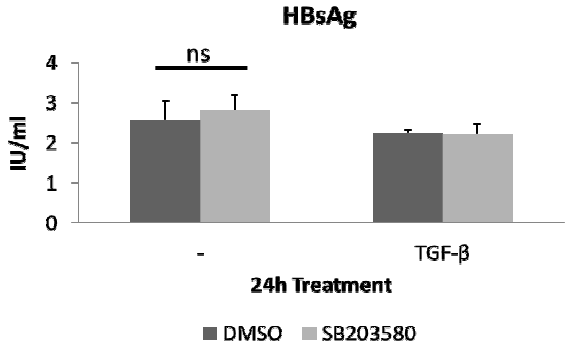

Figure 4.26: SB203580 has no impact on HBV replication. HepG2.2.15 cells were starved overnight and treated with SB203580 (5µM) for 2hrs prior to TGF-β treatment (5ng/ml) for 24hrs.

In summary, HepG2.2.15 cells, able to replicate HBV in contrast to their parental strain HepG2, exhibit reduced Smad3 phosphorylation and transcriptional activity. Elevated Akt activation interfered with TGF-β induced apoptosis, which could be rescued by Akt inhibition. The results suggest that TGF-β induced apoptosis is probably not mediated by canonical Smad3 signaling, as investigated by Smad7 overexpression and Smad3 downregulation. Usage of p38 inhibitor SB203580 was able to reduce TGF-β induced apoptosis upon Akt inhibition. However, lentiviral knockdown of p38 revealed, that p38 might not mediate TGF-β induced apoptosis. A negative effect on HBV replication due to SB203580 was excluded indicating that the effect on TGF-β induced apoptosis of SB203580 might be upstream of p38.

To summarize this chapter, microarray results suggest that HBV is able to interfere with TGF-β signaling pathway, indicated by abrogation of TGF-β target gene expression and reduction of Smad3 phosphorylation levels. HBV infection inhibited TGF-β signaling, but activated the p53 and the mTOR signaling pathways. Further, TGF-β dependent p21 expression was inhibited by HBV infection, indicating inhibition of TGF-β induced apoptosis. In HepG2.2.15 cells, HBV was able to increase Akt activation, thereby probably interfering with TGF-β dependent apoptosis. Increase of Akt activation was reported to be associated with HBV infection before [192] [193]. Further, Conery et al reported that Akt interacts with unphosphorylated Smad3 in the cytoplasm, preventing its phosphorylation and translocation to the nucleus, and thereby inhibiting TGF-β induced apoptosis [54]. Functional analysis of this interaction in this study could not finally explain the mechanistic background. However, it seems obvious, that complex crosstalk of TGF-β mediated apoptotic signals with survival signaling pathways are altered in HBV infected cells inducing survival signaling pathways and inhibiting TGF-β tumor suppressive effects.

4.2 Impact of HCV on TGF-β signaling in human hepatocytes

TGF-β signaling controls tissue homeostasis by cytostatic effects, e.g. apoptosis and proliferation inhibition. In HCV infected patients, TGF-β levels are upregulated [197-199] and in progressed disease stages, it can facilitate development of liver cancer and metastasis. Investigating the impact of HCV infection on TGF-β signaling can lead to efficient HCC treatment in HCV infected patients. However, research using complete and infectious HCV virus is often limited due to safety issues. Elucidating the impact of HCV on TGF-β signaling in more detail can be approached by studying effects of single HCV proteins. One of the most prominent HCV proteins, HCV core protein, is known to have an impact on cell growth, apoptosis and carcinogenesis [125]. In this study the interaction between TGF-β signaling and HCV core protein, and full HCV virus, respectively, was investigated.

4.2.1 HCV core protein impairs TGF-β induced apoptosis in Huh7 cells

As Huh7 cells are sensitive for an apoptotic response upon TGF-β [200], Huh7 cells stably expressing HCV core protein were generated. Cells were transfected with the

plasmid coding for the HCV core protein and selected by Neomycin (400µg/ml) for 21 days until single cell clones had developed. To assure proper expression of HCV core protein, primers flanking the sequence of HCV core protein were used. Control cells, which were stably transfected with empty vector, served as a negative control for subsequent PCR against HCV core protein, as well as control cell line for following experiments (Figure 4.27). Due to these specific mutations, immunoblot detection of overexpressed HCV core protein by a commercially available antibody was not possible in this study. Instead, proper HCV core protein expression was initially proven by PCR.

Figure 4.27: Generation of Huh7-HCV core cells. Huh7 cells were transfected for 6h with 4µg plasmid, encoding HCV core protein, using Lipofectamine 2000. Afterwards, cells were placed on starvation medium for 48h prior to selection of successful transfected cells by Neomycin (400µg/ml). Medium was changed every 2-3 days. Selection took place for 21 days until single cell clones had developed. Expression of HCV core protein was proven by PCR using designed primers flanking the sequence of HCV core protein.

4.2.1.1 HCV core protein interferes with canonical TGF-β signaling

Cheng et al reported that HCV core protein interacts with Smad3 and inhibits its transcriptional activity [120]. To assess interference of HCV core protein with canonical TGF-β signaling in Huh7-HCV core cells, phosphorylation levels and transcriptional activity of Smad3 were investigated. Huh7-HCV core cells and Huh7-empty vector cells were treated with TGF-β for 1 and 24hrs. HCV core protein reduced Smad3 phosphorylation levels from prolonged to transient compared to Huh7-empty vector cells (Figure 4.28). Smad3 expression levels were equal in both cell lines. No differences were seen at Smad2 phosphorylation levels at 24hrs TGF-β.

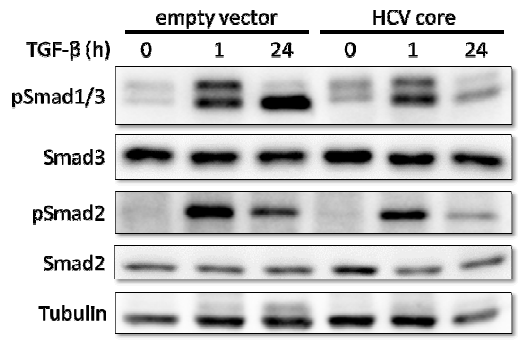

Figure 4.28: HCV core protein reduced Smad3 phosphorylation levels. Cells were starved overnight prior to treatment with TGF-β (5ng/ml) for the indicated time points. Protein lysates were subjected to immunoblot analysis of pSmad3, Smad3, Smad2, and pSmad2. Tubulin served as loading control.

CAGA reporter assay was performed to investigate the impact of impaired Smad3 phosphorylation on its transcriptional activity. A reduced Smad3 transcriptional activity was detected upon TGF-β treatment in Huh7-HCV core cells compared to Huh7-empty vector cells (Figure 4.29) after 6 and 12hrs. This confirmed the results already reported before [120].

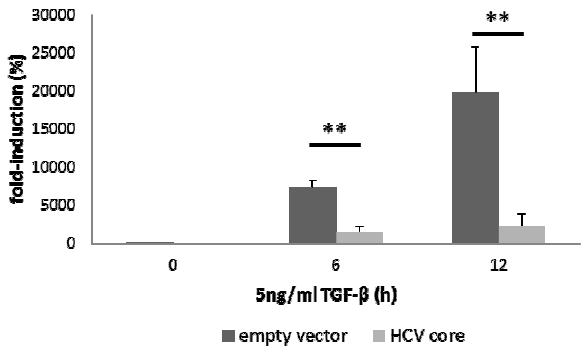

Figure 4.29: Smad3 transcriptional activity is reduced in Huh7-HCV core cells. Cells were cotransfected with plasmid encoding β-Gal and the CAGA sequence, respectively, using Lipofectamine 2000 for 4hrs. Cells were starved overnight prior to treatment with TGF-β (5ng/ml) for the indicated time points. **p<0.02.

Smad7 is a target gene of TGF-β. To investigate the downstream impact of impaired Smad3 phosphorylation and activity on the induction of Smad7 promoter, Huh7-HCV core cells and Huh7-empty vector cells were transfected with plasmid encoding Smad7 promoter. As investigated by qPCR, endogenous Smad7 expression levels were equal in both cell lines (Figure 4.30 A). As expected from downregulated Smad3 activation, reduced Smad7 promoter activity was demonstrated in Huh7-HCV core cells. Upon TGF-β treatment (Figure 4.30 B). This suggests that the interference of HCV core protein and Smad3 indeed have downstream impact on TGF-β induced gene expression.

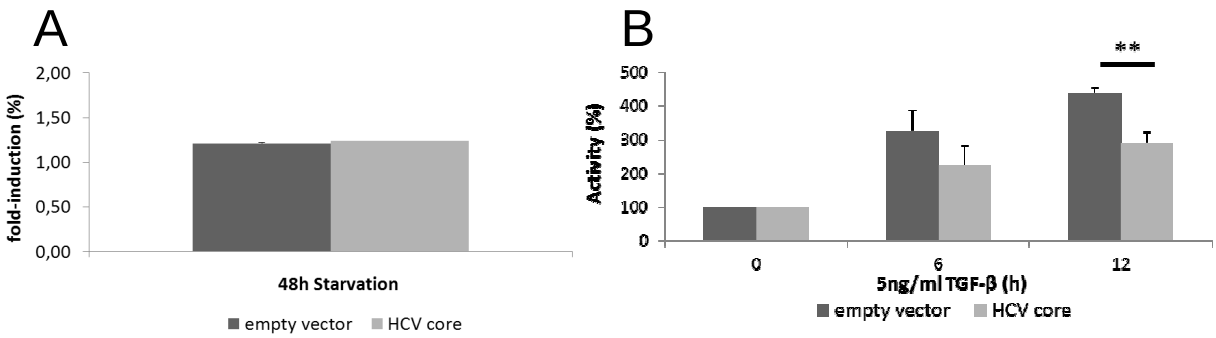

Figure 4.30: HCV core protein reduced Smad7 Promoter Activity. (A) Basal Smad7 expression was investigated by qPCR in Huh7-empty vector and Huh7-HCV core cells after 48h starvation. (B) Smad7 promoter activity assay. Cells were cotransfected with plasmid encoding β-Gal and Smad7 promoter sequence, respectively, using Lipofectamine 2000 for 4hrs. Cells were starved overnight, prior to treatment with 5ng/ml TGF-β for the indicated time points. **p<0.02

4.2.1.2 HCV core protein reduced TGF-β induced apoptosis

It was reported before that HCV core protein and Smad3 interact with each other, which results in reduced TGF-β induced apoptosis [120]. To verify reduced TGF-β induced apoptosis in Huh7-HCV core cells, generated in this study, a LDH assay was performed after 48 and 72hrs TGF-β treatment. In Huh7-HCV core cells LDH release was reduced compared to Huh7-empty vector cells (Figure 4.31). After 72hrs TGF-β treatment, this effect was even more prominent and the number of dead cells increased up to 50%.

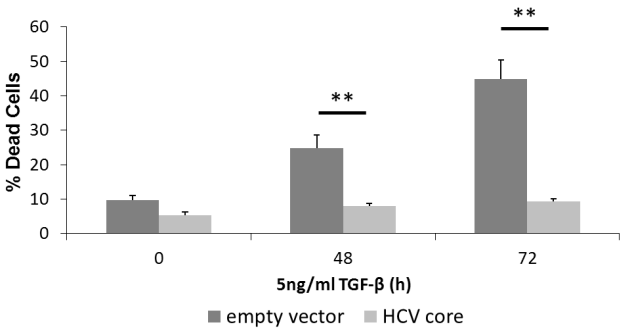

Figure 4.31: HCV core protein reduced TGF-β induced apoptosis. Cells were starved overnight prior to treatment with TGF-β (5ng/ml) for the indicated time points. LDH release was measured in the supernatant. **p<0.02

Reduced TGF-β dependent signaling was also confirmed by investigation of TGF-β target genes responsible for cell cycle arrest. In Huh7-HCV core cells, cell cycle arrest protein p21, as well as p15, were not elevated upon TGF-β for 24hrs as found in Huh7-

empty vector cells (Figure 4.32). Further, the growth arrest and DNA-damage-inducible gene β, GADD45β, was not induced in Huh7-HCV core cells upon TGF-β treatment. These results suggest that interference of HCV core protein with TGF-β signaling results in a reduced apoptotic response upon TGF-β treatment.

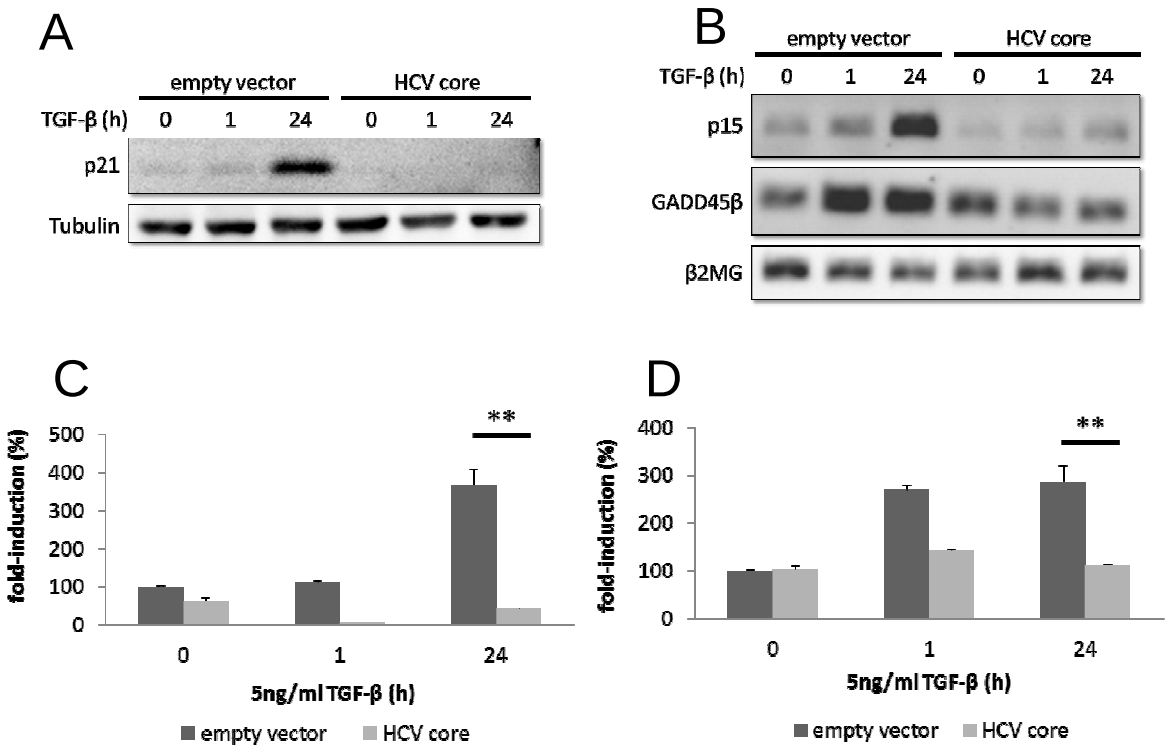

Figure 4.32: HCV core protein abolishes expression of TGF-β dependent cell cycle proteins p21 and p15, as well as of GADD45β. Cells were starved overnight prior to treatment with TGF-β (5ng/ml) for the indicated time points. (A) Protein lysates were subjected to immunoblot analysis of p21. Tubulin served as loading control. (B, C, D) cDNA was subjected to semi-quantitative PCR of p15 and GADD45β. β2MG served as housekeeping gene. Quantitative evaluation of (C) p15 and (D) GADD45β. **p<0.02

4.2.1.3 HCV core protein induces proliferation and migration TGF-β independently

Proliferation and migration are hallmarks of EMT. It was reported before, that HCV core protein induces proliferation [114] and migration [201] [202]. The impact of TGF-β in the course of HCC can shift from tumor suppressor towards tumor promoter and facilitate proliferation and migration [203] [204]. To investigate whether HCV core protein and

TGF-β induce these typical characteristics of EMT, MTT and transwell assays were performed.

As HCV core protein is also reported to induce TGF-β expression [109], basal TGF-β expression levels in both cell lines were measured by qPCR. However, TGF-β expression levels were equal (Figure 4.33 A) excluding enhanced autocrine TGF-β signaling in Huh7-HCV core cells.

Expression of HCV core protein increased basal proliferation about 2-fold (Figure 4.33 B). Treatment with TGF-β had no further impact on proliferation in Huh7-HCV core cells. TGF-β independency of proliferation was shown by usage of TGF-β type I receptor inhibitor SB431542 which did not reduce proliferation of Huh7-HCV core cells and Huh7-empty vector cells.

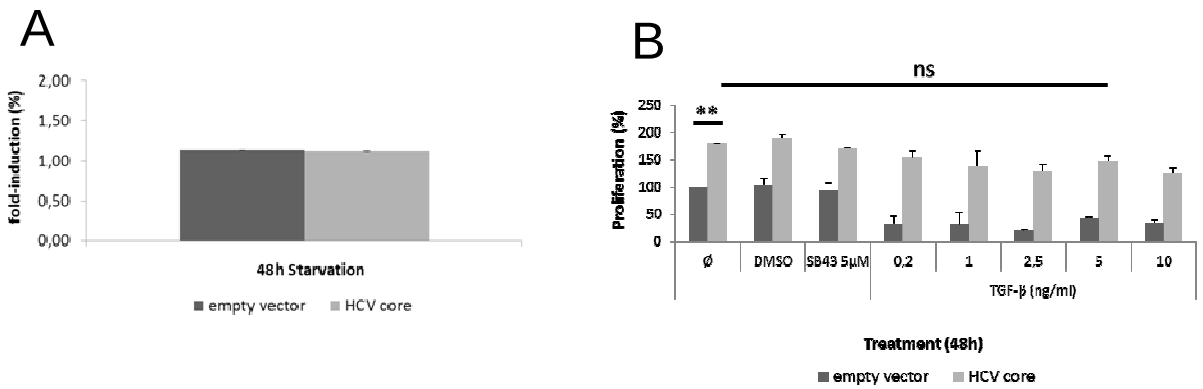

Figure 4.33: Increased proliferation of Huh7-HCV core cells is TGF-β independent. (A) Basal TGF-β expression was investigated by qPCR in Huh7-empty vector and Huh7-HCV core cells after 48h starvation. (B) Cells were starved overnight prior to treatment with TGF-β for 48hrs or type I TGF-β receptor inhibitor SB431542 (SB43). MTT was added to the cells for 4hrs until measurement. ns = not significant. **p<0.02

To assess the impact of HCV core protein and TGF-β in regard to migration, a transwell assay was performed. The basal migration rate of Huh7-HCV core cells was increased around 40% compared to Huh7-empty vector cells (Figure 4.34). However, cell migration in both cell types was not significantly increased upon TGF-β treatment.

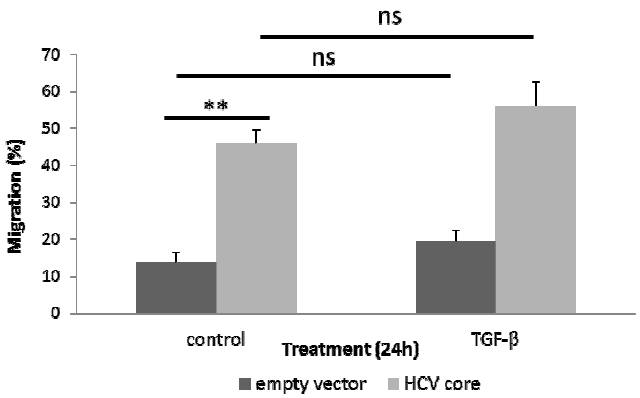

Figure 4.34: Migration is induced in Huh7-HCV core cells. Migration was investigated by transwell assay, comparing TGF-β treated (5ng/ml) to PBS (control) treated cells after 24hrs. ns = not significant. **p<0.02

Although TGF-β has been reported to be involved in the transition of an epithelial cell into a mesenchymal cell during cancer progression [17], induced proliferation and migration were TGF-β independent in Huh7-HCV-core cells. However, the results described here suggest that HCV core protein may induce EMT in Huh7-HCV core cells and direct impact of TGF-β on this cancer related mechanism needs to be investigated.

4.2.1.4 HCV core protein induces Vimentin expression independent of TGF-β

EMT changes a cells morphology and phenotype; cells lose their typical epithelial phenotype and adopt a spindle-shaped phenotype [205]. To investigate EMT in Huh7-HCV core cells, the morphology was regarded and the expression of typical EMT markers was measured.

Expression of HCV core protein altered the morphology of Huh7-HCV core cells compared to Huh7-empty vector cells (Figure 4.35 A). Huh7-HCV core cells had a more rounded morphology and a smoother cell surface compared to Huh7-empty vector cells.

ZO-I delocalization, increased Vimentin expression and stress fiber formation are hallmarks of EMT. To elucidate, whether Huh7-HCV core cells are more prone to TGF-β induced EMT, cells were investigated by immunofluorescence for markers of EMT. After 48h TGF-β treatment, Huh7-HCV core cells displayed no delocalization of ZO-I compared to Huh7-empty vector cells (Figure 4.35 B). The same result holds true for stress fiber formation; only Huh7-empty vector cells had stress fiber formation and ZO-I delocalization after 48hrs TGF-β treatment. However, this effect can also be assigned to

TGF-β induced apoptosis, as apoptosis facilitates stress fiber formation and membrane degradation. EMT is considered to be without signs of apoptosis. Expression of Vimentin, a marker of mesenchymal cells, was not changed upon TGF-β treatment, neither in Huh7-empty vector or Huh7-HCV core cells. However, basal Vimentin expression was higher in Huh7-HCV core cells as in Huh7-empty vector cells. These results suggest that HCV core protein induces EMT in Huh7 cells indicated by a higher basal Vimentin expression.

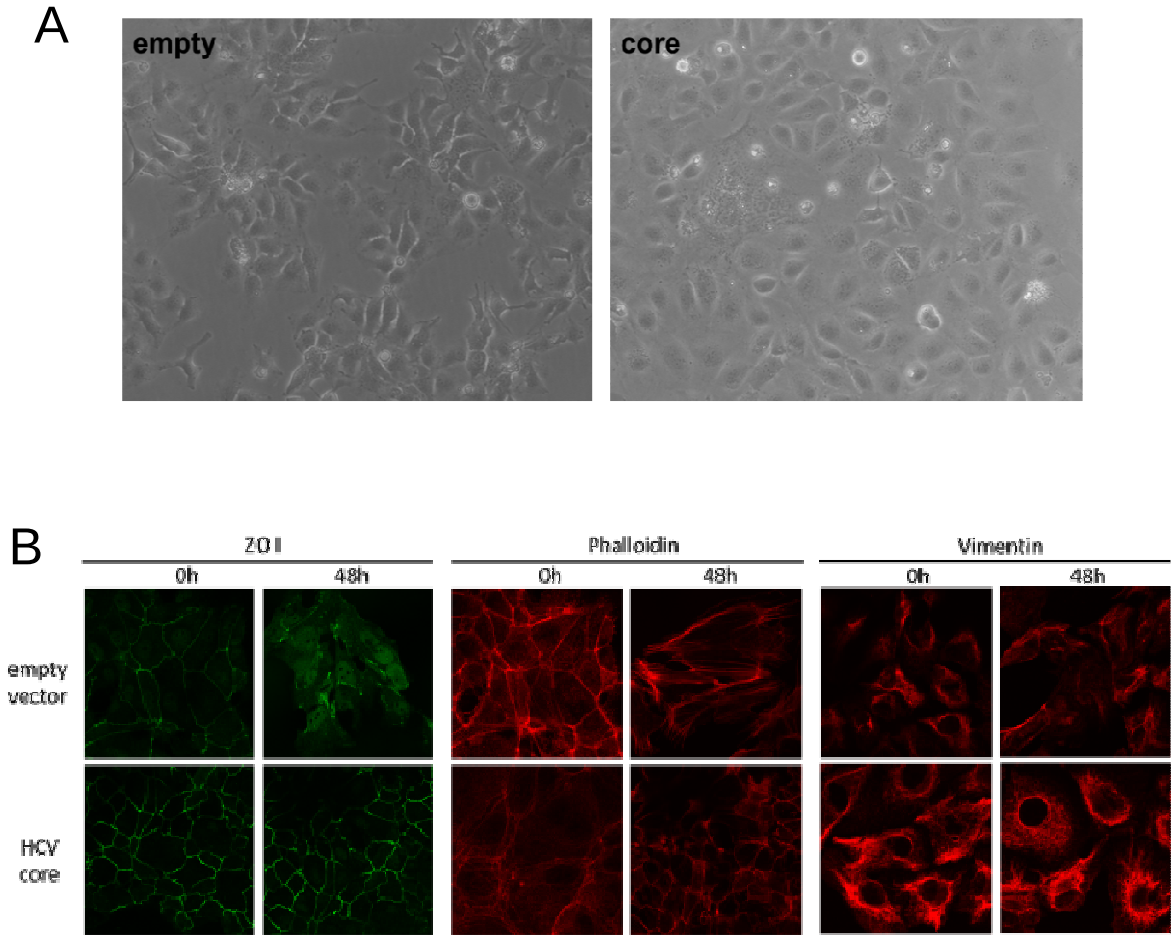

Figure 4.35: HCV core protein induces Vimentin expression. (A) Morphology of cells examined by light microscopy (B) Cells were grown on cover slips and treated with TGF-β or not for 48hrs. For fixation, cells were incubated with 4% PFA (20min) until incubation with indicated antibodies or Phalloidin, respectively.

4.2.1.5 Impact of HCV core protein on other cell signaling pathways and apoptosis related proteins

TGF-β induced apoptosis and Smad signaling is inhibited by HCV core protein in this study. HCV core protein might induce EMT in Huh7 cells, as migration and proliferation, as well as Vimentin expression, were elevated. Hence, it was of major interest to investigate the effect of HCV core protein on other cell signaling pathways, which might lead to increased cell proliferation, migration and survival. Immunoblot analysis showed that protein levels of anti-apoptotic Bcl-2 were higher in Huh7-HCV core cells compared to Huh7-empty vector cells (Figure 4.36 A). The increased levels of Bcl-2 can counteract TGF-β induced apoptosis. No changes were observed in Erk or p38 phosphorylation levels, which play a role in cell proliferation and apoptosis, respectively. Akt signaling plays a role in cell survival by antagonizing apoptotic pathways, like e.g. TGF-β signaling. Huh7-HCV core cells had higher Akt phosphorylation which decreased upon TGF-β treatment. This might indicate that Akt signaling plays no significant role in the inhibition of TGF-β induced apoptosis, and apoptosis has to be inhibited by other mechanisms. E-Cadherin expression, a marker of epithelial cells, was equal in Huh7-HCV core and Huh7-empty vector cells. Interestingly, CTGF a fibrotic cytokine, involved in growth and migration [206] [207] [208], was highly increased in HCV core expressing cells. Although CTGF is a target gene of TGF-β signaling, it was not further increased upon TGF-β treatment (Figure 4.36 B). This suggests that HCV core protein induced CTGF expression is one driver of HCV dependent fibrosis.

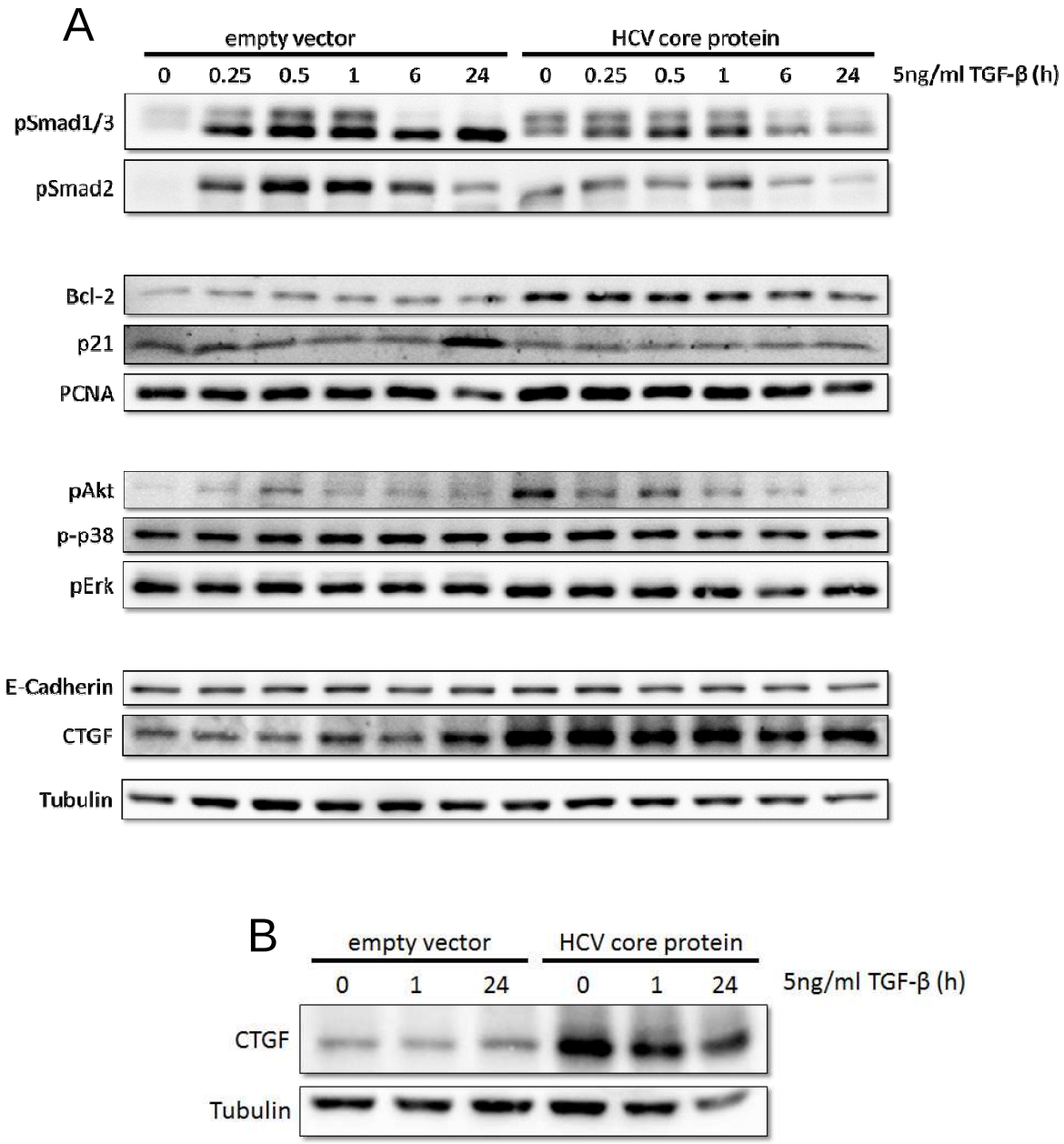

Figure 4.36: HCV core protein induces CTGF expression. Cells were starved overnight prior to treatment with TGF-β (5ng/ml). Protein lysates were subjected to immunoblot analysis of pSmad3, pSmad2, Bcl-2, p21, PCNA, pAkt, p-p38, pErk, E-Cadherin, CTGF levels. Tubulin served as loading control. (A) Impact of HCV core protein on cell signaling pathways. (B) Elevated CTGF expression in Huh7-HCV core cells.

Taken together, results obtained show that HCV core protein interferes with TGF-β tumor-suppressor effects, indicated by the abrogation of TGF-β induced apoptosis and Smad3 signaling. However, investigations further suggest, that the effects of TGF-β are not shifted towards tumor promotion by HCV core protein; rather HCV core protein induces cell proliferation and migration independent of TGF-β. Which pathways or

cellular changes are responsible for induced migration and proliferation has to be clarified in detail. Subsequently, the observation that HCV core protein induced CTGF expression was of great interest. CTGF is known to play a major role in liver fibrosis and elucidation of the cellular mechanism responsible for CTGF expression could have therapeutic value in HCV infection.

4.2.2 Influence of HCV on TGF-β signaling

Overexpression of HCV core protein impaired TGF-β induced apoptosis and reduced Smad3 phosphorylation and transcriptional activity. In order to confirm these results, Huh7.5 cells sensitive for full HCV replication were used. Due to safety reasons, most assays performed in HCV-core cells were not possible to perform with HCV infected Huh7.5 cells. Assays, possible to perform were limited to Immunoblot analysis and luciferase reporter assay.

4.2.2.1 TGF-β has no influence on HCV replication

To assess influence of TGF-β on HCV replication, Huh7.5 cells were electroporated with HCV RNA and treated with TGF-β for 1 or 24hrs, respectively. Huh7.5 cells electroporated with water served as control cells (uninfected). Attached to the HCV RNA is a Renilla luciferase reporter, which allows for the verification of HCV replication in Huh7.5 cells (see 3.1.8). Luciferase reporter activity revealed equal levels of replication within the different experiments. Further, HCV replication was not influenced by TGF-β treatment (Figure 4.37).

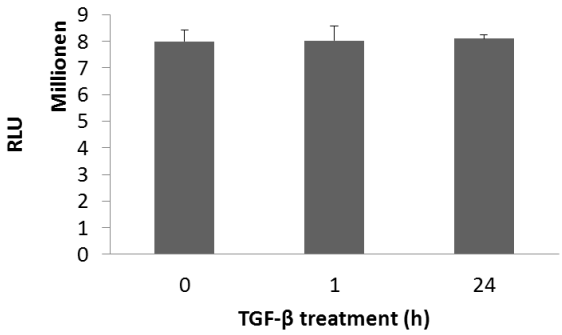

Figure 4.37: HCV replication levels were equal within the different experiments and independent of TGF-β treatment. Cells were electroporated with in vitro transcribed HCV RNA. The next day, cells were treated with TGF-β for the indicated time points and harvested to determine viral replication by Luciferase Assay.

4.2.2.2 Interference of HCV and Smad signaling

To assess interference of HCV replication in Huh7.5 cells with canonical TGF-β signaling, phosphorylation levels of Smad3 were investigated. Therefore, Huh7.5 cells, electroporated with HCV RNA, were treated with TGF-β for 1 or 24hrs, respectively. Huh7.5 cells electroporated with water served as control cells (uninfected). The experiment was performed four times (#1-4), however, Smad3 phosphorylation was not reduced in Huh7.5 cells replicating HCV as found in HCV-core cells (Figure 4.38 A and B). CAGA reporter assay revealed no differences in Smad3 transcriptional activity between control cells and HCV replicating cells (Figure 4.38 C).

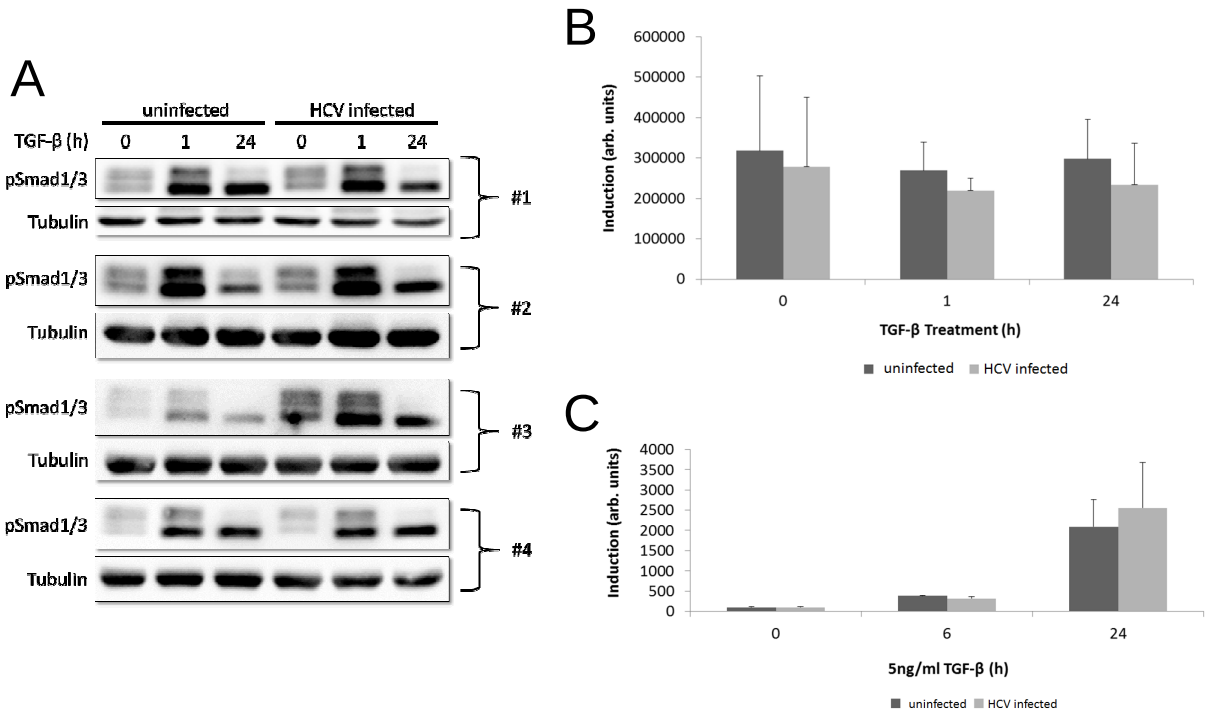

Figure 4.38: Full HCV infection has no impact on Smad3 phosphorylation. Cells were electroporated with in vitro transcribed HCV RNA or water. (A, B) The next day, cells were treated with TGF-β for the indicated time points. Protein lysates of four independent experiments (#1, 2, 3, 4) were subjected to immunoblot analysis of pSmad3. Tubulin served as loading control. (B) Quantitative evaluation of pSmad3. (C) To assess Smad3 transcriptional activity, cells were cotransfected with plasmid encoding β-Gal and the CAGA sequence, respectively, using Lipofectamine 2000 for 4hrs. Cells were starved overnight prior to treatment with TGF-β (5ng/ml) for the indicated time points.

5 DISCUSSION

TGF-β plays a pivotal role in liver cell signaling. In healthy tissue and early stages of liver disease, TGF-β signaling controls tissue homeostasis by promoting cytostatic effects, e.g. apoptosis and proliferation inhibition towards injured and regenerating hepatocytes, and wound closure via activating fibroblasts and stellate cells in injured liver [10] [82]. Chronic HBV and HCV infection have been clearly recognized as an etiological and significant risk factor for HCC development. HBV and HCV induce deregulation of cellular signaling on which the subsequent development of liver inflammation further promotes tumor development [209]. Elucidating the role of HBV/ HCV – TGF-β crosstalk may be beneficial for the development of successful medication. The aim of this study was to investigate the impact of viral infection on TGF-β-dependent signaling pathway, its outcome and progression to HCC. The group of Prof. Dooley has previously shown that in some HCC cell lines with transcriptional Smad3 activity TGF-β induces apoptosis and inhibits cell proliferation. In contrast, TGF-β-dependent cytostatic effects are inhibited in other HCC cell lines which have low Smad3 transcriptional activity. The results obtained in this study hypothesize that HBV and HCV counteract TGF-β tumor suppressive effects by reducing Smad3 activity, thereby facilitating the escape of virus-infected hepatocytes from TGF-β-induced apoptosis.

5.1 Impact of HBV on TGF-β signaling in human hepatocytes

5.1.1 HBV infection impairs TGF-β signaling in primary human hepatocytes

As TGF-β is an important liver cytokine, this study investigated the impact of HBV infection on TGF-β signaling. To elucidate the effects of HBV on host gene expression in the absence of e.g. pathogenic reactions of the immune system and other cell types, isolated PHHs as experimental model were chosen. This also exhibits an advantage compared to former studies using cell lines as model system, as cell lines are transformed cells which have many physiological properties that are altered in the original state of hepatocytes [210]. Although the cultivation of PHHs is more complex and expensive, PHHs are easier to infect with HBV as cell lines. However, if PHHs were used in the past, infection efficiency with HBV was only up to 50% [183]. In the study

presented here HBV infection efficiency of PHHs of nearly 100% was reached, thus representing a valuable model for the investigation of HBV infection and replication impact on the PHH transcriptome.

PHHs from three independent donors were infected with HBV and cultivated for 7 days until treatment with TGF-β for 1 and 24hrs, respectively. It has been reported that HBV has evolved mechanisms to maintain its replication rate at a low level that does not compromise the normal functions of hepatocytes; this allows the host cell to remain healthy. The low replication rate is achieved through the regulation of the level of HBV cccDNA that accumulates in the nucleus [211]. In regard to this, array analysis was performed at the highest peak of viral replication 8 days post infection, as determined in pre-experiments upon measurement of HBsAg and HBeAg levels in the supernatant. RNA was isolated and cRNA was hybridized to Affymetrix Human Genome 1.0 ST Array with subsequent analysis of genomic data by encapsulated R application. To elucidate common and solid influences of HBV infection, gene alterations which were identical in all three donors were taken into account for further studies; donor-specific regulations were disregarded.

Comparison and comprehensive investigation of the alterations in the gene expression profile of PHHs infected with HBV or not revealed that only 12 genes were regulated upon HBV infection. The most upregulated gene was TYMS, actually involved in DNA synthesis and repair. It is induced by the transcription factor LSF/TFCP2. LSF and TYMS have recently been associated to liver cancer proliferation and progression. LSF was found to be overexpressed in HCC cell lines and HCC patients. Stages and grades of the disease correlated with LSF expression levels. Hep3B cells stably overexpressing LSF displayed a significant increase in proliferation, colony formation and Matrigel invasion [155] [156]. The oncogene MDM2, which plays a role in p53 signaling pathway [212] [146], was upregulated as well. p53 signaling pathway is involved in apoptosis and DNA repair, and deregulated p53 signaling can lead to impaired apoptosis and increased proliferation. MDM2 binds to p53 and leads to its degradation. An increase in MDM2 results in the direct inhibition of p53 transcriptional activity, enabling the damaged cells to escape the cell-cycle checkpoint control and to become tumorigenic. MDM2 was shown to be upregulated in several human tumors and reported to be involved in tumor formation. In vitro studies showed, that in Huh7 cells, replicating HBV, deregulation of cell cycle and cell viability was due to increased upregulation of MDM2 [213]. The protein DDB2 was also upregulated upon HBV infection. In contrary, DDB2

was reported to counteract HBx stabilization upon protein interaction [214]. SPATA18 was upregulated, which is known to regulate the quality of mitochondria by repairing or degrading damaged mitochondria. Recently, SPATA18 was reported to be a transcriptional target of p53 and p63. Due to their homology, p63 can compensate for a loss of p53 activity. As in this study p53 activity may be inhibited, upregulation of SPATA18 and maintenance of p53 signaling could be triggered by p63. These results suggest that upon upregulation of DDB2 and SPATA18 the cell tries to minimize the damage of HBV by counteracting HBx stabilization, and to maintain mitochondria quality and p53 signaling.

KEGG Pathway analysis revealed that the p53 signaling pathway was regulated upon HBV infection. Its deregulation was associated to several types of cancer, like glioma, chronic myeloid leukemia, bladder cancer, melanoma, and prostate cancer before. This shows that HBV infection caused carcinogenesis-related changes in host cell gene expression, with p53 signaling pathway as the most prominent one. A similar experiment has been done by Ryu et al. 2006, although PHH infection efficiency was around 50% only in their study. They infected PHHs of 3 independent donors for 8 days [183] and identified 45 downregulated genes, most of them were transcription factors related to RNA polymerase II; around 53 genes were upregulated, including many growth and tumor-related genes, positive genes for tumor growth and proliferation, like GDF11 and NOL1; Hence, gene regulation of uninfected PHHs can cover the impact of HBV. Another study by Iizuka et al. 2002 investigated liver biopsies of HBV-associated HCC. They found 31 upregulated genes, including imprinted genes (H19 and IGF2) and genes related to signal transduction, transcription and metastasis (MAP2K4, MAP2K5, SFI, SIAHBPI, MYOG, MMP9, VEGF) [215]. Another study by Nakanishi et al. 2005 using Huh6 cells transfected with HBV plasmid identified only 14 regulated genes; CD44, high mobility group protein-1, thymosin beta-10, 27kD heat shock protein were upregulated and NM23-H1, caspase-3, BAX were downregulated [216]. In line with our study, much evidence accumulates showing that HBV is well adapted to noncytopathic replication in hepatocytes inducing only minor alteration in gene expression and little or no damage to the cell [143] [65]. It is reported, that HBV has rather the preference to replicate in quiescent cells, since virus replication can be maintained in hepatocytes without signs of apoptosis during prolonged chronic infection [217]. Generally, liver disease is probably produced and induced through immune mediated mechanism aiming on downregulation of virus replication and elimination of infected hepatocytes [144] [145].

Furthermore, no uniform signature of HBV-induced gene alterations could be identified yet. This highlights that HBV infection may cause different outcomes depending on the diverse genetic and epigenetic background of each patient. As identified in the Heat Map analysis, basal gene expression of each donor was quite different. HBV infection had only a minor impact on gene regulation but led to individual alterations in each donor, with only a few common ones. TGF-β treatment had the most impact on gene expression in each donor, but was unexpectedly less influenced by HBV infection. Interestingly, HBV infection decreased the number of TGF-β regulated target genes; this can be due to the impairment of TGF-β signaling pathway by HBV.

Comparison of the gene expression profiles of HBV infected to uninfected PHHs treated with TGF-β identified an upregulation of typical early TGF-β target genes, like Smad7, Serpine1 (PAI-1), p21, or ID1 in uninfected PHHs only [218]. Significant regulated pathways were identified by KEGG pathway analysis. This revealed that TGF-β treatment of uninfected PHHs, but not of HBV infected PHHs, resulted in regulation of TGF-β signaling pathway. In HBV infected PHHs regulation of TGF-β signaling pathway was inhibited. Immunoblot analysis of HBV infected PHHs revealed reduced Smad3 phosphorylation upon 48hrs TGF-β treatment. Investigations of mechanistical details made in HBV replicating HepG2.2.15 cells support the hypothesis of impaired TGF-β signaling and reduced Smad3 phosphorylation levels upon TGF-β treatment. Furthermore, Akt signaling was found to be activated in HepG2.2.15 cells. mTOR, which was found to be regulated in the microarray analysis of HBV infected PHHs, is a downstream target of Akt survival pathway. These results support current knowledge, showing that viruses induce activation of cell survival pathways to inhibit death of cells they infect [89] [188] [189] [190] [191].

In summary, the data are consistent with the hypothesis that HBV infection is noncytopathic, and that carcinogenesis-related transformations are mainly mediated by the impact of the immune system on the infected cell. Results reported before showed that there is no uniform set of genes regulated within the HBV DNA profile during the initial host response to HBV infection [219]. Several reasons account for this. First, obtained microarray results can be different depending on the bioinformatic tools used for analysis of genomic data. Second, usage of different microarrays and different experimental protocols hamper the comparison of genomic analysis of HBV infection among each other. Third, diversity of donor PHHs, due to for example age, gender, race and nutritional status, could result in an unwanted bias. Generalizing gene expression

patterns to establish an overall applicable treatment option upon microarray analysis for HBV-infected patients is apparently impossible. However thorough mechanistical studies of positive hits improve our understanding of TGF-β signaling in HBV infected patients and thus might help to provide personalized therapeutical possibilities in the future. As this study examined a relatively small number of donors, further validation in a larger set of donors will be required. Nevertheless, these results suggest that HBV infection induces the host cell to adopt a malignant phenotype upon TGF-β treatment through alterations in the expression levels of a set of carcinogenesis-related genes and the inhibition of TGF-β signaling pathway regulation. However, the biologic significance of some of the HBV mediated alterations in TGF-β treated hepatocytes still remain unclear. These findings may serve as a first step towards the comprehensive understanding of TGF-β effects on HBV infected hepatocytes and its relation to the development or progression of HCC; And determination of differentially expressed genes may have diagnostic and prognostic value for HBV infected patients with HCC.

5.1.2 Akt deactivation sensitizes HepG2.2.15 cells for TGF-β induced apoptosis

Microarray analysis revealed an impaired TGF-β signaling pathway in HBV infected PHHs upon treatment with TGF-β. Due to the limited availability of PHHs, microarray results were confirmed in HepG2.2.15 cells, replicating HBV. HepG2.2.15 cells showed that TGF-β dependent Smad3 transcriptional activity was reduced and Smad3 phosphorylation levels were transient compared to their parental HepG2 cells. Both, HepG2.2.15 and HepG2 cells were insensitive towards TGF-β induced apoptosis. However, there had to be different regulation mechanisms responsible for apoptosis resistance maybe via additional impact of HBV in HepG2.2.15 cells. One explanation for the cytostatic insensitivity of HepG2.2.15 could be that HBV impair Smad3 activity which ultimately leads to the abrogation of canonical TGF-β signaling responsible for apoptosis. The impaired TGF-β induced apoptosis is further supported by a significant upregulation of Akt signaling pathway in HepG2.2.15 cells. This is in line with the observation of an upregulated mTOR signaling pathway in HBV infected PHHs, which is a downstream target of Akt signaling [220]. Generally Akt signaling plays a role in cell survival by antagonizing apoptotic pathways, like e.g. TGF-β signaling. An increase in Akt activation has been reported to be associated with viral infection [192] [193]. Viral

replication is reported to induce cell stress which leads to an increase in cell apoptosis. To prevent apoptosis of cells they infect, HBV and other viruses upregulate PI3K/Akt signaling pathway, which ultimately may contribute to uncontrolled proliferation of host cells [188] [89] [189] [190]. Shih et al. 2000 reported further, that HBx overexpression in Hep3B cells inhibits TGF-β induced apoptosis through activation of PI3K pathway; however, they did not elucidate the exact mechanism of TGF-β induced apoptosis [89]. Thus, I asked whether upregulation of Akt signaling found in this study may directly counteract TGF-β induced apoptosis. Akt deactivation by its specific inhibitor LY294002 sensitized HepG2.2.15 cells for TGF-β induced apoptosis. Further investigations revealed that induction of apoptosis by TGF-β occurred most likely Smad3 independent, as Smad3 activity was decreased in HepG2.2.15 cells; And inhibition of canonical Smad signaling by overexpression of Smad7, as well as partial knockdown of Smad3, did not decrease TGF-β induced apoptosis upon Akt inhibition. Vice versa, overexpression of Smad3 did not further increase TGF-β induced apoptosis upon Akt inhibition.

It is well accepted that TGF-β is able to exert its effect also via non-canonical signaling pathways. SB203580, a selective inhibitor of p38 MAPK signaling, inhibits the activation of MAPKAPK-2 by p38MAPK and subsequent phosphorylation of HSP27 [221]. Upon usage of SB203580, TGF-β induced apoptosis upon Akt deactivation could be decreased. This suggests in line with previous reports, that TGF-β can mediate its apoptotic effect via the p38 pathway [51] [52]. However, I could not prove p38 phosphorylation by immunoblot analysis. Since there was no basal p38 phosphorylation detectable it was of further interest to investigate whether reduction of TGF-β induced apoptosis upon Akt deactivation is dependent on p38 MAPK or whether it is impaired due to some unspecific effect of the inhibitor SB203580. Therefore, p38 was downregulated in HepG2.2.15 cells by lentivirus carrying siRNA against p38 MAPK. A complete downregulation of p38 was not achieved and this approach did not reduce TGF-β induced apoptosis upon Akt deactivation as compared to usage of SB203580. Thus a satisfying interpretation of the data is not yet possible. So far the data basically suggests that p38 MAPK is not involved in TGF-β induced apoptosis and the effect of SB203580 has to be either upstream of p38 MAPK or is due to another unspecific effect. Unspecificity of SB203580 has already been reported before several times, e.g. SB203580 is able to inhibit Akt phosphorylation and retinoblastoma hyperphosphorylation in interleukin-2-stimulated T cells independently of p38 [222]; SB203580 is able to inhibit cyclooxygenase-1 and -2 non-specifically [223], and it

enhances nuclear factor-kappa B transcriptional activity by a non-specific effect upon ERK pathway [224].

One other unspecific mechanism how SB203580 can exert its TGF-β desensitizing function could be a negative impact on HBV replication, which in turn leads to less cell stress making the cells more resistant towards TGF-β induced apoptosis. Accordingly, Chang et al. published in 2008 that suppression of phosphorylation of p38 by inhibitor SB203580 could inhibit intracellular HBV replication in Huh7 cells transiently transfected with HBV plasmid [225]. However, measurement of HBsAg levels in HepG2.2.15 could not confirm any effect on HBV replication upon treatment with SB203580. High basal p38 phosphorylation levels in Huh7 cells could play a role for this different observation.

In future experiments, one approach to elucidate the influence of HBV replication on TGF-β induced apoptosis upon Akt inhibition could be the usage of HBV-specific 3p-siRNAs, which is able to target HBV RNAs to inhibit HBV replication [226]. Then, HBV could be easily switched “on” and “off” within the same cell model with the same genetic and cellular background.

In summary, the study presented contributes to knowledge about the impact of HBV infection on TGF-β signaling. The obtained results show that the tumor-suppressive effect of TGF-β signaling is abrogated due to upregulation of survival pathways by HBV. HBV induced activation of Akt survival signaling pathway to counteract the cytostatic effects of TGF-β, which could be rescued by inhibition of Akt activation by its inhibitor LY294002. However, mechanistical background of TGF-β induced apoptosis upon Akt deactivation, influence of SB203580 and possible impact of HBV replication could not be solved in this study and remains to be elucidated.

In the future, it is important to understand the molecular mechanism leading to the abrogation of TGF-β induced apoptosis and the upregulation of survival pathways by HBV in order to develop treatment strategies interrupting the responsible pathways to prevent viral carcinogenesis.

5.2 Impact of HCV infection on TGF-β signaling in human hepatocytes

5.2.1 Impact of HCV core protein on TGF-β signaling in Huh7 cells

Huh7 cells represent an ideal model system to investigate the impact of HCV core protein on TGF-β signaling as they are sensitive for cytostatic TGF-β effects and canonical Smad3 dependent signaling is inducible by TGF-β treatment. Huh7 cells were stably transfected with plasmid encoding HCV core protein (kind gift of S. Battaglia, France). This HCV core protein is a natural variant which was isolated from a liver tumor and exhibits a limited number of non-synonymous mutations when compared to a core reference sequence of the same genotype (C1b) [124]. Further, the substitutions found in the HCV core variant were unique to the tumor tissue and not to HCV core protein as found in non-tumor tissue. The tumor sequence did not exhibit any hot-spot mutations, but displayed amino-acid substitutions in the central (aa 59–126) and C-terminal (aa 127–191) domains. Overall, this highlights that even though core is a structural protein and highly conserved within the different genotypes, quasispecies develop during the course of chronic infection due to the high error rate of the RNA-Polymerase. These non-synonymous mutations can be specific to tumor tissue [94].

Several groups reported the influence of HCV core protein expression on TGF-β dependent cell cycle control, resulting in a downregulation of cyclin-dependent kinase inhibitor p21 in HepG2 and in murine fibroblast NIH 3T3 cells, respectively. Mechanistic background of this inhibitory effect was elucidated later, showing decreased DNA binding abilities of Smad3 due to an interaction with HCV core protein [116] [117]. HCV core protein may directly interact with the MH1 domain of Smad3; thereby blocking TGF-β/Smad3 mediated transcriptional activation through interference with the DNA binding ability of Smad3, but not with its nuclear translocation ability. This interaction leads to repression of TGF-β/Smad3 mediated apoptosis as investigated by TGF-β induced p21 promoter activation.

In this study, a reduced Smad3 phosphorylation and transcriptional activity, concomitant with an inhibition of TGF-β induced apoptosis was confirmed in Huh7-HCV core cells. Aim of this study was then to investigate whether and how HCV core protein shifts TGF-β signaling from tumor suppressor towards tumor promoter. As TGF-β can induce

proliferation and migration during disease progression [203] [204], the impact of HCV core protein was analyzed using MTT and transwell assays. Huh7-HCV core cells showed increased proliferation and migration rates, however independent of TGF-β, which might be associated with EMT. Indeed Huh7-HCV core cells exhibited a change in shape and morphology compared to Huh7-empty vector cells. ZO-I delocalization and stress fiber formation are hallmarks of EMT and can be induced upon TGF-β [15] [227]. Huh7-empty vector cells displayed ZO-I delocalization and stress fiber formation upon TGF-β. Apoptosis induces cell stress and membrane degradation, which leads to ZO-I delocalization and stress fiber formation. However, Huh7-empty vector cells are sensitive for TGF-β induced apoptosis and EMT is regarded to be without signs of apoptosis. Another hallmark of EMT is Vimentin expression. Huh7-HCV core cells had higher levels of Vimentin expression as Huh7-empty vector cells, which were however, TGF-β independent. It was reported, that Vimentin negatively regulates HCV core protein levels and HCV production [228] suggesting that modulation of hepatic Vimentin expression may critically influence the outcome of an HCV infection. As mentioned above no antibody is available for detection of mutated HCV core protein, meaning that this hypothesis could not be investigated in this study.

Several investigations consistently found that overexpression of HCV core protein in hepatoma cells results in an upregulation of TGF-β1 protein by activation of MAPK signaling pathways [121] [122] [123]. An upregulation of TGF-β could not be confirmed in this study. However, the expression of CTGF, a downstream target of TGF-β, was highly upregulated in Huh7-HCV core cells, independent of exogenous TGF-β treatment. In contrast, Nagaraja et al. 2012 reported recently, that CTGF upregulation in Huh7.5 cells is dependent on TGF-β through sequential activation of MAP kinase and Smad dependent pathways [229]. Similarly, Shin et al published, that overexpression of HCV core protein promotes liver fibrogenesis via upregulation of CTGF and TGF-β1 in HepG2 cells co-cultured with HSCs [122]. CTGF has been linked to TGF-β pathways in fibro-proliferative diseases before [230]. In regard to this, the role of CTGF upregulation and its suitability for the assessment of liver fibrosis in HCV infected patients was investigated by Kovalenk et al. 2009. It was shown that HCV infected patients had significantly higher serum CTGF levels than healthy controls and that CTGF correlated with the histological degree of liver fibrosis [126]. Overall these data suggest that infection with HCV is associated with an upregulation of CTGF expression.

However, results obtained in this study which are related to the impact of TGF-β in this process are in contrast to results of current literature. This might be due to the different investigational cell models used. In sum, this study shows the ability of the HCV core protein to activate cell survival, while inhibiting apoptotic pathways; it interferes with inhibitors of cell cycle progression, while inducing expression of mitogenic factors, which promote proliferation and migration. Taken together, data obtained in this study suggest that HCV core protein modulates the TGF-β signaling pathway. In Huh7-HCV core cells, reduced Smad3 activity resulted in decreased TGF-β induced cell death, indicating that virus infection provides the escape of neoplastic hepatocytes from the TGF-β cytostatic response, thereby facilitating cancer progression. However, no indices of the induction of tumor promoting TGF-β effects like EMT and migration in dependency of TGF-β and HCV core protein could be shown. Instead, downstream signaling promoting fibrogenesis and tumorigenesis, like enhanced proliferation and migration, increased Vimentin and CTGF expression, was induced by HCV core protein expression and independent of TGF-β.

5.2.2 Interference of HCV with TGF-β signaling

Overexpression of HCV core protein in Huh7 cells revealed impaired Smad3 phosphorylation and transcriptional activity. To investigate these results in a model with full HCV, Huh7.5 cells sensitive for full HCV replication, were used. Huh7.5 cells were electroporated with HCV RNA and treated with TGF-β. HCV replication levels were equal between the different experiments, and TGF-β treatment had no impact on HCV replication. Immunoblot analysis of Smad phosphorylation levels upon TGF-β treatment in Huh7.5 cells revealed no difference between different experiments conducted. CAGA reporter activity assay revealed no changes upon TGF-β treatment in HCV infected or uninfected cells. Rapid development of quasispecies due to the high error rate of the RNA-Polymerase is one reason why HCV replication in vitro is not stable for longer periods. Thus, Huh7.5 cells might be suitable for investigations of HCV replication on either one hand, but on the other hand probably display a rather unstable model for investigations of cell signaling events. In general, these results show that elucidation of HCV induced HCC in cell culture models remain difficult; the development of quasispecies, the high cell death rate induced by the rapid depletion of cellular resources due to the high replication rate, and the safety issues, hamper this research.

REFERENCES

1. El-Serag, H.B., *Epidemiology of viral hepatitis and hepatocellular carcinoma.* Gastroenterology, 2012. 142(6): p. 1264-1273 e1.

2. Bosch, F.X., et al., *Primary liver cancer: worldwide incidence and trends.* Gastroenterology, 2004. 127(5 Suppl 1): p. S5-S16.

3. Ruggeri, M., *Hepatocellular carcinoma: cost-effectiveness of screening. A systematic review.* Risk Manag Healthc Policy, 2012. 5: p. 49-54.

4. Tsoulfas, G., et al., *Surgical treatment for large hepatocellular carcinoma: does size matter?* ANZ J Surg, 2012. 82(7-8): p. 510-7.

5. Tanaka, S. and S. Arii, *Molecular targeted therapies in hepatocellular carcinoma.* Semin Oncol, 2012. 39(4): p. 486-92.

6. Yue, J. and K.M. Mulder, *Requirement of Ras/MAPK pathway activation by transforming growth factor beta for transforming growth factor beta 1 production in a Smad-dependent pathway.* J Biol Chem, 2000. 275(40): p. 30765-73.

7. Ito, N., et al., *Elevated levels of transforming growth factor beta messenger RNA and its polypeptide in human hepatocellular carcinoma.* Cancer Res, 1991. 51(15): p. 4080-3.

8. Kudo, M., et al., *Liver Cancer Working Group report.* Jpn J Clin Oncol, 2010. 40 Suppl 1: p. i19-27.

9. Derynck, R., et al., *Synthesis of messenger RNAs for transforming growth factors alpha and beta and the epidermal growth factor receptor by human tumors.* Cancer Res, 1987. 47(3): p. 707-12.

10. Massague, J., *TGFbeta in Cancer.* Cell, 2008. 134(2): p. 215-30.

11. Shirai, Y., et al., *Plasma transforming growth factor-beta 1 in patients with hepatocellular carcinoma. Comparison with chronic liver diseases.* Cancer, 1994. 73(9): p. 2275-9.

12. Brenner, D.A., *Molecular pathogenesis of liver fibrosis.* Trans Am Clin Climatol Assoc, 2009. 120: p. 361-8.

13. Laiho, M., et al., *Growth inhibition by TGF-beta linked to suppression of retinoblastoma protein phosphorylation.* Cell, 1990. 62(1): p. 175-85.

14. Moses, H.L., E.Y. Yang, and J.A. Pietenpol, *TGF-beta stimulation and inhibition of cell proliferation: new mechanistic insights.* Cell, 1990. 63(2): p. 245-7.

15. van Zijl, F., et al., *Epithelial-mesenchymal transition in hepatocellular carcinoma.* Future Oncol, 2009. 5(8): p. 1169-79.

16. Roberts, A.B. and L.M. Wakefield, *The two faces of transforming growth factor beta in carcinogenesis.* Proc Natl Acad Sci U S A, 2003. 100(15): p. 8621-3.

17. Xu, J., S. Lamouille, and R. Derynck, *TGF-beta-induced epithelial to mesenchymal transition.* Cell Res, 2009. 19(2): p. 156-72.

18. Dooley, S. and P. ten Dijke, *TGF-beta in progression of liver disease.* Cell Tissue Res, 2012. 347(1): p. 245-56.

19. Jou, J. and A.M. Diehl, *Epithelial-mesenchymal transitions and hepatocarcinogenesis.* J Clin Invest, 2010. 120(4): p. 1031-4.

20. Zavadil, J. and E.P. Bottinger, *TGF-beta and epithelial-to-mesenchymal transitions.* Oncogene, 2005. 24(37): p. 5764-74.

21. Heldin, C.H., M. Vanlandewijck, and A. Moustakas, *Regulation of EMT by TGFbeta in cancer.* FEBS Lett, 2012. 586(14): p. 1959-70.

22. Heldin, C.H., M. Landstrom, and A. Moustakas, *Mechanism of TGF-beta signaling to growth arrest, apoptosis, and epithelial-mesenchymal transition.* Curr Opin Cell Biol, 2009. 21(2): p. 166-76.

23. Yamazaki, K., Y. Masugi, and M. Sakamoto, *Molecular pathogenesis of hepatocellular carcinoma: altering transforming growth factor-beta signaling in hepatocarcinogenesis.* Dig Dis, 2011. 29(3): p. 284-8.

24. K. Breitkopf, H.W., S. Dooley, *TGF-β/Smad-signaling in liver cells: Target genes and inhibitors of two parallel pathways.* Signal Transduction, 2006. 6(5): p. 329-337.

25. Derynck, R., R.J. Akhurst, and A. Balmain, *TGF-beta signaling in tumor suppression and cancer progression.* Nat Genet, 2001. 29(2): p. 117-29.

26. Yanagisawa, K., et al., *Induction of apoptosis by Smad3 and down-regulation of Smad3 expression in response to TGF-beta in human normal lung epithelial cells.* Oncogene, 1998. 17(13): p. 1743-7.

27. Yamamura, Y., et al., *Critical role of Smads and AP-1 complex in transforming growth factor-beta -dependent apoptosis.* J Biol Chem, 2000. 275(46): p. 36295-302.

28. Koinuma, D., et al., *Chromatin immunoprecipitation on microarray analysis of Smad2/3 binding sites reveals roles of ETS1 and TFAP2A in transforming growth factor beta signaling.* Mol Cell Biol, 2009. 29(1): p. 172-86.

29. Xu, P., J. Liu, and R. Derynck, *Post-translational regulation of TGF-beta receptor and Smad signaling.* FEBS Lett, 2012. 586(14): p. 1871-84.

30. Moustakas, A. and C.H. Heldin, *Non-Smad TGF-beta signals.* J Cell Sci, 2005. 118(Pt 16): p. 3573-84.

31. Zhang, Y.E., *Non-Smad pathways in TGF-beta signaling.* Cell Res, 2009. 19(1): p. 128-39.

32. Mu, Y., S.K. Gudey, and M. Landstrom, *Non-Smad signaling pathways.* Cell Tissue Res, 2012. 347(1): p. 11-20.

33. Galliher, A.J. and W.P. Schiemann, *Src phosphorylates Tyr284 in TGF-beta type II receptor and regulates TGF-beta stimulation of p38 MAPK during breast cancer cell proliferation and invasion.* Cancer Res, 2007. 67(8): p. 3752-8.

34. Bhowmick, N.A., et al., *Transforming growth factor-beta1 mediates epithelial to mesenchymal transdifferentiation through a RhoA-dependent mechanism.* Mol Biol Cell, 2001. 12(1): p. 27-36.

35. Kretzschmar, M., J. Doody, and J. Massague, *Opposing BMP and EGF signalling pathways converge on the TGF-beta family mediator Smad1.* Nature, 1997. 389(6651): p. 618-22.

36. Pessah, M., et al., *c-Jun interacts with the corepressor TG-interacting factor (TGIF) to suppress Smad2 transcriptional activity.* Proc Natl Acad Sci U S A, 2001. 98(11): p. 6198-203.

37. Davis, B.N., et al., *SMAD proteins control DROSHA-mediated microRNA maturation.* Nature, 2008. 454(7200): p. 56-61.

38. Imoto, S., et al., *Regulation of transforming growth factor-beta signaling by protein inhibitor of activated STAT, PIASy through Smad3.* J Biol Chem, 2003. 278(36): p. 34253-8.

39. Inman, G.J., *Switching TGFbeta from a tumor suppressor to a tumor promoter.* Curr Opin Genet Dev, 2011. 21(1): p. 93-9.

40. Valderrama-Carvajal, H., et al., *Activin/TGF-beta induce apoptosis through Smad-dependent expression of the lipid phosphatase SHIP.* Nat Cell Biol, 2002. 4(12): p. 963-9.

41. Jang, C.W., et al., *TGF-beta induces apoptosis through Smad-mediated expression of DAP-kinase.* Nat Cell Biol, 2002. 4(1): p. 51-8.

42. Cook, T., et al., *Molecular cloning and characterization of TIEG2 reveals a new subfamily of transforming growth factor-beta-inducible Sp1-like zinc finger-encoding genes involved in the regulation of cell growth.* J Biol Chem, 1998. 273(40): p. 25929-36.

43. Ohgushi, M., et al., *Transforming growth factor beta-dependent sequential activation of Smad, Bim, and caspase-9 mediates physiological apoptosis in gastric epithelial cells.* Mol Cell Biol, 2005. 25(22): p. 10017-28.

44. Datto, M.B., et al., *Transforming growth factor beta induces the cyclin-dependent kinase inhibitor p21 through a p53-independent mechanism.* Proc Natl Acad Sci U S A, 1995. 92(12): p. 5545-9.

45. Hannon, G.J. and D. Beach, *p15INK4B is a potential effector of TGF-beta-induced cell cycle arrest.* Nature, 1994. 371(6494): p. 257-61.

46. Yagi, K., et al., *c-myc is a downstream target of the Smad pathway.* J Biol Chem, 2002. 277(1): p. 854-61.

47. Shima, Y., et al., *Activation of caspase-8 in transforming growth factor-beta-induced apoptosis of human hepatoma cells.* Hepatology, 1999. 30(5): p. 1215-22.

48. Takekawa, M., et al., *Smad-dependent GADD45beta expression mediates delayed activation of p38 MAP kinase by TGF-beta.* EMBO J, 2002. 21(23): p. 6473-82.

49. Perlman, R., et al., *TGF-beta-induced apoptosis is mediated by the adapter protein Daxx that facilitates JNK activation.* Nat Cell Biol, 2001. 3(8): p. 708-14.

50. Hofmann, T.G., et al., *HIPK2 regulates transforming growth factor-beta-induced c-Jun NH(2)-terminal kinase activation and apoptosis in human hepatoma cells.* Cancer Res, 2003. 63(23): p. 8271-7.

51. Sorrentino, A., et al., *The type I TGF-beta receptor engages TRAF6 to activate TAK1 in a receptor kinase-independent manner.* Nat Cell Biol, 2008. 10(10): p. 1199-207.

52. Yamashita, M., et al., *TRAF6 mediates Smad-independent activation of JNK and p38 by TGF-beta.* Mol Cell, 2008. 31(6): p. 918-24.

53. Chen, R.H., et al., *Suppression of transforming growth factor-beta-induced apoptosis through a phosphatidylinositol 3-kinase/Akt-dependent pathway.* Oncogene, 1998. 17(15): p. 1959-68.

54. Conery, A.R., et al., *Akt interacts directly with Smad3 to regulate the sensitivity to TGF-beta induced apoptosis.* Nat Cell Biol, 2004. 6(4): p. 366-72.

55. Remy, I., A. Montmarquette, and S.W. Michnick, *PKB/Akt modulates TGF-beta signalling through a direct interaction with Smad3.* Nat Cell Biol, 2004. 6(4): p. 358-65.

56. Song, K., et al., *Novel roles of Akt and mTOR in suppressing TGF-beta/ALK5-mediated Smad3 activation.* EMBO J, 2006. 25(1): p. 58-69.

57. Seoane, J., et al., *Integration of Smad and forkhead pathways in the control of neuroepithelial and glioblastoma cell proliferation.* Cell, 2004. 117(2): p. 211-23.

58. Liu, X., et al., *Transforming growth factor beta-induced phosphorylation of Smad3 is required for growth inhibition and transcriptional induction in epithelial cells.* Proc Natl Acad Sci U S A, 1997. 94(20): p. 10669-74.

59. Wildey, G.M., S. Patil, and P.H. Howe, *Smad3 potentiates transforming growth factor beta (TGFbeta)-induced apoptosis and expression of the BH3-only protein Bim in WEHI 231 B lymphocytes.* J Biol Chem, 2003. 278(20): p. 18069-77.

60. Dane, D.S., C.H. Cameron, and M. Briggs, *Virus-like particles in serum of patients with Australia-antigen-associated hepatitis.* Lancet, 1970. 1(7649): p. 695-8.

61. Hollinger, F.B. and D.T. Lau, *Hepatitis B: the pathway to recovery through treatment.* Gastroenterol Clin North Am, 2006. 35(4): p. 895-931.

62. Neuveut, C., Y. Wei, and M.A. Buendia, *Mechanisms of HBV-related hepatocarcinogenesis.* J Hepatol, 2010. 52(4): p. 594-604.

63. Dienstag, J.L., *Hepatitis B virus infection.* N Engl J Med, 2008. 359(14): p. 1486-500.

64. Gripon, P., C. Diot, and C. Guguen-Guillouzo, *Reproducible high level infection of cultured adult human hepatocytes by hepatitis B virus: effect of polyethylene glycol on adsorption and penetration.* Virology, 1993. 192(2): p. 534-40.

65. Rumin, S., et al., *Long-term productive episomal hepatitis B virus replication in primary cultures of adult human hepatocytes infected in vitro.* J Viral Hepat, 1996. 3(5): p. 227-38.

66. Sureau, C., et al., *Production of hepatitis B virus by a differentiated human hepatoma cell line after transfection with cloned circular HBV DNA.* Cell, 1986. 47(1): p. 37-47.

67. Sells, M.A., M.L. Chen, and G. Acs, *Production of hepatitis B virus particles in Hep G2 cells transfected with cloned hepatitis B virus DNA.* Proc Natl Acad Sci U S A, 1987. 84(4): p. 1005-9.

68. Gripon, P., et al., *Infection of a human hepatoma cell line by hepatitis B virus.* Proc Natl Acad Sci U S A, 2002. 99(24): p. 15655-60.

69. Nassal, M., *Hepatitis B virus replication: novel roles for virus-host interactions.* Intervirology, 1999. 42(2-3): p. 100-16.

70. Arbuthnot, P. and M. Kew, *Hepatitis B virus and hepatocellular carcinoma.* Int J Exp Pathol, 2001. 82(2): p. 77-100.

71. Kramvis, A., M. Kew, and G. Francois, *Hepatitis B virus genotypes.* Vaccine, 2005. 23(19): p. 2409-23.

72. Magnius, L.O. and H. Norder, *Subtypes, genotypes and molecular epidemiology of the hepatitis B virus as reflected by sequence variability of the S-gene.* Intervirology, 1995. 38(1-2): p. 24-34.

73. Kao, J.H., et al., *Hepatitis B genotypes correlate with clinical outcomes in patients with chronic hepatitis B.* Gastroenterology, 2000. 118(3): p. 554-9.

74. Brechot, C., et al., *State of hepatitis B virus DNA in hepatocytes of patients with hepatitis B surface antigen-positive and -negative liver diseases.* Proc Natl Acad Sci U S A, 1981. 78(6): p. 3906-10.

75. Takada, S., et al., *Structural rearrangement of integrated hepatitis B virus DNA as well as cellular flanking DNA is present in chronically infected hepatic tissues.* J Virol, 1990. 64(2): p. 822-8.

76. Brechot, C., et al., *Persistent hepatitis B virus infection in subjects without hepatitis B surface antigen: clinically significant or purely "occult"?* Hepatology, 2001. 34(1): p. 194-203.

77. Murakami, Y., et al., *Large scaled analysis of hepatitis B virus (HBV) DNA integration in HBV related hepatocellular carcinomas.* Gut, 2005. 54(8): p. 1162-8.

78. Brechot, C., *Pathogenesis of hepatitis B virus-related hepatocellular carcinoma: old and new paradigms.* Gastroenterology, 2004. 127(5 Suppl 1): p. S56-61.

79. Bonilla Guerrero, R. and L.R. Roberts, *The role of hepatitis B virus integrations in the pathogenesis of human hepatocellular carcinoma.* J Hepatol, 2005. 42(5): p. 760-77.

80. Yeh, C.T., *Hepatitis B virus X protein: searching for a role in hepatocarcinogenesis.* J Gastroenterol Hepatol, 2000. 15(4): p. 339-41.

81. Loffler-Mary, H., M. Werr, and R. Prange, *Sequence-specific repression of cotranslational translocation of the hepatitis B virus envelope proteins coincides with binding of heat shock protein Hsc70.* Virology, 1997. 235(1): p. 144-52.

82. Gressner, A.M., et al., *Roles of TGF-beta in hepatic fibrosis.* Front Biosci, 2002. 7: p. d793-807.

83. Flisiak, R., et al., *Plasma transforming growth factor-beta(1) in acute viral hepatitis.* Med Sci Monit, 2005. 11(6): p. CR304-308.

84. Guo, G.H., et al., *Hepatitis B virus X protein promotes proliferation and upregulates TGF-beta1 and CTGF in human hepatic stellate cell line, LX-2.* Hepatobiliary Pancreat Dis Int, 2009. 8(1): p. 59-64.

85. Dong, Z.Z., et al., *Clinical impact of plasma TGF-beta1 and circulating TGF-beta1 mRNA in diagnosis of hepatocellular carcinoma.* Hepatobiliary Pancreat Dis Int, 2008. 7(3): p. 288-95.

86. Yoo, Y.D., et al., *Regulation of transforming growth factor-beta 1 expression by the hepatitis B virus (HBV) X transactivator. Role in HBV pathogenesis.* J Clin Invest, 1996. 97(2): p. 388-95.

87. Pan, J., M. Clayton, and M.A. Feitelson, *Hepatitis B virus X antigen promotes transforming growth factor-beta1 (TGF-beta1) activity by up-regulation of TGF-beta1 and down-regulation of alpha2-macroglobulin.* J Gen Virol, 2004. 85(Pt 2): p. 275-82.

88. Oshikawa, O., et al., *The effect of hepatitis B virus X gene expression on response to growth inhibition by transforming growth factor-beta 1.* Biochem Biophys Res Commun, 1996. 222(3): p. 770-3.

89. Shih, W.L., et al., *Hepatitis B virus X protein inhibits transforming growth factor-beta -induced apoptosis through the activation of phosphatidylinositol 3-kinase pathway.* J Biol Chem, 2000. 275(33): p. 25858-64.

90. Lee, D.K., et al., *The hepatitis B virus encoded oncoprotein pX amplifies TGF-beta family signaling through direct interaction with Smad4: potential mechanism of hepatitis B virus-induced liver fibrosis.* Genes Dev, 2001. 15(4): p. 455-66.

91. Choo, Q.L., et al., *Isolation of a cDNA clone derived from a blood-borne non-A, non-B viral hepatitis genome.* Science, 1989. 244(4902): p. 359-62.

92. Clement, S., S. Pascarella, and F. Negro, *Hepatitis C virus infection: molecular pathways to steatosis, insulin resistance and oxidative stress.* Viruses, 2009. 1(2): p. 126-43.

93. Fung, J., C.L. Lai, and M.F. Yuen, *Hepatitis B and C virus-related carcinogenesis.* Clin Microbiol Infect, 2009. 15(11): p. 964-70.

94. Schlutter, J., *Therapeutics: new drugs hit the target.* Nature, 2011. 474(7350): p. S5-7.

95. Kronenberger, B. and S. Zeuzem, *New developments in HCV therapy.* J Viral Hepat, 2012. 19 Suppl 1: p. 48-51.

96. Suzuki, T., *Assembly of hepatitis C virus particles.* Microbiol Immunol, 2011. 55(1): p. 12-8.

97. Thimme, R., et al., *Viral and immunological determinants of hepatitis C virus clearance, persistence, and disease.* Proc Natl Acad Sci U S A, 2002. 99(24): p. 15661-8.

98. Ruster, B., et al., *Comparative sequence analysis of the core- and NS5-region of hepatitis C virus from tumor and adjacent non-tumor tissue.* J Med Virol, 2001. 63(2): p. 128-34.

99. Alam, S.S., et al., *Hepatitis C virus quasispecies in cancerous and noncancerous hepatic lesions: the core protein-encoding region.* Acta Med Okayama, 2002. 56(3): p. 141-7.

100. Anzola, M., *Hepatocellular carcinoma: role of hepatitis B and hepatitis C viruses proteins in hepatocarcinogenesis.* J Viral Hepat, 2004. 11(5): p. 383-93.

101. Lohmann, V., et al., *Replication of subgenomic hepatitis C virus RNAs in a hepatoma cell line.* Science, 1999. 285(5424): p. 110-3.

102. Banaudha, K., et al., *Primary hepatocyte culture supports hepatitis C virus replication: a model for infection-associated hepatocarcinogenesis.* Hepatology, 2010. 51(6): p. 1922-32.

103. Dabrowska, M.M., A. Panasiuk, and R. Flisiak, *Signal transduction pathways in liver and the influence of hepatitis C virus infection on their activities.* World J Gastroenterol, 2009. 15(18): p. 2184-9.

104. Rice, C.M., *New insights into HCV replication: potential antiviral targets.* Top Antivir Med, 2011. 19(3): p. 117-20.

105. Farinati, F., et al., *Oxidative damage, pro-inflammatory cytokines, TGF-alpha and c-myc in chronic HCV-related hepatitis and cirrhosis.* World J Gastroenterol, 2006. 12(13): p. 2065-9.

106. Farinati, F., et al., *Oxidative DNA damage in circulating leukocytes occurs as an early event in chronic HCV infection.* Free Radic Biol Med, 1999. 27(11-12): p. 1284-91.

107. Jain, S.K., et al., *Oxidative stress in chronic hepatitis C: not just a feature of late stage disease.* J Hepatol, 2002. 36(6): p. 805-11.

108. Wu, W.S., *The signaling mechanism of ROS in tumor progression.* Cancer Metastasis Rev, 2006. 25(4): p. 695-705.

109. Lin, W., et al., *Hepatitis C virus regulates transforming growth factor beta1 production through the generation of reactive oxygen species in a nuclear factor kappaB-dependent manner.* Gastroenterology, 2010. 138(7): p. 2509-18, 2518 e1.

110. Wilson, G.K., et al., *A dual role for hypoxia inducible factor-1alpha in the hepatitis C virus lifecycle and hepatoma migration.* J Hepatol, 2012. 56(4): p. 803-9.

111. Roingeard, P. and C. Hourioux, *Hepatitis C virus core protein, lipid droplets and steatosis.* J Viral Hepat, 2008. 15(3): p. 157-64.

112. Dubuisson, J., *Hepatitis C virus proteins.* World J Gastroenterol, 2007. 13(17): p. 2406-15.

113. Krekulova, L., V. Rehak, and L.W. Riley, *Structure and functions of hepatitis C virus proteins: 15 years after.* Folia Microbiol (Praha), 2006. 51(6): p. 665-80.

114. Erhardt, A., et al., *Hepatitis C virus core protein induces cell proliferation and activates ERK, JNK, and p38 MAP kinases together with the MAP kinase phosphatase MKP-1 in a HepG2 Tet-Off cell line.* Virology, 2002. 292(2): p. 272-84.

115. Nakamura, H., et al., *HCV core protein promotes heparin binding EGF-like growth factor expression and activates Akt.* Hepatol Res, 2011. 41(5): p. 455-62.

116. Dubourdeau, M., et al., *Infection of HepG2 cells with recombinant adenovirus encoding the HCV core protein induces p21(WAF1) down-regulation -- effect of transforming growth factor beta.* J Hepatol, 2002. 37(4): p. 486-92.

117. Lee, M.N., et al., *Hepatitis C virus core protein represses the p21 promoter through inhibition of a TGF-beta pathway.* J Gen Virol, 2002. 83(Pt 9): p. 2145-51.

118. Kwun, H.J. and K.L. Jang, *Dual effects of hepatitis C virus Core protein on the transcription of cyclin-dependent kinase inhibitor p21 gene.* J Viral Hepat, 2003. 10(4): p. 249-55.

119. Shrivastava, A., et al., *Ectopic expression of hepatitis C virus core protein differentially regulates nuclear transcription factors.* J Virol, 1998. 72(12): p. 9722-8.

120. Cheng, P.L., et al., *Hepatitis C viral proteins interact with Smad3 and differentially regulate TGF-beta/Smad3-mediated transcriptional activation.* Oncogene, 2004. 23(47): p. 7821-38.

121. Taniguchi, H., et al., *Hepatitis C virus core protein upregulates transforming growth factor-beta 1 transcription.* J Med Virol, 2004. 72(1): p. 52-9.

122. Shin, J.Y., et al., *HCV core protein promotes liver fibrogenesis via up-regulation of CTGF with TGF-beta1.* Exp Mol Med, 2005. 37(2): p. 138-45.

123. Boudreau, H.E., et al., *Hepatitis C virus (HCV) proteins induce NADPH oxidase 4 expression in a transforming growth factor beta-dependent manner: a new contributor to HCV-induced oxidative stress.* J Virol, 2009. 83(24): p. 12934-46.

124. Pavio, N., et al., *Hepatitis C virus core variants isolated from liver tumor but not from adjacent non-tumor tissue interact with Smad3 and inhibit the TGF-beta pathway.* Oncogene, 2005. 24(40): p. 6119-32.

125. Battaglia, S., et al., *Liver cancer-derived hepatitis C virus core proteins shift TGF-beta responses from tumor suppression to epithelial-mesenchymal transition.* PLoS One, 2009. 4(2): p. e4355.

126. Kovalenko, E., et al., *Validation of connective tissue growth factor (CTGF/CCN2) and its gene polymorphisms as noninvasive biomarkers for the assessment of liver fibrosis.* J Viral Hepat, 2009. 16(9): p. 612-20.

127. Wu, C.F., Y.L. Lin, and Y.T. Huang, *Hepatitis C virus core protein stimulates fibrogenesis in hepatic stellate cells involving the obese receptor.* J Cell Biochem, 2013. 114(3): p. 541-50.

128. Aden, D.P., et al., *Controlled synthesis of HBsAg in a differentiated human liver carcinoma-derived cell line.* Nature, 1979. 282(5739): p. 615-6.

129. Buenemann, C.L., et al., *Transforming growth factor-beta1-induced Smad signaling, cell-cycle arrest and apoptosis in hepatoma cells.* Carcinogenesis, 2001. 22(3): p. 447-52.

130. Farshid, M. and E. Tabor, *Expression of oncogenes and tumor suppressor genes in human hepatocellular carcinoma and hepatoblastoma cell lines.* J Med Virol, 1992. 38(4): p. 235-9.

131. Nakabayashi, H., et al., *Growth of human hepatoma cells lines with differentiated functions in chemically defined medium.* Cancer Res, 1982. 42(9): p. 3858-63.

132. Shibuya, H., et al., *TAB1: an activator of the TAK1 MAPKKK in TGF-beta signal transduction.* Science, 1996. 272(5265): p. 1179-82.

133. Blight, K.J., J.A. McKeating, and C.M. Rice, *Highly permissive cell lines for subgenomic and genomic hepatitis C virus RNA replication.* J Virol, 2002. 76(24): p. 13001-14.

134. Weiss, T.S., et al., *Cellular damage to human hepatocytes through repeated application of 5-aminolevulinic acid.* J Hepatol, 2003. 38(4): p. 476-82.

135. Dennler, S., et al., *Direct binding of Smad3 and Smad4 to critical TGF beta-inducible elements in the promoter of human plasminogen activator inhibitor-type 1 gene.* EMBO J, 1998. 17(11): p. 3091-100.

136. Stopa, M., et al., *Participation of Smad2, Smad3, and Smad4 in transforming growth factor beta (TGF-beta)-induced activation of Smad7. THE TGF-beta response element of the promoter requires functional Smad binding element and E-box sequences for transcriptional regulation.* J Biol Chem, 2000. 275(38): p. 29308-17.

137. Ni, Y., et al., *The pre-s2 domain of the hepatitis B virus is dispensable for infectivity but serves a spacer function for L-protein-connected virus assembly.* J Virol, 2010. 84(8): p. 3879-88.

138. Engelke, M., et al., *Characterization of a hepatitis B and hepatitis delta virus receptor binding site.* Hepatology, 2006. 43(4): p. 750-60.

139. Ganzinger, M., et al., *An encapsulated R application for the guided analysis of genomic data.* Stud Health Technol Inform, 2012. 180: p. 1144-6.

140. Brechot, C., et al., *Impact of HBV, HCV and GBV-C/HGV on hepatocellular carcinomas in Europe: results of a European concerted action.* J Hepatol, 1998. 29(2): p. 173-83.

141. Bova, R., M.R. Micheli, and S. Nardiello, *Molecular biology of hepatocellular carcinoma and hepatitis B virus association.* Int J Clin Lab Res, 1991. 21(2): p. 190-8.

142. Schulze, A., et al., *Hepatocyte polarization is essential for the productive entry of the hepatitis B virus.* Hepatology, 2012. 55(2): p. 373-83.

143. Hajjou, M., et al., *cDNA microarray analysis of HBV transgenic mouse liver identifies genes in lipid biosynthetic and growth control pathways affected by HBV.* J Med Virol, 2005. 77(1): p. 57-65.

144. Rehermann, B., et al., *The cytotoxic T lymphocyte response to multiple hepatitis B virus polymerase epitopes during and after acute viral hepatitis.* J Exp Med, 1995. 181(3): p. 1047-58.

145. Guidotti, L.G., et al., *Viral clearance without destruction of infected cells during acute HBV infection.* Science, 1999. 284(5415): p. 825-9.

146. Pei, D., Y. Zhang, and J. Zheng, *Regulation of p53: a collaboration between Mdm2 and Mdmx.* Oncotarget, 2012. 3(3): p. 228-35.

147. Levine, A.J., W. Hu, and Z. Feng, *The P53 pathway: what questions remain to be explored?* Cell Death Differ, 2006. 13(6): p. 1027-36.

148. Sherr, C.J. and J.M. Roberts, *CDK inhibitors: positive and negative regulators of G1-phase progression.* Genes Dev, 1999. 13(12): p. 1501-12.

149. Nakada, M., et al., *Aberrant signaling pathways in glioma.* Cancers (Basel), 2011. 3(3): p. 3242-78.

150. Di Bacco, A., et al., *Molecular abnormalities in chronic myeloid leukemia: deregulation of cell growth and apoptosis.* Oncologist, 2000. 5(5): p. 405-15.

151. Lu, M.L., et al., *Impact of alterations affecting the p53 pathway in bladder cancer on clinical outcome, assessed by conventional and array-based methods.* Clin Cancer Res, 2002. 8(1): p. 171-9.

152. Onel, K. and C. Cordon-Cardo, *MDM2 and prognosis.* Mol Cancer Res, 2004. 2(1): p. 1-8.

153. Osman, I., et al., *Inactivation of the p53 pathway in prostate cancer: impact on tumor progression.* Clin Cancer Res, 1999. 5(8): p. 2082-8.

154. Powell, C.M., et al., *Inhibition of the mammalian transcription factor LSF induces S-phase-dependent apoptosis by downregulating thymidylate synthase expression.* EMBO J, 2000. 19(17): p. 4665-75.

155. Santhekadur, P.K., et al., *The transcription factor LSF: a novel oncogene for hepatocellular carcinoma.* Am J Cancer Res, 2012. 2(3): p. 269-85.

156. Studach, L.L., et al., *Subset of Suz12/PRC2 target genes is activated during hepatitis B virus replication and liver carcinogenesis associated with HBV X protein.* Hepatology, 2012. 56(4): p. 1240-51.

157. Yoo, B.K., et al., *Transcription factor Late SV40 Factor (LSF) functions as an oncogene in hepatocellular carcinoma.* Proc Natl Acad Sci U S A, 2010. 107(18): p. 8357-62.

158. Kitamura, N., et al., *Mieap, a p53-inducible protein, controls mitochondrial quality by repairing or eliminating unhealthy mitochondria.* PLoS One, 2011. 6(1): p. e16060.

159. Wallace, D.C., *A mitochondrial paradigm of metabolic and degenerative diseases, aging, and cancer: a dawn for evolutionary medicine.* Annu Rev Genet, 2005. 39: p. 359-407.

160. Bornstein, C., et al., *SPATA18, a spermatogenesis-associated gene, is a novel transcriptional target of p53 and p63.* Mol Cell Biol, 2011. 31(8): p. 1679-89.

161. Huber, R., et al., *Regulation of C/EBPbeta and resulting functions in cells of the monocytic lineage.* Cell Signal, 2012. 24(6): p. 1287-96.

162. Lopez de Heredia, L., et al., *Bioluminescence imaging of the brain response to acute inflammation in living C/EBP reporter mice.* Neurosci Lett, 2011. 497(2): p. 134-8.

163. Choi, B.H., G.T. Park, and H.M. Rho, *Interaction of hepatitis B viral X protein and CCAAT/ enhancer-binding protein alpha synergistically activates the hepatitis B viral enhancer II/pregenomic promoter.* J Biol Chem, 1999. 274(5): p. 2858-65.

164. Ott, M., S.P. Thyagarajan, and S. Gupta, *Phyllanthus amarus suppresses hepatitis B virus by interrupting interactions between HBV enhancer I and cellular transcription factors.* Eur J Clin Invest, 1997. 27(11): p. 908-15.

165. Xu, Y., et al., *TGF-beta receptor kinase inhibitor LY2109761 reverses the anti-apoptotic effects of TGF-beta1 in myelo-monocytic leukaemic cells co-cultured with stromal cells.* Br J Haematol, 2008. 142(2): p. 192-201.

166. Doherty, M.J., et al., *Amino acid sequence and expression of the hepatic glycogen-binding (GL)-subunit of protein phosphatase-1.* FEBS Lett, 1995. 375(3): p. 294-8.

167. Castanares, C., et al., *Signaling by ALK5 mediates TGF-beta-induced ET-1 expression in endothelial cells: a role for migration and proliferation.* J Cell Sci, 2007. 120(Pt 7): p. 1256-66.

168. Dumont, N., A.V. Bakin, and C.L. Arteaga, *Autocrine transforming growth factor-beta signaling mediates Smad-independent motility in human cancer cells.* J Biol Chem, 2003. 278(5): p. 3275-85.

169. Walsh, J.E. and M.R. Young, *Interrelationship between protein phosphatase 1 and TGF-{beta} in regulating motility and cytoskeletal architecture of endothelial cells.* Anticancer Res, 2010. 30(12): p. 4861-6.

170. Yoshikawa, T., et al., *Silencing of microRNA-122 enhances interferon-alpha signaling in the liver through regulating SOCS3 promoter methylation.* Sci Rep, 2012. 2: p. 637.

171. Yoo, J., et al., *Transforming growth factor-beta-induced apoptosis is mediated by Smad-dependent expression of GADD45b through p38 activation.* J Biol Chem, 2003. 278(44): p. 43001-7.

172. Zawel, L., et al., *DEC1 is a downstream target of TGF-beta with sequence-specific transcriptional repressor activities.* Proc Natl Acad Sci U S A, 2002. 99(5): p. 2848-53.

173. Ogata, S., et al., *TGF-beta signaling-mediated morphogenesis: modulation of cell adhesion via cadherin endocytosis.* Genes Dev, 2007. 21(14): p. 1817-31.

174. Kim, K., K.H. Kim, and J. Cheong, *Hepatitis B virus X protein impairs hepatic insulin signaling through degradation of IRS1 and induction of SOCS3.* PLoS One, 2010. 5(3): p. e8649.

175. Ko, W.H., et al., *Diabetes, hepatitis virus infection and hepatocellular carcinoma: A case-control study in hepatitis endemic area.* Hepatol Res, 2012. 42(8): p. 774-81.

176. Petta, S., et al., *Hepatic steatosis and insulin resistance are associated with severe fibrosis in patients with chronic hepatitis caused by HBV or HCV infection.* Liver Int, 2011. 31(4): p. 507-15.

177. Xie, L., et al., *Transforming growth factor beta-regulated gene expression in a mouse mammary gland epithelial cell line.* Breast Cancer Res, 2003. 5(6): p. R187-98.

178. Chen, H.Z., S.Y. Tsai, and G. Leone, *Emerging roles of E2Fs in cancer: an exit from cell cycle control.* Nat Rev Cancer, 2009. 9(11): p. 785-97.

179. Jiang, Y., et al., *A potential oncogenic role of the commonly observed E2F5 overexpression in hepatocellular carcinoma.* World J Gastroenterol, 2011. 17(4): p. 470-7.

180. Klade, C.S., et al., *Identification and characterization of 9D7, a novel human protein overexpressed in renal cell carcinoma.* Int J Cancer, 2002. 97(2): p. 217-24.

181. von Eyss, B., et al., *The SNF2-like helicase HELLS mediates E2F3-dependent transcription and cellular transformation.* EMBO J, 2012. 31(4): p. 972-85.

182. Vafa, O., et al., *c-Myc can induce DNA damage, increase reactive oxygen species, and mitigate p53 function: a mechanism for oncogene-induced genetic instability.* Mol Cell, 2002. 9(5): p. 1031-44.

183. Ryu, H.M., et al., *Gene expression analysis of primary normal human hepatocytes infected with human hepatitis B virus.* World J Gastroenterol, 2006. 12(31): p. 4986-95.

184. Honda, M., et al., *Different signaling pathways in the livers of patients with chronic hepatitis B or chronic hepatitis C.* Hepatology, 2006. 44(5): p. 1122-38.

185. Lu, S., et al., *Smad3 is overexpressed in advanced human prostate cancer and necessary for progressive growth of prostate cancer cells in nude mice.* Clin Cancer Res, 2007. 13(19): p. 5692-702.

186. Dzieran, J., et al., *Comparative analysis of TGF-beta/Smad signaling dependent cytostasis in human hepatocellular carcinoma cell lines.* PLoS One, 2013. 8(8): p. e72252.

187. Lara-Pezzi, E., et al., *The hepatitis B virus X protein up-regulates tumor necrosis factor alpha gene expression in hepatocytes.* Hepatology, 1998. 28(4): p. 1013-21.

188. Cooray, S., *The pivotal role of phosphatidylinositol 3-kinase-Akt signal transduction in virus survival.* J Gen Virol, 2004. 85(Pt 5): p. 1065-76.

189. Scholle, F., K.M. Bendt, and N. Raab-Traub, *Epstein-Barr virus LMP2A transforms epithelial cells, inhibits cell differentiation, and activates Akt.* J Virol, 2000. 74(22): p. 10681-9.

190. Huang, W.C., et al., *Hepatitis B virus X protein induces IKKalpha nuclear translocation via Akt-dependent phosphorylation to promote the motility of hepatocarcinoma cells.* J Cell Physiol, 2012. 227(4): p. 1446-54.

191. Khattar, E., A. Mukherji, and V. Kumar, *Akt augments the oncogenic potential of the HBx protein of hepatitis B virus by phosphorylation.* FEBS J, 2012. 279(7): p. 1220-30.

192. Chin, R., et al., *Modulation of MAPK pathways and cell cycle by replicating hepatitis B virus: factors contributing to hepatocarcinogenesis.* J Hepatol, 2007. 47(3): p. 325-37.

193. Kong, G., et al., *Upregulated microRNA-29a by hepatitis B virus X protein enhances hepatoma cell migration by targeting PTEN in cell culture model.* PLoS One, 2011. 6(5): p. e19518.

194. Godoy, P., et al., *Extracellular matrix modulates sensitivity of hepatocytes to fibroblastoid dedifferentiation and transforming growth factor beta-induced apoptosis.* Hepatology, 2009. 49(6): p. 2031-43.

195. Hoppe-Seyler, K., et al., *The inhibitors of nucleotide biosynthesis leflunomide, FK778, and mycophenolic acid activate hepatitis B virus replication in vitro.* Hepatology, 2012. 56(1): p. 9-16.

196. Lloyd, R.E., *How do viruses interact with stress-associated RNA granules?* PLoS Pathog, 2012. 8(6): p. e1002741.

197. Gabriel, A., et al., *Hepatocyte steatosis in HCV patients promotes fibrosis by enhancing TGF-beta liver expression.* Hepatol Res, 2008. 38(2): p. 141-6.

198. Kanzler, S., et al., *Prediction of progressive liver fibrosis in hepatitis C infection by serum and tissue levels of transforming growth factor-beta.* J Viral Hepat, 2001. 8(6): p. 430-7.

199. Verma, V., A. Chakravarti, and P. Kar, *Cytokine levels of TGF-beta, IL-10, and sTNFalphaRII in type C chronic liver disease.* Dig Dis Sci, 2008. 53(8): p. 2233-7.

200. Caja, L., et al., *Dissecting the effect of targeting the epidermal growth factor receptor on TGF-beta-induced-apoptosis in human hepatocellular carcinoma cells.* J Hepatol, 2011. 55(2): p. 351-8.

201. Feng, X., et al., *Hepatitis C virus core protein promotes the migration and invasion of hepatocyte via activating transcription of extracellular matrix metalloproteinase inducer.* Virus Res, 2011. 158(1-2): p. 146-53.

202. Zeng, B., et al., *Epigenetic regulation of miR-124 by hepatitis C virus core protein promotes migration and invasion of intrahepatic cholangiocarcinoma cells by targeting SMYD3.* FEBS Lett, 2012. 586(19): p. 3271-8.

203. Vo, B.T., et al., *TGF-beta effects on prostate cancer cell migration and invasion are mediated by PGE2 through activation of PI3K/AKT/mTOR pathway.* Endocrinology, 2013. 154(5): p. 1768-79.

204. Zhang, H., et al., *KLF8 involves in TGF-beta-induced EMT and promotes invasion and migration in gastric cancer cells.* J Cancer Res Clin Oncol, 2013. 139(6): p. 1033-42.

205. Thiery, J.P. and J.P. Sleeman, *Complex networks orchestrate epithelial-mesenchymal transitions.* Nat Rev Mol Cell Biol, 2006. 7(2): p. 131-42.

206. Jiang, C.G., et al., *Downregulation of connective tissue growth factor inhibits the growth and invasion of gastric cancer cells and attenuates peritoneal dissemination.* Mol Cancer, 2011. 10: p. 122.

207. Braig, S., et al., *CTGF is overexpressed in malignant melanoma and promotes cell invasion and migration.* Br J Cancer, 2011. 105(2): p. 231-8.

208. Cui, L., et al., *CTGF is overexpressed in papillary thyroid carcinoma and promotes the growth of papillary thyroid cancer cells.* Tumour Biol, 2011. 32(4): p. 721-8.

209. Butel, J.S., *Viral carcinogenesis: revelation of molecular mechanisms and etiology of human disease.* Carcinogenesis, 2000. 21(3): p. 405-26.

210. Galle, P.R., et al., *In vitro experimental infection of primary human hepatocytes with hepatitis B virus.* Gastroenterology, 1994. 106(3): p. 664-73.

211. Summers, J., et al., *Morphogenetic and regulatory effects of mutations in the envelope proteins of an avian hepadnavirus.* J Virol, 1991. 65(3): p. 1310-7.

212. Adimoolam, S. and J.M. Ford, *p53 and regulation of DNA damage recognition during nucleotide excision repair.* DNA Repair (Amst), 2003. 2(9): p. 947-54.

213. Chin, R., et al., *Dysregulation of hepatocyte cell cycle and cell viability by hepatitis B virus.* Virus Res, 2010. 147(1): p. 7-16.

214. Bergametti, F., D. Sitterlin, and C. Transy, *Turnover of hepatitis B virus X protein is regulated by damaged DNA-binding complex.* J Virol, 2002. 76(13): p. 6495-501.

215. Iizuka, N., et al., *Comparison of gene expression profiles between hepatitis B virus- and hepatitis C virus-infected hepatocellular carcinoma by oligonucleotide microarray data on the basis of a supervised learning method.* Cancer Res, 2002. 62(14): p. 3939-44.

216. Nakanishi, F., et al., *Alteration in gene expression profile by full-length hepatitis B virus genome.* Intervirology, 2005. 48(2-3): p. 77-83.

217. Ozer, A., et al., *Effect of hepatocyte proliferation and cellular DNA synthesis on hepatitis B virus replication.* Gastroenterology, 1996. 110(5): p. 1519-28.

218. Coulouarn, C., V.M. Factor, and S.S. Thorgeirsson, *Transforming growth factor-beta gene expression signature in mouse hepatocytes predicts clinical outcome in human cancer.* Hepatology, 2008. 47(6): p. 2059-67.

219. Wieland, S., et al., *Genomic analysis of the host response to hepatitis B virus infection.* Proc Natl Acad Sci U S A, 2004. 101(17): p. 6669-74.

220. Nave, B.T., et al., *Mammalian target of rapamycin is a direct target for protein kinase B: identification of a convergence point for opposing effects of insulin and amino-acid deficiency on protein translation.* Biochem J, 1999. 344 Pt 2: p. 427-31.

221. Cuenda, A., et al., *SB 203580 is a specific inhibitor of a MAP kinase homologue which is stimulated by cellular stresses and interleukin-1.* FEBS Lett, 1995. 364(2): p. 229-33.

222. Lali, F.V., et al., *The pyridinyl imidazole inhibitor SB203580 blocks phosphoinositide-dependent protein kinase activity, protein kinase B phosphorylation, and retinoblastoma hyperphosphorylation in interleukin-2-stimulated T cells independently of p38 mitogen-activated protein kinase.* J Biol Chem, 2000. 275(10): p. 7395-402.

223. Borsch-Haubold, A.G., S. Pasquet, and S.P. Watson, *Direct inhibition of cyclooxygenase-1 and -2 by the kinase inhibitors SB 203580 and PD 98059. SB 203580 also inhibits thromboxane synthase.* J Biol Chem, 1998. 273(44): p. 28766-72.

224. Birkenkamp, K.U., et al., *The p38 MAP kinase inhibitor SB203580 enhances nuclear factor-kappa B transcriptional activity by a non-specific effect upon the ERK pathway.* Br J Pharmacol, 2000. 131(1): p. 99-107.

225. Chang, W.W., et al., *Suppression of p38 mitogen-activated protein kinase inhibits hepatitis B virus replication in human hepatoma cell: the antiviral role of nitric oxide.* J Viral Hepat, 2008. 15(7): p. 490-7.

226. Ebert, G., et al., *5' Triphosphorylated small interfering RNAs control replication of hepatitis B virus and induce an interferon response in human liver cells and mice.* Gastroenterology, 2011. 141(2): p. 696-706, 706 e1-3.

227. Wendt, M.K., T.M. Allington, and W.P. Schiemann, *Mechanisms of the epithelial-mesenchymal transition by TGF-beta.* Future Oncol, 2009. 5(8): p. 1145-68.

228. Nitahara-Kasahara, Y., et al., *Cellular vimentin content regulates the protein level of hepatitis C virus core protein and the hepatitis C virus production in cultured cells.* Virology, 2009. 383(2): p. 319-27.

229. Nagaraja, T., et al., *Activation of the connective tissue growth factor (CTGF)-transforming growth factor beta 1 (TGF-beta 1) axis in hepatitis C virus-expressing hepatocytes.* PLoS One, 2012. 7(10): p. e46526.

230. Weng, H.L., et al., *Profibrogenic transforming growth factor-beta/activin receptor-like kinase 5 signaling via connective tissue growth factor expression in hepatocytes.* Hepatology, 2007. 46(4): p. 1257-70.

DECLARATION

I hereby declare that this dissertation is, to the best of my knowledge and belief, a presentation of my own work, except where otherwise acknowledged.

Jasmin Fabian

DANKSAGUNG

In erster Linie gilt mein Dank meinem Doktorvater Prof. Dr. Steven Dooley (Molekulare Hepatologie – Alkoholfolgeerkrankungen, II. Medizinische Klinik, Fakultät für klinische Medizin Mannheim, Universität Heidelberg), der mir die Möglichkeit gegeben hat, meine Doktorarbeit über das Thema HBV / HCV zu schreiben, welches mir persönlich sehr am Herzen liegt.
Lieber Steven, vielen Dank für Deine Führung und Unterstützung in den Höhen und Tiefen meiner Doktorarbeit. Auch wenn es nicht immer leicht war, ich möchte die Zeit nicht missen.

Des Weiteren danke ich meiner Betreuerin Dr. Nadja Meindl-Beinker, die sich immer mit mir auseindergesetzt hat und immer eine gute Idee hatte.
Liebe Nadja, vielen Dank für Deine Unterstützung, oft auch auf menschlicher Ebene; und vielen Dank für Deine Geduld, mir das wissenschaftliche Schreiben etwas näher zu bringen.

Auch möchte ich meinen Kollegen danken, vor allem Chris und Johanna, die mir immer mit Rat und Tat zur Seite standen.
Lieber Chris, Liebe Johanna, vielen Dank für die schöne Zeit, ohne Euch hätte es nur halb so viel Spaß gemacht.

Ganz im Besonderen möchte ich meiner Mutter danken, die mir diesen Weg geebnet hat.
Liebe Mama, vielen Dank, dass Du immer für mich da warst und durch sämtliche Lebensphasen mit mir gegangen bist. Ich weiß, dass ich immer auf Dich zählen kann und Du auch auf mich.

Zu guter Letzt danke ich meinem Partner, bei dem ich immer neue Kraft tanken konnte.
Mein lieber Schatz, ich bin froh, dass wir uns kennengelernt haben. Deine Gelassenheit und Leichtigkeit des Lebens hat mich um einiges entspannter werden lassen.